Chapter 1

Structure of Microsporidia

Jiří Vávra
Faculty of Sciences, Charles University in Prague (Emeritus), Czech Republic
Institute of Parasitology, Biology Centre, Academy of Sciences of the Czech Republic, Czech Republic
Faculty of Sciences, University of South Bohemia, Czech Republic

J. I. Ronny Larsson
Department of Biology, University of Lund (Emeritus), Sweden

1.1 INTRODUCTION

Microsporidia are intracellular parasites ranked among the protists, which means that they are eukaryotic and unicellular. The microsporidian cell exhibits, however, a number of unique features, some of them are reductions, and others are structural innovations. The main morphological characteristic of the microsporidia is the profound difference between multiplicative (vegetative) stages on one hand and disseminated spores (and their immediate precursors) on the other hand. Vegetative stages are rather inconspicuous cells showing several seemingly primitive characters: instead of typical mitochondria, they possess mitosomes, which are mitochondrial remnants (Williams et al. 2002; Vávra 2005), their Golgi apparatus is of an unstacked type (Vávra 1965, 1976a; Beznoussenko et al. 2007), their ribosomes are not of the typical eukaryotic type but resemble ribosomes of prokaryotic organisms (Ishihara & Hayashi 1968; Curgy et al. 1980), and the microsporidian cells lack typical microbody-like organelles (peroxisomes) (Vávra & Lukeš 2013). Microsporidian spores, on the other hand, are equipped with an infection apparatus, composed of a unique set of organelles, which during spore germination injects the spore content into a host cell and perpetuates thus the life cycle of the parasite (Lom & Vávra 1963a; Vávra 1976a; Weidner 1976a; Vávra & Lukeš 2013). Spores are the only stage that survives outside the host, and due to their durability and structural complexity, the spores are essential for microsporidium recognition and classification.

1.2 STRUCTURAL CHARACTERS AND CLASSIFICATION OF MICROSPORIDIA

Structural characters are still basic for microsporidian classification, despite that molecular biology characters are progressively gaining importance for revealing relationships between individual taxons of the phylum and between microsporidia and other organisms. Molecular biology also provides unique possibilities to identify developmental stages of microsporidia with complex life cycles comprising dissimilar life cycle stages (see Section 1.3.4).

The first microsporidium was described in 1857 (Nägeli 1857), and during the more than 150 years' long history of formal existence, based on cytology, microsporidia have successively been classified as yeastlike fungi, protozoans of various taxonomic ranks, as well as Archezoa, primitive organisms from the premitochondrial era of eukaryotic cell genesis (see Corradi & Keeling 2009, for the history of microsporidia taxonomy). Recent views, however, consider microsporidia to be related to fungi. Microsporidia–Fungi relationship is supported almost exclusively by molecular biology data (see Chapter 5). The structural support for such relationships is inconclusive, being limited to a number of characters, like deposition of cell wall material on the plasma membrane of certain developmental stages, the structure of the spindle pole terminus, presence of chitin in spores, closed type of mitosis, presence of nuclear twins in some microsporidia, and some features of meiosis

Microsporidia: Pathogens of Opportunity, First Edition. Edited by Louis M. Weiss and James J. Becnel.

(Cavalier-Smith 2001; Thomarat et al. 2004). These characters which, however, are not quite fungi-specific (Vávra & Lukeš 2013) are discussed in detail in the following text.

The unique structural and biological characters of microsporidia justify their ranking as a phylum of their own, named Microspora Sprague, 1977, or Microsporidia Balbiani, 1882, depending on the interpretation of Balbiani's intentions as it was not specified as a phylum (Balbiani 1882), within the superkingdom Opisthokonta (Adl et al. 2012). However, microsporidia lack a posteriorly directed flagellum, which is a characteristic of the Opisthokonta, and they have no 9+2 microtubular structures in their cells. In this character, microsporidia resemble fungi which have lost flagella almost totally (James et al. 2006; Liu et al. 2006).

By tradition, names, descriptions, and type requirements of new microsporidian taxa follow the rules of the International Code of Zoological Nomenclature (ICZN 1999). It has been recommended that this practice is maintained even if microsporidia at present time are believed to be related to the kingdom Fungi which are treated under the botanical code ICBN (Redhead et al. 2009). The last census of microsporidian genera is that of Larsson (1999), Sprague et al. (1992), and Canning and Vávra (2000), with the paper by Larsson (1999) providing extensive information on structural characters of microsporidian genera described up to the year 1999. As about 43 genera have been added since 1999, presently, there exist about 197 genera (see Appendix 1) and totally 1300–1500 microsporidian species (Vávra & Lukeš 2013). As stated earlier, the comprehensive classifications of microsporidia have mostly been based on structural characters, and several classifications below the phylum level exist (Sprague 1977; Weiser 1977; Issi 1986). The classifications based mostly on other characters than morphology have the limitation that they cover only part of existing genera (Sprague et al. 1992; Vossbrinck & Debrunner-Vossbrinck 2005).

Although microsporidia structurally are a very homogeneous group of organisms, nevertheless, two main branches, conspicuously differing in structure and development, can be recognized. The groups are the typical microsporidia and the supposedly evolutionary primitive (or reduced?) atypical microsporidia. The last group can be divided into two structurally diverse subgroups.

Microsporidia with a cytology typical for these protists are by far the largest group, with more than 1000 named species in nearly 190 genera. Their hosts are found in all groups of animals, from protists to humans. They exhibit the most complex life cycles and produce spores in a great variety of shapes, from spherical to rodlike.

Life cycle and cytology distinguish typical microsporidia from the other two groups: chytridiopsids and metchnikovellideans. Our knowledge of these groups is superficial. The two groups share an extrusion apparatus of similar, although not identical, construction that diverges from the common type of extrusion apparatus. They also share a life cycle that differs from that of typical microsporidia. Whether these similarities indicate that the two groups are closely related is unknown. The chytridiopsids, represented by about 15 species in 8 genera, are parasites of terrestrial or freshwater invertebrates, mostly insects. Their spores are spherical. The metchnikovellideans (about 25 species in 4 genera) are hyperparasites of gregarines. The spores are more or less subspherical or, exceptionally, rod-shaped. Spores lack a typical polaroplast, and the polar filament is of a special construction.

1.2.1 Microsporidia under the Light Microscope

The presence of spores, or sometimes of grouped presporal stages (sporoblasts), in examined material indicates in a reliable way that microsporidia might be involved. There is no reliable way to recognize presporogonic stages using light microscopy. Spores or cells resembling microsporidian spores are produced by many other protists. A number of specific techniques, described later in this chapter, can be applied to determine if an organism is a microsporidium. The ultimate diagnostic test of a microsporidium is the ejection of the polar filament from fresh, unfixed spores (Fig. 1.8e and g). This might occur spontaneously or can be forced by mechanical or chemical stimulation. The periodic acid–Schiff (PAS) staining of spores in smears and sections of fixed material, described in the following text, is also a reliable diagnostic method. Techniques for the priming and staining of spores are presented in Section 1.11.

1.2.1.1 Microsporidia in Fresh Materials

Very seldom are presporal stages so characteristic and well preserved in fresh material that they allow recognition. Spores, in contrast, are resistant to harsh conditions of the environment and not destroyed by the handling of ordinary squashed materials. The spore is thus the main diagnostic element. Living spores of most microsporidia are only a few micrometers long, but the size range between the smallest and the largest species is considerable. Spores of the human parasite *Enterocytozoon bieneusi* measure about 1 µm in length, while spores of *Bacillidium filiferum*, a parasite of freshwater oligochaetes, approach 40 µm. A sample of microsporidian spores is fairly uniform in shape and size, although sometimes two distinct size classes might occur together, while in a sample of yeast cells, which can erroneously be taken for microsporidia, there is a gradient of spore sizes.

The spore shape of most species is oval or pyriform, but rodlike, spherical, and other shapes are not unusual. About 20% of microsporidian genera have rodlike spores (Vávra & Lukeš 2013) (Fig. 1.1). Fixation and staining may change the shape of spores. For example, the predominantly insect-parasitic *Amblyospora* species produce in one of their alternate hosts

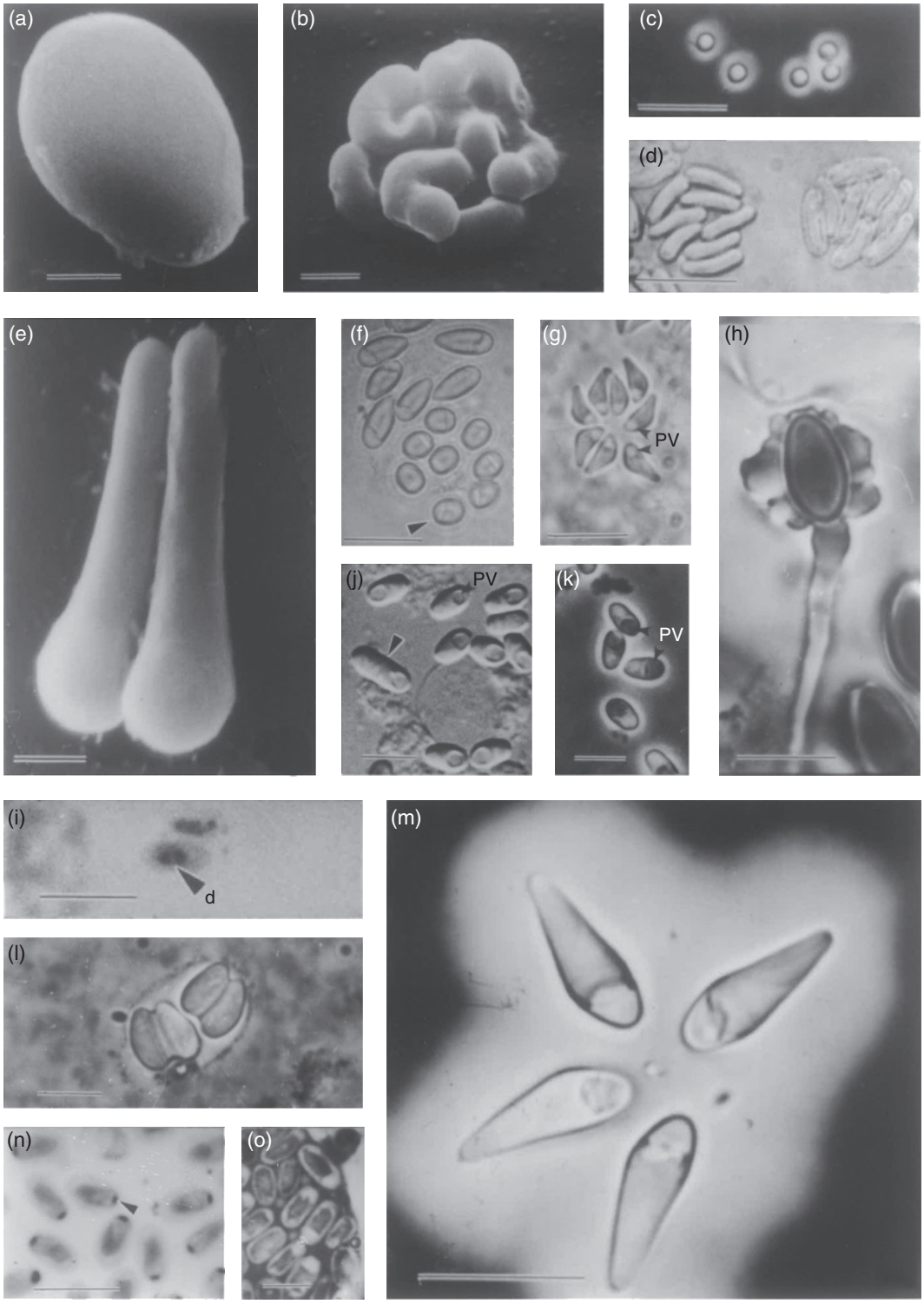

Figure 1.1 Shape and staining reactions of microsporidian spores. (a) Lightly pyriform (*Episeptum invadens*); (b) horseshoe-shaped (*Toxoglugea variabilis*); (c) spherical (*Coccospora micrococcus*); (d) rod-shaped (*Resiomeria odonatae*); (e) lageniform (*Paraepiseptum* (formerly *Cougourdella*) *polycentropi*); (f) dimorphic sporogony with pyriform free spores and ovoid octospores (arrowhead) (*Amblyospora callosa*); (g) angular octospores (*Bohuslavia asterias*); (h) ovoid spore with prominent exospore projections (*Caudospora simulii*); (i) diplokaryon (*Vairimorpha mesnili*); (j and k) live ovoid spores (*Glugea anomala*); (l) coupled spores (*Norlevinea daphniae*); (m) tetraspores with prominent mucus production (*Marssoniella elegans*); (n) PAS reaction stains the "polar cap" of the spores, which actually is the polar sac–anchoring disk complex (arrowhead) (*Nosema lepiduri*); (o) spores in stained smear (*Nosema apis*). (a, b and e) SEM; (c) dark field; (d, j) interference phase contrast; (f, g, h, k) phase contrast; (i, o) Giemsa stain; (l, m) India ink negative staining; (n) PAS. Scale bars = 1 µm (a, b, e); 10 µm (c, d, f, h); 5 µm (i–o). d, diplokaryon; PV, posterior vacuole. Reprinted from Wittner, M., Weiss, L. M. (eds.) 1999. *The Microsporidia and Microsporidiosis*. ASM Press, Washington, DC.

uniform spores in groups of eight. While living spores are nearly oval in shape, they appear barrel-shaped in a stained smear (Hazard & Oldacre 1975).

Live microsporidian spores are refractive, and usually, only a vacuole (ranging in size from very small to more than one-third of the spore volume) is visible at the posterior pole of the spore (Fig. 1.1g, j, k, and m). Only exceptionally are traces of the coiled, threadlike infection apparatus visible in large and living immature spores (Fig. 1.8e). It is not unusual that spores produced in aquatic hosts are ornamented with spore expansions and filamentous projections, like the genus characteristic spores of the blackfly parasites *Caudospora* (Fig. 1.1h) and *Hirsutosporos* (Batson 1983), and the mosquito parasite *Trichoctosporea* (Larsson 1994b). Spores of microsporidia from aquatic invertebrate hosts often produce a mucous coat when released into water (Fig. 1.1c and m) (Lom & Vávra 1963b) (see Section 1.11.3.5).

1.2.1.2 Microsporidia in Fixed and Stained Materials

Fixed and stained preparations do not only allow the recognition of spores, but also of vegetative stages. Identification of presporal stages in the absence of spores is difficult even for a specialist, but it is an important element for the recognition of the life cycle of the organism. Most commonly Giemsa staining is used for smears. This staining allows recognition of nuclei of presporal stages. Mature spores exhibit a dark band across the center of the spore, where the nucleus lies (Fig. 1.1o), a dark spot at the anterior pole (the anchor for the extrusion apparatus), and sometimes a reddish granule, the posterosome, in the posterior vacuole. If the spores are fully mature, nuclei are seldom clearly revealed using Giemsa staining (Fig. 1.1i) unless the staining is performed after an acid hydrolysis (see Section 1.11.3.6).

Another useful staining is the PAS method, which stains a red dot at one pole of the spore, corresponding to the location of the apical part ("anchoring disk") of the polar filament (see Section 1.11.2.2) (Fig. 1.1n). This staining reaction is microsporidia-specific and of diagnostic value.

A number of microsporidia produce their spores in packets. The envelopes of the packets are rarely visible in light microscopic preparations, neither in fresh preparations nor in stained smears, but a technique for revealing their existence by in vivo staining is described in Section 1.11.3.7 (Fig. 1.33). If groups with 2, 4, 8, 16, or other regular numbers of spores are seen in carefully made smears or, better, squash preparations, it might be suspected that the organism is a microsporidium (Fig. 1.1d, f, g, l and m and Fig. 1.2g).

1.3 STRUCTURAL ASPECTS OF REPRODUCTION AND LIFE CYCLES

Microsporidian life cycles are treated in detail in Chapter 2. However, as basic knowledge of the life cycle, and of the terminology applied to the various stages, is necessary for the presentation of the cytology, a brief introduction is given here. Further information on microsporidian life cycles and terminology can be found in Vávra (1976b), Vávra and Sprague (1976), Larsson (1986b, 1988c), and Sprague et al. (1992).

1.3.1 Basic Life Cycle

The microsporidia are most frequently encountered in the spore stage. This is the infectious stage and the only life cycle stage able to survive outside the host cell. The spore normally reaches the new host through the gut even if other routes of transmission are known to occur.

When the spore is inside an appropriate host, a minute infectious cell, the sporoplasm is injected from the spore into a host cell via an evaginable tube, resulting in the transmission of the infection. In the new host, the sporoplasm starts a reproduction cycle which terminates with the production of spores. In a typical case, the host cell is finally completely filled up with parasite spores with few or none of the earlier developmental stages left behind. In most microsporidia, two sequences of reproduction follow each other: an initial vegetative reproduction (merogony) yielding daughter cells (merozoites) with the potential either to repeat merogony or to enter the second reproductive phase, the production of spores (sporogony). Some microsporidia, like the *Nosema* species, reproduce weakly in the sporogony, where each cell initiating sporogony ("sporont") yields only two spores (Brooks et al. 1985). Species with a weak sporogony reproduce more efficiently during the merogony, where several cycles of divisions might follow each other.

In a small number of microsporidia, merogonial reproduction has never been observed and is presumed to be absent. The only reproduction known to occur is the production of spores. This is characteristic for the genera *Chytridiopsis* (Larsson 1993) and *Metchnikovella* (Vivier & Schrével 1973) and a few other related genera. The recently described unusual merogonial budding-like process described for *Chytridiopsis* by Tonka et al. (2010) probably involved the beginning of sporogony by plasmotomy (see Section 1.3.2).

1.3.2 Reproduction Modes

Both merogony and sporogony proceed as binary fission, plasmotomy, or schizogony depending on the species (Fig. 1.2). The manner in which the divisions occur is often best visible in stained light microscopic preparations.

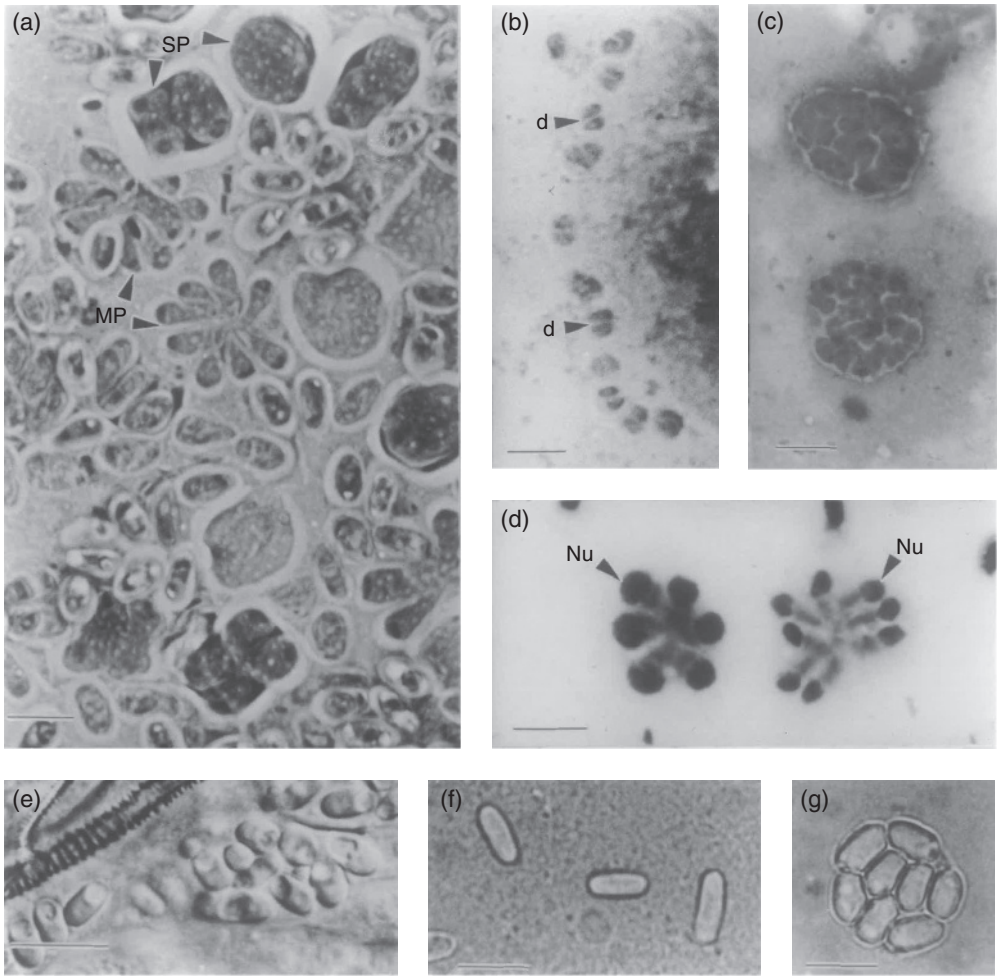

Figure 1.2 Reproduction and spore morphs. (a) Merogony, sporogony, and mature spores (*Systenostrema corethrae*); (b) chain of diplokaryotic merozoites (*Nosema* sp.); (c) two stages of plasmotomy (*Vavraia holocentropi*); (d) two stages of schizogony (*Trichotuzetia guttata*); (e–g) spore morphs of *Vairimorpha* sp. from the gypsy moth *Lymantria dispar* larvae. (e) First-generation spores for intertissue transmission; (f) *Nosema*-type binucleate spores for interhost transmission; (g) *Thelohania*-like uninucleate spores for interhost transmission. (a, b, d) Giemsa stain; (c) hematoxylin; (e) interference phase contrast; (f, g) phase contrast. Scale bars = 10 µm (a, c, d–g); 5 µm (b). d, diplokaryon; MP, merogonial plasmodium; Nu, nucleus; SP, sporogonial plasmodium. Reprinted from Wittner, M., Weiss, L. M. (eds.) 1999. *The Microsporidia and Microsporidiosis*. ASM Press, Washington, DC.

When reproduction involves binary fission, two daughter cells are formed by each mother cell. Often the division products adhere to each other, forming chains of cells (Fig. 1.2b and Fig. 1.26d). Plasmotomy and schizogony start with a series of nuclear fissions, producing a cell with numerous nuclei, which is called a plasmodium. A plasmodium is usually more or less rounded (Fig. 1.2c, Fig. 1.22d, Fig. 1.23b), but ribbonlike plasmodia with lined nuclei occur frequently (Larsson et al. 1997a). If the plasmodium splits into smaller parts by a series of successive divisions, the division process is called plasmotomy (Fig. 1.2c). In a small number of microsporidia, the plasmodium splits endogenously in that vacuoles are formed inside the plasmodium, and the plasmodium is fragmented into cells by the expanding vacuoles. This process has been named vacuolation (Beard et al. 1990).

Schizogony proceeds in three stages: the nuclei of the multinucleate plasmodium, after ended nuclear fission, accumulate at the periphery; lobes are formed at the periphery, in the same number as there are nuclei (Fig. 1.2d), and finally all lobes bud off simultaneously, each lobe yielding one daughter cell.

1.3.3 Sexual Processes

Structural evidence of the existence of sexual reproduction has been reported from a fairly small number of microsporidia. The events are not well known, as they have been described only from static observations with light and electron microscopes.

The first well-documented light microscopic observation of karyogamy and meiosis at the transition from merogony to sporogony was made from a mosquito parasite of the genus *Amblyospora* (Hazard & Brookbank 1984) (see Section 1.4.2.2). This

work was followed by the description of a unique type of cell with an anterior nipple-like protrusion ("papilla") formed as doubled and thickened plasma membrane, occurring early in merogony (Hazard et al. 1985; Becnel et al. 1987; Becnel 1992, 1994). The cell was interpreted to be a uninucleate gamete, destined for fusion with another such cell by plasmogamy (fusion of cells without nuclear fusion) to restore the diplokaryotic state (with two apposed nuclei) of a meront. In a number of microsporidia, sexuality has been deduced from more or less clear observations in ultrathin sections of structures resembling synaptonemal complexes (see the following text for details). Despite the limited structural evidence of the sexual process in microsporidia, methods of molecular genetics have confirmed the existence of sexual recombination in microsporidia indicating that cryptic sexual reproduction in microsporidia actually exists (Haag et al. 2013; Ironside 2013) (see Chapter 8 of the present volume).

1.3.4 Life Cycle Types

Complete life cycles have only been elucidated for a small fraction of microsporidian species, and recent evidence shows that apparently many microsporidia have complex life cycles. According to the present knowledge, many microsporidia produce spores of a single type and of similar size and shape. Other microsporidia produce spores of several types (Fig. 1.1f and Fig. 1.2e–g), differing in size (microspores, macrospores) or in size, shape, and cytology. Different spores are produced within the same infected host and tissue (Pilley 1976), within different tissues of the same host, or even in tissues of different hosts (Becnel 1994). So far, four is the maximum number of cytologically different spore types revealed from a single species (Sokolova & Fuxa 2008). If two cytologically different kinds of spores (differing not only in size) are produced, the life cycles are considered dimorphic, and with three or more kinds of spores polymorphic. Thus, *Trachipleistophora anthropophthera* forms two types of spores, sometimes in the same brain cell of its human host (Vávra et al. 1998) (see Fig. 1.29e–i and Section 1.10.3). *Spraguea lophii* forms two types of spores in different layers of the gigantic infected cell (a xenoma) of its fish host *Lophius* (Weissenberg 1976). *Vairimorpha necatrix* forms two types of spores within the fat body of its lepidopteran hosts (Pilley 1976). Two extremely different spore types, one in cardiac muscles and the other in skeletal muscles of the crab *Carcinus maenas*, are produced by a microsporidium close to *Nadelspora canceri* (Stentiford et al. 2013). *Vairimorpha disparis* forms three different spore morphs in its host, the gypsy moth *Lymantria dispar*. One type is formed in muscles surrounding the gut, and two other types are formed, respectively, in the fat body and in the salivary and silk glands (Vávra et al. 2006) (Fig. 1.2e–g). Finally, the fire ant parasite *Kneallhazia* forms four spore morphs in different castes and stages of its social hymenopteran host *Solenopsis* (Sokolova & Fuxa 2008). The most complex cycles need alternation of hosts and involvement of more than one host generation. Thus, microsporidia of the family Amblyosporidae and of the genus *Desmozoon* (family Enterocytozoonidae) circulate between copepods and mosquitoes and copepods and salmonid fish, respectively (Vossbrinck et al. 2004; Freeman & Sommerville 2011) (Fig. 1.1f). The sporogonial divisions and the cytology of the respective spore morphs may differ to such an extent that without the knowledge of the whole cycle, some organisms in different hosts or tissues might be considered to belong to different genera. The significance of life cycle and sporal polymorphism in microsporidia is not fully understood. Molecular methods are frequently the only tool to prove or to disprove the identity of the microsporidian morphs involved in a life cycle (Stentiford et al. 2013). Detailed consideration of life cycles is presented in Chapter 2 of the present volume.

1.4 ESSENTIALS OF MICROSPORIDIAN CYTOLOGY

Our presentation of the microsporidian cytology starts with a review of general cytological features. The specific structures of the merogonial and sporogonial stages, and of the mature spores, will be dealt with separately.

1.4.1 The Plasma Membrane

The plasma membrane of microsporidia is a unit membrane of classical trilaminar structure, about 7 nm thick. In the merogonial stage, this membrane may show evidence of active interaction with the host cell cytoplasm in the form of vesicular or tubular projections, increasing the surface area of the parasite (Vávra 1976a). A thick layer of a glycocalyx-like material (frequently in the form of tubules) covers the outer face of the plasma membrane of meronts in some microsporidia (Koudela et al. 2001; Franzen et al. 2005) (Fig. 1.32). At a certain moment of the life cycle, the cell membrane becomes the site of deposition of electron-dense material which will later be incorporated into the spore wall or form various kinds of sporogonial envelopes. The appearance of spore wall primordial material on the plasma membrane of the merozoite indicates that merogony ends and the second life cycle phase, the sporogony, begins (Vávra 1976a).

1.4.2 The Nucleus

The microsporidian nucleus is usually round or oval. The size of the nucleus varies during the life cycle. In meronts, it is usually several micrometers in diameter; during sporulation, its size decreases; and in spores, it is usually very small (1–2 μm or even less).

The nucleus is of the typical eukaryotic type. It is limited by double unit membranes separated by a perinuclear space. Normally pores are visible (Fig. 1.3c and e; Fig. 1.10f). The nucleoplasm is usually homogeneous. Condensations of chromatin, corresponding to chromosomes, have been reported occasionally. Nucleoli are seldom seen in microsporidian nuclei (Larsson 1986b), except in stages preceding spore formation (Fig. 1.3c) (Vávra 1976a).

1.4.2.1 Nuclear Configuration

Two types of nuclear configurations exist in microsporidia: monokaryon, an individual nucleus (Fig. 1.3a), and diplokaryon, two apposed nuclei (Fig. 1.3b, Fig. 1.30b and f; Fig. 1.31a; Fig. 1.32b and g). Some life cycles are monokaryotic throughout, having multiple monokarya in dividing stages, while others are diplokaryotic, having multiple diplokarya in dividing stages. There are also microsporidia that shift from one nuclear type to another in different life cycle stages. In such cases, diplokaryotic nuclei are typical of merogony and the transition to sporogony, while monokarya are seen in sporogony (Canning 1988). Polymorphic species shift between the nuclear configurations when changing hosts or tissues.

Structurally, the diplokaryon consists of two nuclei in a coffee bean-like association, each member of the twin having its complete nuclear membrane, which, in the area where the two nuclei abut, is flat and devoid of nuclear pores (Vávra 1976a) (Fig. 1.3c and d; Fig. 1.10f). Both nuclei of the diplokaryon are structurally identical and divide synchronously (Vávra 1976b). There is ultrastructural evidence, from some microsporidia having diplokaryotic meronts but monokaryotic sporonts and spores, that the diplokaryon originates by the association of nuclei during a sexual event (copulation of cells considered to be gametes) in the initial phase of the life cycle (Hazard et al. 1985). In some diplokaryotic microsporidia, the monokaryotic state is restored either by nuclear separation or fusion (this last event postulated in the absence of structural evidence) (Sprague et al. 1992). The separation is achieved by progressive dissociation of the twin nuclei (Mitchell & Cali 1993). The fusion of the two nuclei of the diplokaryon is presumed to occur as a part of the meiosis.

1.4.2.2 The Microsporidian Nucleus in Mitosis and Meiosis

Microsporidia express closed intranuclear pleuromitosis (Hollande 1972; Raikov 1982), which means that the nuclear membrane is preserved during mitosis and meiosis, and the mitotic spindle is intranuclear. The microtubules of the mitotic spindle attach at one end to the kinetochores of the chromosomes (Fig. 1.3f) and converge at the other end to a microtubule-organizing center, the spindle (or centriolar) plaque (Fig. 1.3f and g; Fig. 1.7b). Some microtubules run from one spindle plaque to the opposite one, and others radiate away from the spindle plaque into the cytoplasm (Desportes 1976; Desportes-Livage et al. 1996). There is no centriole in the microsporidian cell, and the fine structure of the spindle plaque closely resembles that of yeasts and other ascomycetous fungi (Vávra 1976a; Desportes & Théodoridès 1979). Like microtubule-organizing centers of yeasts (Alfa & Hyams 1990), their components are found both internally and externally to the nuclear envelope. Externally, the centriolar plaque is a lenticular, electron-dense area of more or less stratified material, situated in a depression of the nuclear envelope. Several (usually three to six) "polar vesicles," electron-opaque vesicles with double membranes, are present close to the spindle plaque. They represent mitochondrial remnants, termed mitosomes (see Section 1.4.3). The internal part of the plaque, where the spindle microtubules converge, is an aggregation of electron-dense material on the internal nuclear membrane (Fig. 1.3g and Fig. 1.7b, d, and e). Some variations of the aforementioned structure of the spindle plaque were described (e.g., in the appearance and number of strata in the lenticular area). Whether these variations are artifacts of preparation, are true structural characters of different microsporidia, or express different spindle plaque organization in different life cycle events is not known. It should be mentioned that in yeast the structure of the spindle plaque changes during mitosis and meiosis (Zickler & Olson 1975).

Usually more than two spindle plaques are present in a nucleus during active growth and divisions of the parasite. Supernumerary plaques are ready for the next mitosis (Vávra 1976b). The new spindle plaques arise by division of the old ones (Larsson 1986b), and they migrate along the nuclear surface to their final site (Vávra 1976a). It is not known if spindle plaques persist in some form in the spores, but their presence in young sporoblasts has been reported (Walker & Hinsch 1972).

Meiosis of microsporidia has been ascertained both by light microscopical cytology (Hazard & Brookbank 1984; Chen & Barr 1995) and electron microscopy (Loubès et al. 1976; Loubès 1979). With the latter method, synaptonemal complexes, representing coupled meiotic chromosomes, have been reported from a number of microsporidia representing about 20 genera (Loubès 1979; Larsson 1986b). Synaptonemal complexes of microsporidia are similar to those of other eukaryotes. The complex is about 100 nm wide, with three parallel dark strands (Fig. 1.3h): two lateral elements and one central element. Perpendicularly to the longitudinal strands is a system of microfibrils.

It was originally thought that synaptonemal complexes appeared in the transition from merogony to sporogony in microsporidia shifting from diplokarya in merogony to monokaryon in the spore (Loubès et al. 1976; Loubès 1979). Synaptonemal complexes have also been reported from species with isolated nuclei in all life cycle stages, such as *Amphiamblys bhatiellae*

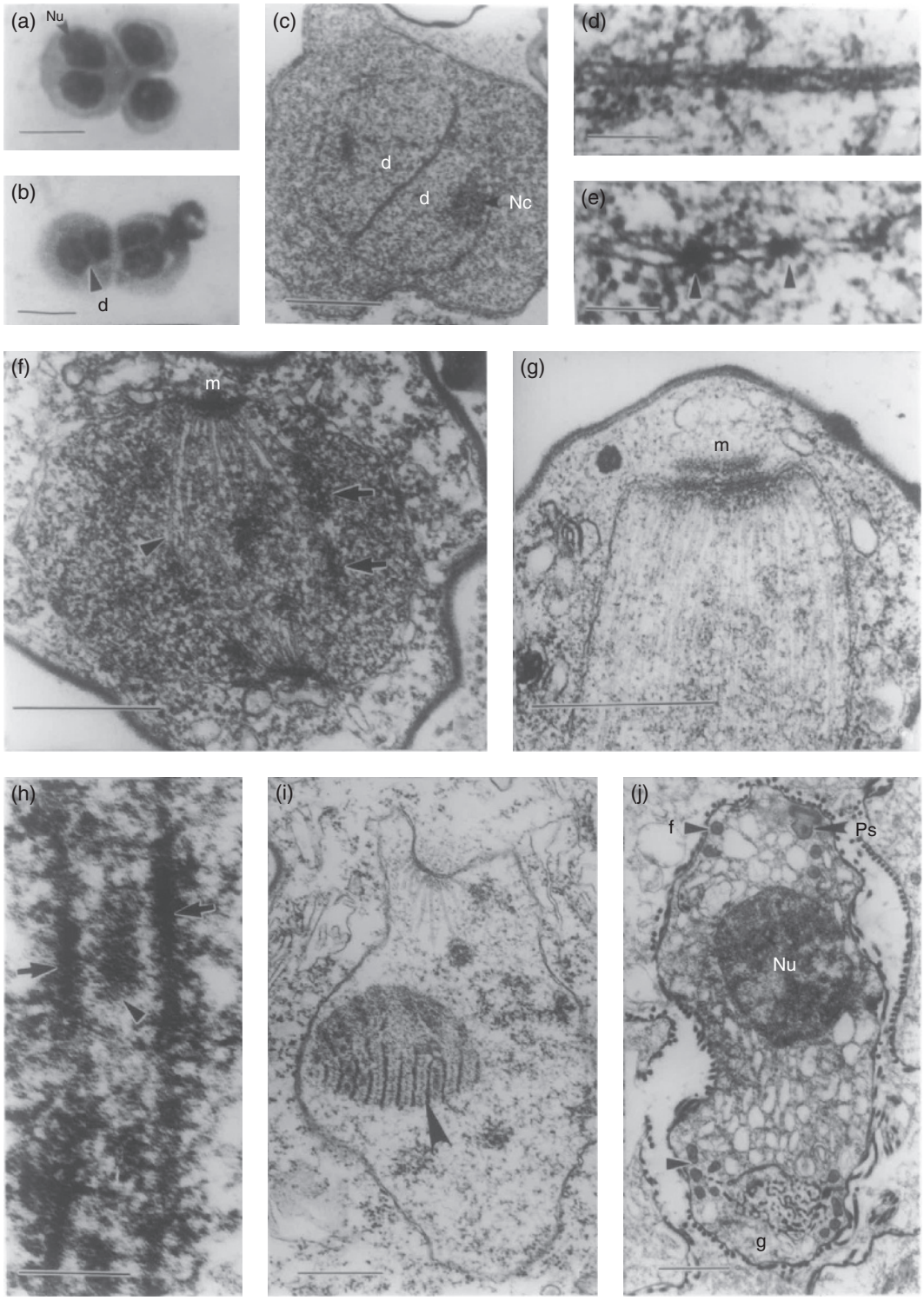

Figure 1.3 Cytology of early stages. (a) Monokaryotic meronts (*Berwaldia schaefernai*); (b) diplokaryotic sporonts (*Nosema tractabile*); (c–e) diplokaryotic sporont with details of the zone of nuclear apposition (d) and nuclear periphery (e) (arrowheads indicate nuclear pores) (*Helmichia aggregata*); (f) mitotic spindle exhibiting microtubules (arrowhead), spindle plaques, polar vesicles, and chromosomes (arrows) (*Toxoglugea variabilis*); (g) two-layered spindle plaque (*Hyalinocysta expilatoria*); (h) synaptonemal complex with lateral (arrows) and central (arrowhead) elements (*H. aggregata*); (i) synaptonemal polycomplex (arrowhead) (*Systenostrema alba*); (j) sporoblast exhibiting Golgi apparatus, primordial anchoring apparatus, and polar filament (*Janacekia debaisieuxi*). Giemsa stain (a, b), TEM (c–j). Scale bars = 1 µm (a–c, j), 100 nm (d, e, h), 0.5 µm (e, g, i). d, diplokaryon; f, polar filament; g, Golgi apparatus; m, mitotic spindle plaque; Nu, nucleus; Nc, nucleolus; Ps, polar sac; V, polar vesicle. Reprinted from Wittner, M., Weiss, L. M. (eds.) 1999. *The Microsporidia and Microsporidiosis*. ASM Press, Washington, DC.

(Ormières et al. 1981), and from species with diplokaryotic nuclei throughout, such as *Nosema rivulogammari* and *Paranosema grylli* (Larsson 1983b; Nassonova & Smirnov 2005). Of unknown significance are synaptonemal polycomplexes (Fig. 1.3i), observed in *Systenostrema tabani* and two other species of the same genus (Larsson 1988a, unpublished data). However, intranuclear dark material in parallel arrangement is not necessarily a synaptonemal complex, and all observations are not sufficiently documented.

Whether microsporidian meiosis is a special process, or if its course can be explained in conventional way, has been debated (Hurst 1993; Flegel & Pasharawipas 1995).

1.4.3 Mitosomes

Mitosomes are highly reduced mitochondrial remnants appearing as small (about 100–200 × 100 nm, sometimes even larger up to 500 nm) vesicles with double membranes, forming a small cluster of three to six members, close to the terminus of the nuclear spindle plaque. Some mitosomes occur also scattered in the cytoplasm (Williams et al. 2002, 2008; Vávra 2005) (Fig. 1.7c–e). In *Trachipleistophora hominis*, there are about 28 (7–47) mitosomes per cell (Williams et al. 2002). As mentioned earlier (Section 1.4.2.2), the mitosomes assembled near the spindle terminus were known as "polar vesicles" of unknown function (Vávra 1976a). For details of the physiological function of mitosomes, see Chapter 9 of the present volume.

1.4.4 Endoplasmic Reticulum

Very few membranous elements are present in early merogonial cells, but their number and order of arrangement increase as the life cycle proceeds toward sporogony (Fig. 1.3c and g and Fig. 1.6d and e). Some of the membranous elements belong to the rough endoplasmic reticulum (ER), as evidenced by their arrangement as parallel cisternae covered by ribosomes. Numerous single-membrane-covered vesicles with lucent interiors exist in microsporidian cells other than spores. Whether they belong to the smooth type of ER or if they are exocytic or endocytic vesicles cannot be determined with certainty.

1.4.5 Ribosomes

Ribosomes are a predominant component of the microsporidian cytoplasm. The large amount of these elements reveals a very high rate of protein synthesis which is also obvious from the high rate of reproduction. Within the first 48 h after the sporoplasm has reached the host cell, several rounds of division, and even spore formation, may occur (Vávra & Lukeš 2013).

In early developmental stages, ribosomes are dispersed mostly freely in the cytoplasm (Fig. 1.6d), while in late merogonial and in sporogonial stages, ribosomes attached to lamellae of the ER become prominent (Fig. 1.3c and g and Fig. 1.6e). In sporoblasts and young spores, polyribosomes, ribosomes arranged in a crystalline pattern, are frequently observed (Fig. 1.4).

Ribosomes of microsporidia express prokaryote-like properties, being of the 70S sedimentation type for the monosome with subunits of 50S and 30S. They also lack 5.8S rRNA and, as in prokaryotes, have a region corresponding to a part of the 5.8S rRNA in the large subunit (Ishihara & Hayashi 1968; Curgy et al. 1980; Vossbrinck & Woese 1986; Vávra & Lukeš 2013) (see also Chapters 6 and 9 of the present volume).

1.4.6 Golgi Apparatus

In one or several areas of the cytoplasm of presporal stages, accumulations of small opaque vesicles enclosed by a single membrane are present (Fig. 1.3j, Fig. 1.7a, and Fig. 1.8a). The vesicles form a meshwork in which the central components are smaller than the marginal ones. No ribosomes are present in the area of the vesicles (Vávra 1976a), which are actually embedded in a matrix having greater density than the surrounding cytoplasm. The area of vesicles was called a "primitive Golgi zone" by Vávra (1965), because it does not resemble the classical Golgi apparatus of eukaryotic cells, which is composed of stacked lamellar cisternae. The idea that microsporidia possess a structurally atypical, yet physiologically functional Golgi apparatus has originally been corroborated by histochemical detection of thiamine pyrophosphatase, which is specific for the transmembrane components of the Golgi apparatus (Takvorian & Cali 1994, 1996). Refined methods of transmission electron microscopy (TEM) finally recognized the microsporidian Golgi as a 300 nm network of thin, branching or varicose tubules (Beznoussenko et al. 2007; Takvorian et al. 2013). It is a general feature of the microsporidian Golgi apparatus that it becomes more prominent as development progresses toward the formation of spores. In late sporonts and in sporoblasts, this area occupies a progressively greater volume of the cell and assumes a central role in the elaboration of various spore organelles (Vávra 1976a) (Fig. 1.7a and Fig. 1.14a). Of interest is the recent histochemistry identification of both the cis- and the transmembrane enzymatic Golgi activity in a "multilayered interlaced network" (MIN), a membranous reticulum occurring in freshly extruded sporoplasms of *Anncaliia algerae* (Cali et al. 2002; Takvorian et al. 2005, 2013) (Fig. 1.32d and e).

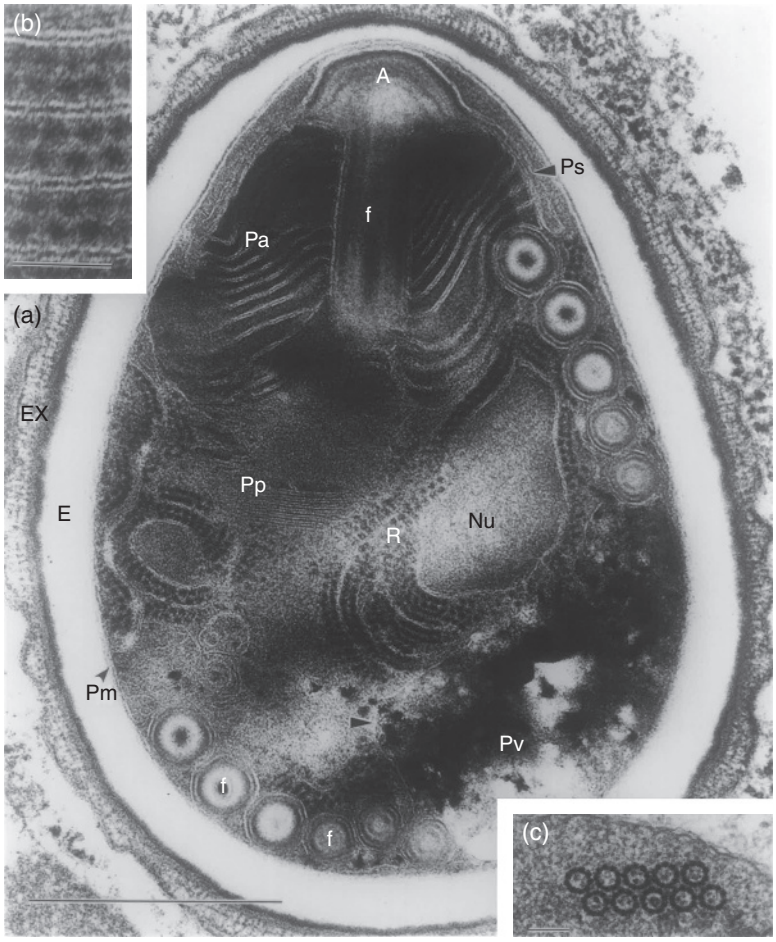

Figure 1.4 Ultrastructure of the mature spore. (a) Longitudinally sectioned spore exhibiting the characteristic organelles (arrowhead indicates vacuolar membrane) (*Episeptum inversum*); (b) polyribosomes attached to membranes (*Napamichum dispersus*); (c) circularly arranged polyribosomes (*Hamiltosporidium magnivora*). All images TEM. Scale bars = 0.5 µm (a); 100 nm (b, c). A, anchoring disk; E, endospore; EX, exospore; f, polar filament; Nu, nucleus; Pa, anterior polaroplast region; Pm, plasma membrane; Pp, posterior polaroplast region; Ps, polar sac; Pv, posterior vacuole; R, polyribosomes. Reprinted from Wittner, M., Weiss, L. M. (eds.) 1999. *The Microsporidia and Microsporidiosis*. ASM Press, Washington, DC.

1.5 STRUCTURE OF MICROSPORIDIAN DEVELOPMENTAL STAGES

When occurring together, merogonial stages can usually be distinguished from sporogonial stages under the light microscope, using a combination of characters like the size of the stages and of their nuclei, the density of the staining of the cytoplasm, and the presence of a membranous sachet (sporophorous vesicle (SPOV)) around spore packets, eventually revealed by grouped spores. However, the point of transition from merogony to sporogony, expressed by the appearance of spore wall material deposits on the plasma membrane of sporonts, is only visible with the use of electron microscopy.

1.5.1 The Spore

Microsporidian development starts and ends with a spore (Fig. 1.4a and Fig. 1.5a). The spore has a thick wall, with exospore and endospore layers outside the plasma membrane and a unique infection apparatus, composed of three parts: a long thread-like polar filament ("polar tube," "invasion tube," "injection tube"—see the following text), which is a multilayered structure; a polaroplast, which is a system of membrane-lined compartments, appearing as lamellae, sacs, or tubules in the anterior half of the spore; and a posterior vacuole close to the posterior pole of the spore (for details of the spore structure, see Section 1.6). As mentioned earlier (Section 1.3.4), many microsporidia produce two or more spore morphs, differing both in cytology and in germination characters (Vávra & Lukeš 2013) (see the following text for details).

Infection starts with the germination of the spore. The spore is triggered by an appropriate stimulus (see Chapter 10 of the present volume). The polar filament everts from the spore and during this process turns inside out, like the finger of a glove, and forms a tube through which the spore contents are expelled (Fig. 1.5c, Fig. 1.8g, and Fig. 1.29j). The structure was originally called a filament, for example, by Henneguy and Thélohan (1892), and as it will not be a functional tube until it is everted,

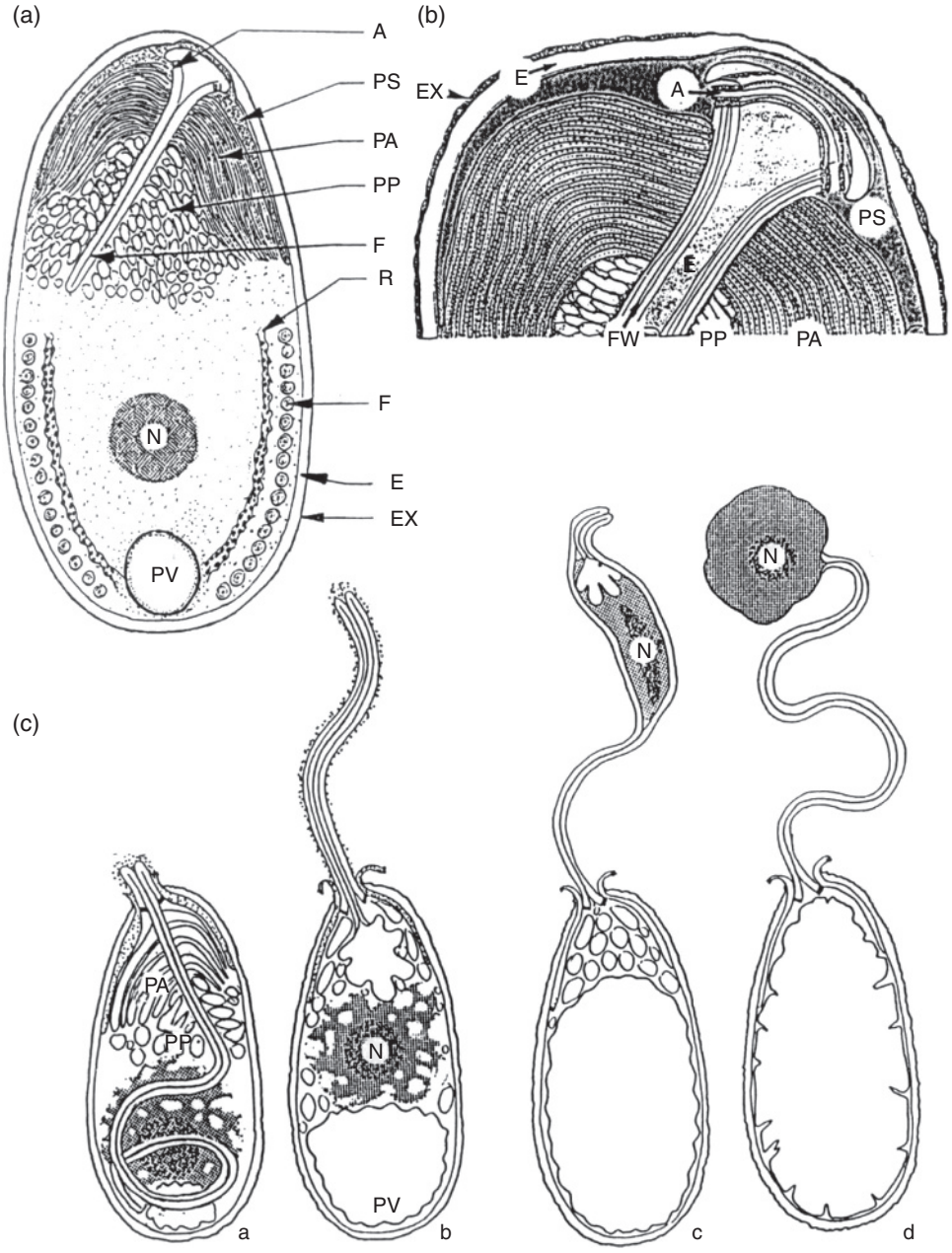

Figure 1.5 Schematic drawings of a microsporidian spore (a) and of the anterior part of the spore (b). (c) Schematic representation of the spore germination: polar filament eversion (a and b), passage of the spore contents (sporoplasm) through the lumen of the everted polar tube (c), and exit of the sporoplasm as a minute cell at the tip of the everted polar tube (d) (*Glugea atherinae*). A, anchoring disk; E, endospore; EX, exospore; F, polar filament; PW, polar filament wall; N, nucleus; PA, anterior (lamellar) polaroplast; PP, posterior (vesicular) polaroplast; PV, posterior vacuole; PS, polar sac; R, endoplasmic reticulum with (poly)ribosomes. Reprinted from Wittner, M., Weiss, L. M. (eds.) 1999. *The Microsporidia and Microsporidiosis*. ASM Press, Washington, DC.

Weidner distinguished between the two states by retaining the terminology polar filament for the condition inside the spore and used polar tube, or invasion tube, for the tubular ejected state (Weidner 1976a, 1982). Recently, Vávra and Lukeš (2013) termed the structure "injection tube," stressing thus the way in which the microsporidian infective cell is introduced into the host cell.

The polaroplast is active during the germination. It swells, resulting in increased volume of the intralamellar matrix and disturbed arrangement of the membranous lamellae, thereby increasing the turgor within the spore. It is responsible for the initial stage of polar filament evagination (Lom & Vávra 1963a). In the later stage of germination, when the infective cell, the sporoplasm, is being formed, the membranes of the polaroplast contribute the plasma membrane of the sporoplasm (Weidner et al. 1984). The nascent sporoplasm is nothing else than the cytoplasmic content of the spore (including the nucleus). When passing through the polar tube, it is enveloped by polaroplast membranes, drawn into the lumen of the tube together with other spore contents (see the following text).

The posterior vacuole expands during spore germination and pushes the spore contents into the developing polar tube (Fig. 1.5c). Spore germination is evidently an osmotic event even if its physical explanation remains unknown. Trehalose splitting into glucose and the concomitant increase in osmotic pressure were proposed as the propellant for spore germination (Undeen 1990; Undeen & Vander Meer 1994). Trehalose is present in microsporidian spores, and it seems that it serves rather as an energy store for the spore and as an antidessicant agent (Undeen & Solter 1996; Metenier & Vivarés 2001; Vávra & Lukeš 2013). After the spores have emptied their contents, most of the inner space is filled by the enormously expanded vacuole, which is enclosed by a wrinkled membrane. This membrane is apposed to the plasma membrane that subtends the endospore layer of the spore wall.

The spore content is injected through the polar tube into the cytoplasm of the host cell. It appears at the tip of the tube as a minute cell, the sporoplasm, with one nucleus in some species and with a diplokaryon in other species (Fig. 1.5c, Fig. 1.6a, and Fig. 1.8g). The sporoplasm remains connected to the tip of the extruded tube for a short while after extrusion (Weidner 1972) (Fig. 1.32d), but after a few seconds, it becomes detached from the tube which retracts by elasticity (Lom & Vávra 1963a). Freshly extruded sporoplasms were reported to be surrounded by two membranes. One of them, continuous with the outer sheath of the extruded tube, disappears quickly (Weidner 1972). The released sporoplasm has an external unit membrane, some vesicles, and a weakly developed ER with ribosomes and approximately equivalent to the cytoplasmic contents of the spore. As mentioned earlier (Section 1.4.6), an MIN of membranes with Golgi activity is present in freshly extruded sporoplasms of *Anncaliia algerae* (Cali et al. 2002; Takvorian et al. 2005, 2013) (Fig. 1.32d and e). Surplus membranous material similar to MIN may be of general occurrence in the sporoplasms (Fig. 1.6a).

1.5.2 Meronts and Merozoites

The sporoplasm injected from the spore into a suitable host cell matures into a meront which, after a period of growth and nuclear fission, divides into daughter cells, merozoites. Meronts and merozoites (Fig. 1.6b) are morphologically identical: rounded or slightly irregular cells covered by a unit membrane. They have from one to many nuclear components which, depending on species, occur as isolated nuclei or coupled as diplokarya. The cytoplasm is homogeneously granular with weakly developed or even nonexistent ER and numerous free ribosomes (Fig. 1.6d). There are one or several areas in which comparatively electron-dense Golgi vesicles are accumulated (Section 1.4.6). In Giemsa-stained light microscopic preparations, the cytoplasm of meronts and merozoites is less densely stained than the sporoplasm, and the nuclei are larger and more distinct.

If several bouts of merogony occur, the increase in lamellae of ribosome-covered ER is the only difference between successive merogonial generations.

At the end of merogony, patches of electron-dense material are deposited on the external face of the plasma membrane (Fig. 1.6f–h). Secretion of this material is the ultrastructural evidence of the parasite entering the sporogonial phase of reproduction. When the cells are covered by the electron-dense material, they are classified as sporonts, the initial stage of sporogony. The trigger for the switch from merogony to sporogony is not known. Obviously, after a microsporidian cell has entered sporogony, it cannot revert to merogony.

1.5.3 Sporogony

Sporogony involves divisions of the sporont and of its daughter cells until formation of the final division product: the sporoblast (Fig. 1.3j, Fig. 1.24a, Fig. 1.25c, Fig. 1.26f, Fig. 1.27f, and Fig. 1.30e). This stage matures and transforms into a spore. Depending on the microsporidian species, the number of sporont divisions varies from one, bisporous sporogony, in which two sporoblasts are formed, to many, polysporous sporogony. In some species, the sporogony yields a regular number of spores, often 4, 8, or 16, with 8 spores being the most frequent number (octosporous sporogony). Bisporous sporogony proceeds as simple binary fission, and polysporous sporogony can proceed in different ways: plasmotomy, schizogony, or vacuolation. Sporogony can take place in direct contact with the cytoplasm of the host cell, open sporogony, or inside an envelope of microsporidian origin, closed sporogony.

In a stained smear viewed under the light microscope, sporogonial stages are usually less intensely stained than merogonial stages, and their nuclei are smaller (Fig. 1.6b and c). In ultrathin sections, the cytoplasm is less electron dense and less packed with free ribosomes but contains more membranous elements in the form of vesicles and cisternae of rough ER. The cisternae are characteristically arranged in concentrical layers around the nucleus (Fig. 1.6e). The cluster of small vesicles representing the Golgi apparatus becomes more prominent in the sporont.

1.5.3.1 The Electron-Dense Material on the Sporont Surface

The appearance and progressive accumulation of electron-dense material on the outer face of the plasma membrane of the sporont (Fig. 1.6e–h) indicate that the microsporidian cell is entering sporogony. Depending on the species, this material has the potential to develop in one of three directions.

1. It may immediately become the primordium of the exospore layer of the spore wall, which occurs frequently. The dense material on the sporont plasma membrane gradually covers the cell as a uniform layer, which divides with the parasite

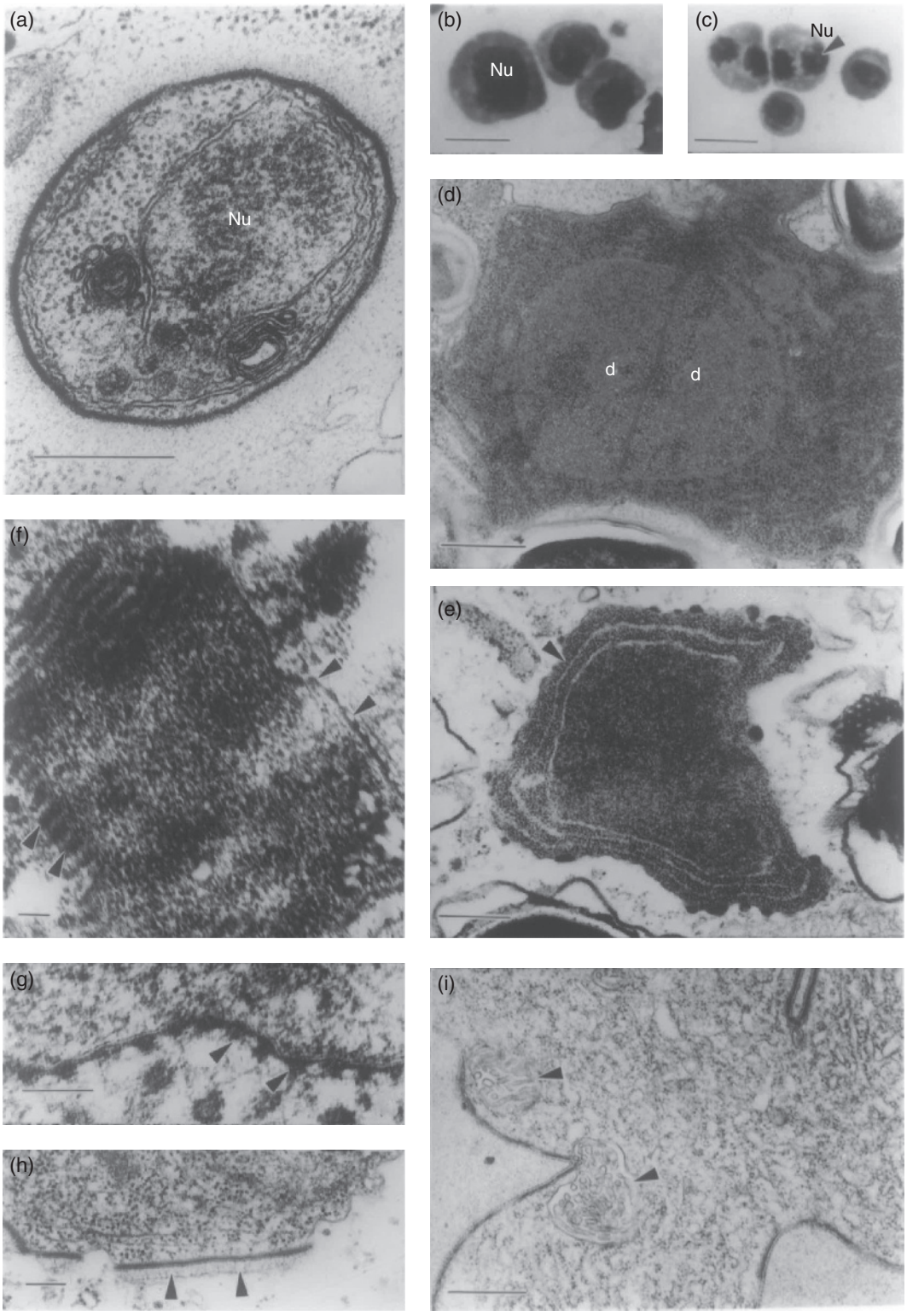

Figure 1.6 From sporoplasm to early sporogony. (a) Sporoplasm (*Ameson michaelis*); (b, c) meronts and sporonts (*Berwaldia schaefernai*); (d) diplokaryotic meront (*Helmichia aggregata*); (e) sporont with electron-dense material (arrowheads) accumulating spotwise (arrowhead indicates concentric layers of endoplasmic reticulum) (*B. schaefernai*); (f, g) strandlike initiation of the exospore (arrowheads) (*Nosema tractabile*); (h) wide initiation of the exospore (arrowheads) (*Episeptum inversum*); (i) paramural bodies (arrowheads) (*Microsporidium* sp. ex *Daphnia longispina*). All images TEM (a, d–i), Giemsa stain (b, c). Scale bars = 1 µm (b, c, i), 0.5 µm (a, d, e), 100 nm (f–h). d, diplokaryon; Nu, nucleus. Reprinted from Wittner, M., Weiss, L. M. (eds.) 1999. *The Microsporidia and Microsporidiosis*. ASM Press, Washington, DC.

and becomes the spore wall. The wall material is in direct contact with the cytoplasm matrix of the host cell in open sporogony. The first signs of a future exospore layer look differently depending on species. In *Encephalitozoon cuniculi* (Barker 1975), *Nosema tractabile* (Larsson 1981c), and *Unikaryon slaptonleyi* (Canning et al. 1983), the primordial exospore material is laid down as uniform electron-dense strands in a parallel arrangement (Fig. 1.6f and g). More commonly, the material is spread from a few foci over wide surface areas (Fig. 1.6h). Either the exospore primordium grows into an exospore of uniform electron-dense material (Fig. 1.9a), as, for example, in *Loma fontinalis* (Morrison & Sprague 1981), or it develops into layers of different electron density and thickness (Fig. 1.9b and c). In some microsporidia, the electron-dense material envelopes and couples two spores (Fig. 1.1l) (Codreanu & Vávra 1970; Larsson 1981a; Vávra 1984) (see Section 1.6.1).

2. It may form a thin, membranous sac, a SPOV, enclosing the sporont and its division products, including spores (Fig. 1.28c, and Fig. 1.29b, e, g, and h). In this case, the exospore is formed secondarily from a second production of electron-dense material. This mode also occurs frequently (see Section 1.7.1).
3. It may form a cyst-like envelope together with the plasma membrane, a sporont-derived sac (Fig. 1.20). The electron-dense material of the spore wall is formed secondarily. This is the most unusual fate of the dense material (see Section 1.7.3).

Aberrant Sporonts

There are two situations where electron-dense surface material does not indicate the sporont stage. In microsporidia of the family Pleistophoridae (*Pleistophora*, *Trachipleistophora*, and *Vavraia*), the dense surface material is produced already by the meront, generating a merontogenetic SPOV enclosing the sporont (Fig. 1.18g and Fig. 1.28a). On the contrary, there are also a few microsporidia, for example, *Enterocytozoon bieneusi*, with a delayed production of a small amount of electron-dense material. Their sporogonial plasmodia have little or no reinforcement of the plasma membrane until the moment when the sporoblasts are formed (Cali & Owen 1990) (Fig. 1.22, Fig. 1.23, and Fig. 1.24). Molecular biology reveals that some of the genes involved in spore wall material synthesis are activated well before this material is microscopically visible on the surface of the sporont (Taupin et al. 2006; Vávra & Lukeš 2013).

1.5.3.2 Paramural Bodies

When a multinucleate sporogonial stage divides into unicellular daughter cells, cell separation is achieved by formation of grooves in the plasmodium which deepen progressively until complete separation of daughter cells is achieved. The electron-dense material on the surface of the sporogonial plasmodium does not cover the bottom of the groove. At this site, the plasma membrane is sometimes folded like a whorl (Fig. 1.6i). It probably represents the site where more plasma membrane material, required to cover the increasing cell surface, is being formed. The membranous whorl was originally called a scindosome ("a body occurring at a cleaving site") (Vávra 1975, 1976a), but this name was later replaced by paramural body ("a body occurring close to the wall") because it resembles structurally and probably also functionally similar structures in fungi (Vávra 1976c).

1.5.4 The Sporoblast

The transformation of the sporont to sporoblasts is a continuous process during which the nuclei divide, electron-dense material accumulates on the plasma membrane to form a thick, continuous surface cover, and the extrusion apparatus starts to develop. The sporoblast is the cell which gradually assumes the shape of the spore and continues to build the wall of the future spore. The specific organelles of the spore start to assume their final form in the sporoblast (Fig. 1.3j and Fig. 1.25). In ultrastructural studies, technical problems make young sporoblasts appear as wrinkled cells of considerable electron density in which it is difficult to observe the organelles. The wrinkling at a certain stage of sporoblast maturation is probably due to the increased osmotic sensitivity of the cell. The sporoblast is enclosed by a plasma membrane covered by an almost continuous layer of electron-dense material which will develop into the exospore layer of the future spore. In microsporidia with a closed type of sporogony, this layer frequently forms tubular or fibrillar expansions protruding from the surface of the sporoblast. Even if the transition from sporoblast to spore is a continuous process, for terminological reasons, it is useful to agree on a point at which a cell is no longer called a sporoblast but a spore. Larsson (1986b) considers polarization of a cell the turning point: after the cell initiates polarization (cell organelles are no longer randomly distributed), it is designated a spore.

1.5.5 The Origin of the Extrusion Apparatus

The formation of the extrusion apparatus, which is a synapomorphic structure of microsporidia, usually begins at the sporoblast stage. It is universally agreed that the Golgi apparatus is the organelle forming the individual parts of the extrusion apparatus (Fig. 1.3j and Fig. 1.7a).

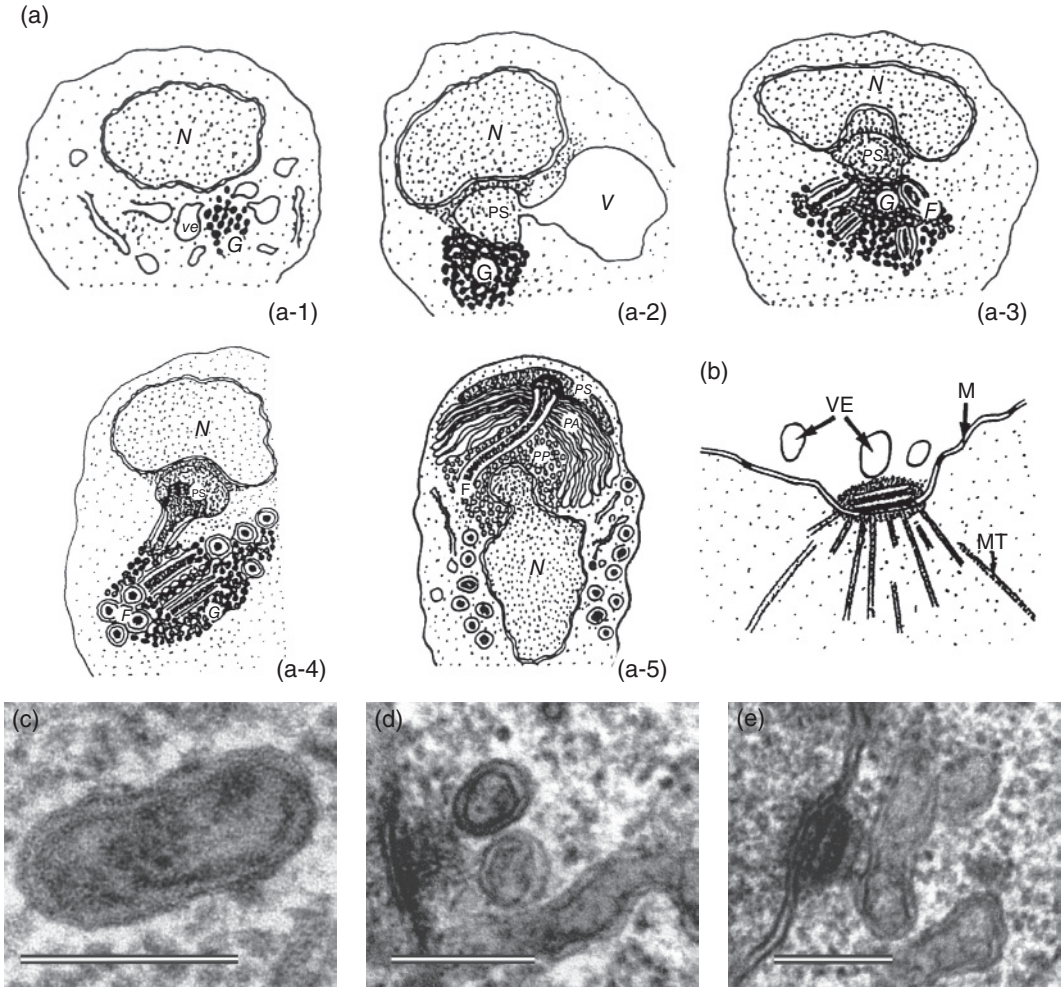

Figure 1.7 (a) Schematic representation of the development of the extrusion apparatus during sporont-to-spore transition (*Nosemoides vivieri*). (a-1) A small vacuole (ve) and Golgi vesicles (G) assemble close to the nucleus; (a-2) the polar sac (PS) primordium and a large vacuole appear close to the nucleus, and the Golgi vesicles (G) abut the PS; (a-3) coils of the polar filament (F) start to form by coalescence of Golgi vesicles; (a-4) the polar sac and polar filament material start to be organized into layers; (a-5) the polar sac migrates toward the tip of the forming spore and the polaroplast with anterior (PA) and posterior (PP) parts appears. (b) Schematic representation of the spindle plaque of microsporidia (*Glugea atherinae*). The plaque, which is the organizing center of the mitotic microtubules, is situated in a depression of the nuclear membrane (M), and it consists of a stack of flattened electron-lucent vesicles surrounded by dense granular material from which microtubules (MT) radiate. Several "polar vesicles" (mitosomes) (VE) are situated close to the plaque on its cytoplasmic side. (c–e) mitosomes: an isolated mitosome (c), and a group of mitosomes close to the spindle plaque (d, e) (*Vavraia culicis*). Scale bars = 200 nm. Reprinted from Wittner, M., Weiss, L. M. (eds.) 1999. *The Microsporidia and Microsporidiosis*. ASM Press, Washington, DC (a, b), Vávra, Folia Parasitologica 2005 (c–e).

The first traces of the extrusion apparatus may appear as dilated distal ends of the tubular vesicles of the ER, containing electron-dense material. This material is probably exported to the Golgi apparatus, and by fusion of its vesicles, the extrusion apparatus is generated (Fig. 1.7a and Fig. 1.8a).

1.5.5.1 The Polar Filament

The first traces of the future polar filament appear in some cases in life cycle stages preceding the sporoblasts (Fig. 1.7a). The first sign is an accumulation of electron-dense Golgi vesicles in an area immediately adjacent to the nucleus (Fig. 1.7a-1). Next, a small, round vacuole containing some dense granular material appears at the same site. The vacuole is surrounded at most of its circumference by a unit membrane, but the remaining part, not covered by the membrane, is in direct contact with a large reticulum of anastomosing Golgi vesicles. The vacuole represents the future polar sac (Vinckier 1973, 1975, 1990; Vávra 1976a) (Fig. 1.7a-2). The polar filament appears initially as rings with thick, dense borders and a dark center situated at the edge of the Golgi reticulum. These rings are in fact cross sections of a coiled tube (Fig. 1.7a-3). The outer limiting border (a membrane?) of the tube is continuous with the vacuole borders, and the central dense material of the tube penetrates for some distance into the polar sac. This penetrating material is the primordium of the anchoring disk (Fig. 1.7a-4). The reticulum of the Golgi vesicles is progressively displaced away from the nucleus toward the future posterior end of the spore, and during this process, more filament coils are formed at its edges (Fig. 1.7a-4 and a-5). When the Golgi vesicular reticulum

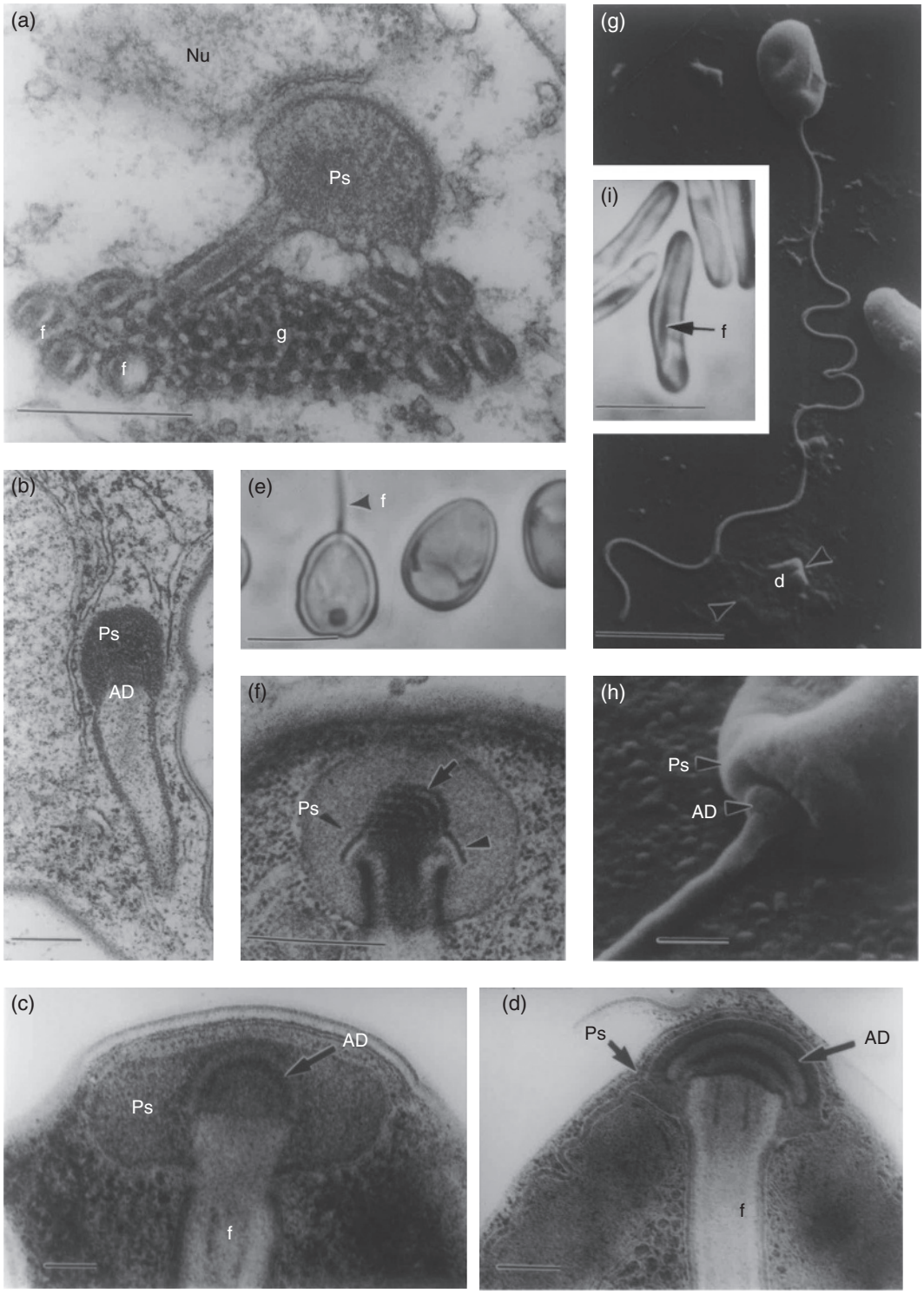

Figure 1.8 Initiation of the extrusion apparatus and ejection. (a) Initiation of the polar filament and polar sac, note the close association of the sac with the nucleus (*Nosemoides vivieri*). (b–d) Polar sac and anchoring disk in the sporoblast (b), immature spore (c), and mature spore (d). *Systenostrema alba*; (c) *S. candida*. (e) Polar filament in situ in one spore and ejected in the other (*Amblyospora* sp. ex *Aedes* sp.). (f) Polar sac and anchoring disk during formation (*Amblyospora culicis*). Note the layering of the developing anchoring disk (arrow) and the presence of layered material to which the walls of the polar filament (arrowhead) abut. This structure serves as a "hinge" and turns inside up during filament eversion. (g) Extruded polar tube and ejected sporoplasm (arrowhead) (*Nosema tractabile*). (h) Details of the anterior pole of the spore, the polar sac, and the penetrated anchoring disk are visible (*N. tractabile*). (i) Polar filament of the manubrium type (*Mrazekia cyclopis*). TEM (a–d, f) TEM; phase contrast (e); SEM (g and h); fresh, unstained (i). Scale bars = 0.5 µm (a, f), 25 nm (b), 100 nm (c, d), 5 µm (e, g, i), 0.5 µm (h). AD, anchoring disk; d, diplokaryon; f, polar filament; g, Golgi apparatus; Nu, nucleus; Pa, anterior polaroplast; Ps, polar sac. Reprinted from Wittner, M., Weiss, L. M. (eds.) 1999. *The Microsporidia and Microsporidiosis*. ASM Press, Washington, DC.

reaches the posterior end of the future spore, a vacuolar space appears there with the remnants of the reticulum inside. This mode of formation was confirmed by the freeze-fracture technique (Vinckier 1990; Vinckier et al. 1993). The Golgi apparatus at this time is a large, spongiform structure occupying a considerable part of the cell volume (Fig. 1.14a).

1.5.5.2 The Polaroplast

Because the polaroplast is a delicate membranous structure, the earliest signs of its appearance are easily overlooked. There are divergent opinions about its origin, and it is possible that the time and mode of initiation vary among different microsporidia. In any case, there is a close association between the polaroplast and the polar filament, which has led to speculation that both these organelles are parts of the same polar filament–polaroplast membrane complex (Lom & Corliss 1967). One mode of formation presumes that the polaroplast lamellae originate from progressive infolding of the membrane surrounding the vacuole, which occurs in some microsporidia (e.g., *Nosemoides vivieri*) (Vinckier 1973, 1975) close to the nucleus during polar sac and polar filament formation (Vávra 1976a) (Fig. 1.7a-2 and a-3). Other observations, for example, from *Amblyospora culicis* (Toguebaye & Marchand 1986) and *Bacillidium criodrili* (Larsson 1994a), suggest that the polaroplast is initiated at a later stage in the maturing sporoblast (Fig. 1.8b–d). The primordia of the polaroplast are small, membrane-lined protuberances from the unit membrane cover of the filament which are first seen in the proximity of the polar sac. They widen to become membrane-lined sacs, new compartments are added in posterior direction, and finally the compartments become packed in various arrangements.

1.5.5.3 The Posterior Vacuole

The posterior vacuole is not fully formed until the spore is mature (Fig. 1.4 and Fig. 1.5a). Its primordium appears in late sporoblasts in the form of a meshwork of vesicles and tubules of the Golgi apparatus located in the area where the vacuole later appears (Vinckier 1975). Remnants of the meshwork appear as an inclusion body, the posterosome, in the posterior vacuole of young spores of some microsporidia (Weiser & Žižka 1974, 1975). The posterosome is stained intensely red using Giemsa stain, and it is easily mistaken for a nucleus by an inexperienced observer.

1.6 THE MATURE SPORE

Shape and size are important structural characters, as they tend to be rather constant and characteristic of respective genera and species, but possible polymorphism and alternation of hosts must be considered (Section 1.3.4). Shape and size are best evaluated using a light microscope, but to be able to correctly evaluate the construction of the spore, it is necessary to make ultrathin sections and examine them by TEM. A longitudinal section taken through the center of the spore reveals a unique, complex organization, the principal parts of which are treated in greater detail under separate headings.

1.6.1 Spore Shape

The spore shape (Fig. 1.1) is more or less constant for all species of a genus. Spores are most commonly oval, as in the genera *Enterocytozoon* (Fig. 1.22d and Fig. 1.24c) and *Nosema* (Fig. 1.1o), or pyriform, as in *Marssoniella* (Fig. 1.1m) and *Agglomerata*. Spherical spores are, for example, found in the genera *Pilosporella* and *Chytridiopsis*, and rodlike spores are characteristic of several genera. Spores of *Bacillidium*, *Helmichia*, and *Mrazekia* are stout rods (Fig. 1.1d, Fig. 1.8i, and Fig. 1.11c–e) (Vávra 1962; Larsson 1982; Larsson et al. 1993), *Cylindrospora* spores are slender rods (Larsson 1986c), and the spores of *Nadelspora* are almost filiform (Olson et al. 1994). Some genera produce spores of unique or nearly unique shape for the genus. The spores of *Toxoglugea* (Fig. 1.1b) and *Toxospora* are bent like horseshoes, *Campanulospora* spores are bell-shaped, and *Paraepiseptum* (formerly *Cougourdella*) spores are lageniform (Fig. 1.1e).

In some microsporidian genera, spores are joined in pairs, completely embedded in an amorphous substance as in *Telomyxa glugeiformis* (Fig. 1.17g–j), or cemented together by patches of electron-dense material as in *Berwaldia singularis* (Larsson 1981b), *Norlevinea daphniae* (Fig. 1.1l) (Vávra 1984), and *Microsporidium fluviatilis* (Voronin 1994). In *Telomyxa*, the coupling is so intimate that electron microscopy was needed to show that the body interpreted as the spore of *Telomyxa*, originally described in 1910, actually is a couple of spores (Codreanu & Vávra 1970).

1.6.2 Spore Size

Most commonly, all spores produced belong to the same size class, but a number of genera produce a small number of macrospores together with the more common microspores (Fig. 1.17f). This sporogony is characteristic of the polysporoblastic genera *Pleistophora* (Canning & Nicholas 1980) and *Vavraia* (Larsson 1986d) and is also frequently observed in *Amblyospora* (Hazard & Oldacre 1975). *Hyalinocysta expilatoria* produces spores of three size classes: octosporous microspores, tetraspores of intermediate size, and diplospores of the largest size class (Larsson 1983c). *Kneallhazia* (formerly *Thelohania*)

solenopsae forms four structurally distinctive (size included) spore types in various life cycle stages and tissues of its host, the fire ant *Solenopsis*. Diplokaryotic spores develop only in brood, octospores and *Nosema*-like diplokaryotic spores occur in adults, and megaspores occur in various larval and pupal tissues and gonadal tissues of adults (Sokolova & Fuxa 2008).

1.6.3 The Spore Wall

The spore wall is built in such a way that for some time it withstands osmotic pressure during spore germination but ruptures at a certain moment. The rupture occurs at the spore apex where the spore wall is thin, creating an exit for the polar tube. The wall consists of two layers externally to the plasma membrane.

1.6.3.1 The Exospore

The exospore is the surface layer (Fig. 1.4 and Fig. 1.9). It is electron dense and forms a coat of uniform thickness all around the spore. Its thickness and construction vary in different microsporidia from a thin, dense, unstratified layer about 10 nm to a complex, multilayered structure about 200 nm thick (Larsson 1986b).

High resolution by TEM must be used in order to evaluate the exospore structure. For example, in the genus *Encephalitozoon*, the exospore has been described as a homogeneous layer (Barker 1975), but high resolution shows that it actually consists of three layers of different electron density and structure (Bigliardi et al. 1996). Freeze fracture of the exospore of *Amblyospora* species shows it as a granulofibrillar stratum in which short, coarse fibers are scattered among abundant granules (Vávra et al. 1986) (Fig. 1.10a). Bigliardi et al. (1996) recognized in freeze-fractured and freeze-etched exospores of *Encephalitozoon hellem* two layers in which 4-nm fibrils were arranged in different spatial orientations. The fine structure of the exospore is evidently worthy of more attention by researchers as it could be used in taxonomy: the

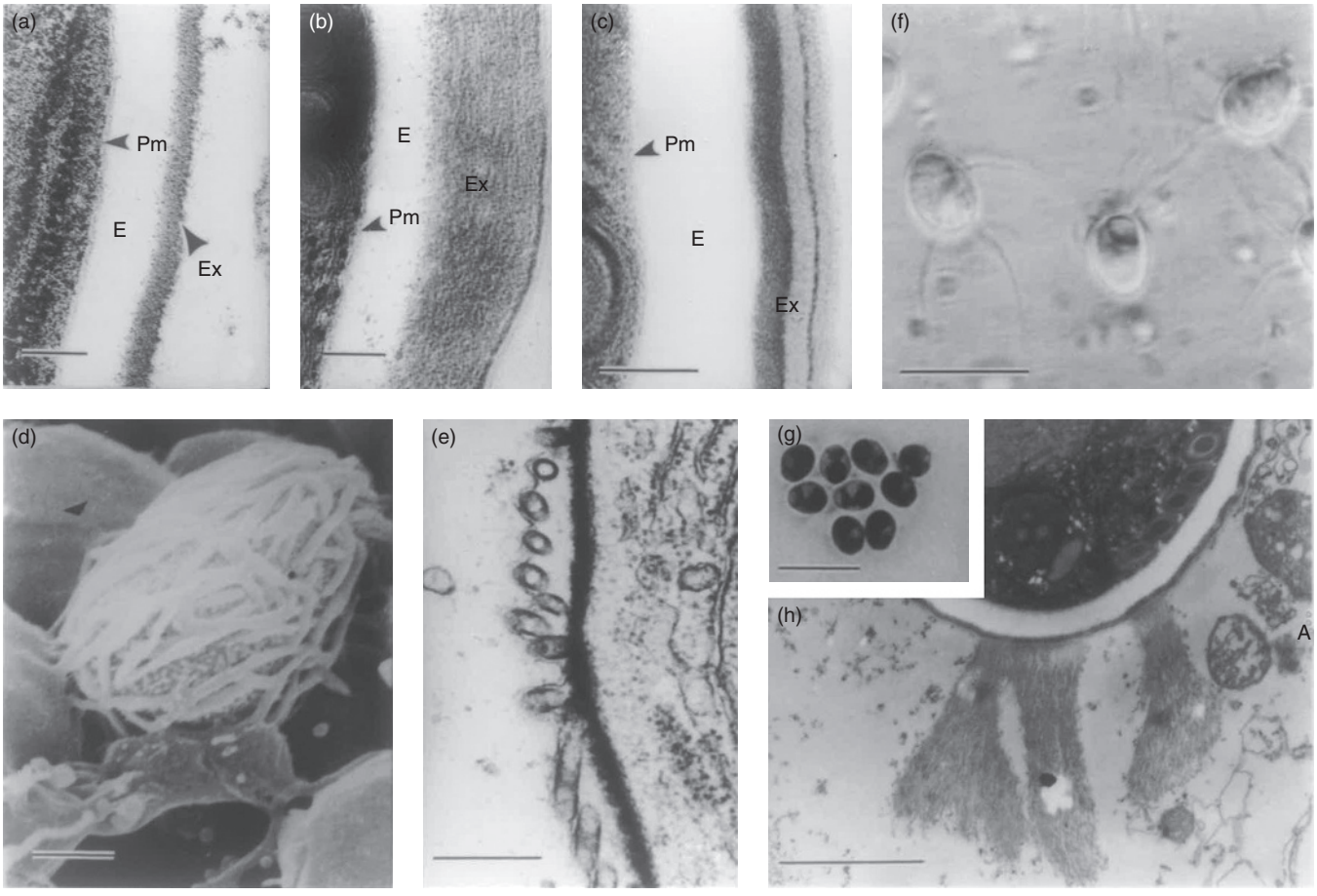

Figure 1.9 The spore wall. (a) Uniform exospore (free spore) (*Amblyospora callosa*); (b) spore wall of the *Amblyospora* type (octospore) (*A. callosa*); (c) layered exospore (*Napamichum dispersus*); (d, e) exospore with tubular projections (*Janacekia debaisieuxi*); (f–h) exospore with filamentous projections invisible in stained smears (g) (*Trichoctosporea pygopellita*). All images TEM (a–c, e, h), SEM (d), interference phase contrast (f), Giemsa stain (g). Scale bars = 100 nm (a–c), 1 µm (d), 0.5 µm (e), 10 µm (f–h). E, endospore; EX, exospore; Pm, plasma membrane. Reprinted from Wittner, M., Weiss, L. M. (eds.) 1999. *The Microsporidia and Microsporidiosis*. ASM Press, Washington, DC.

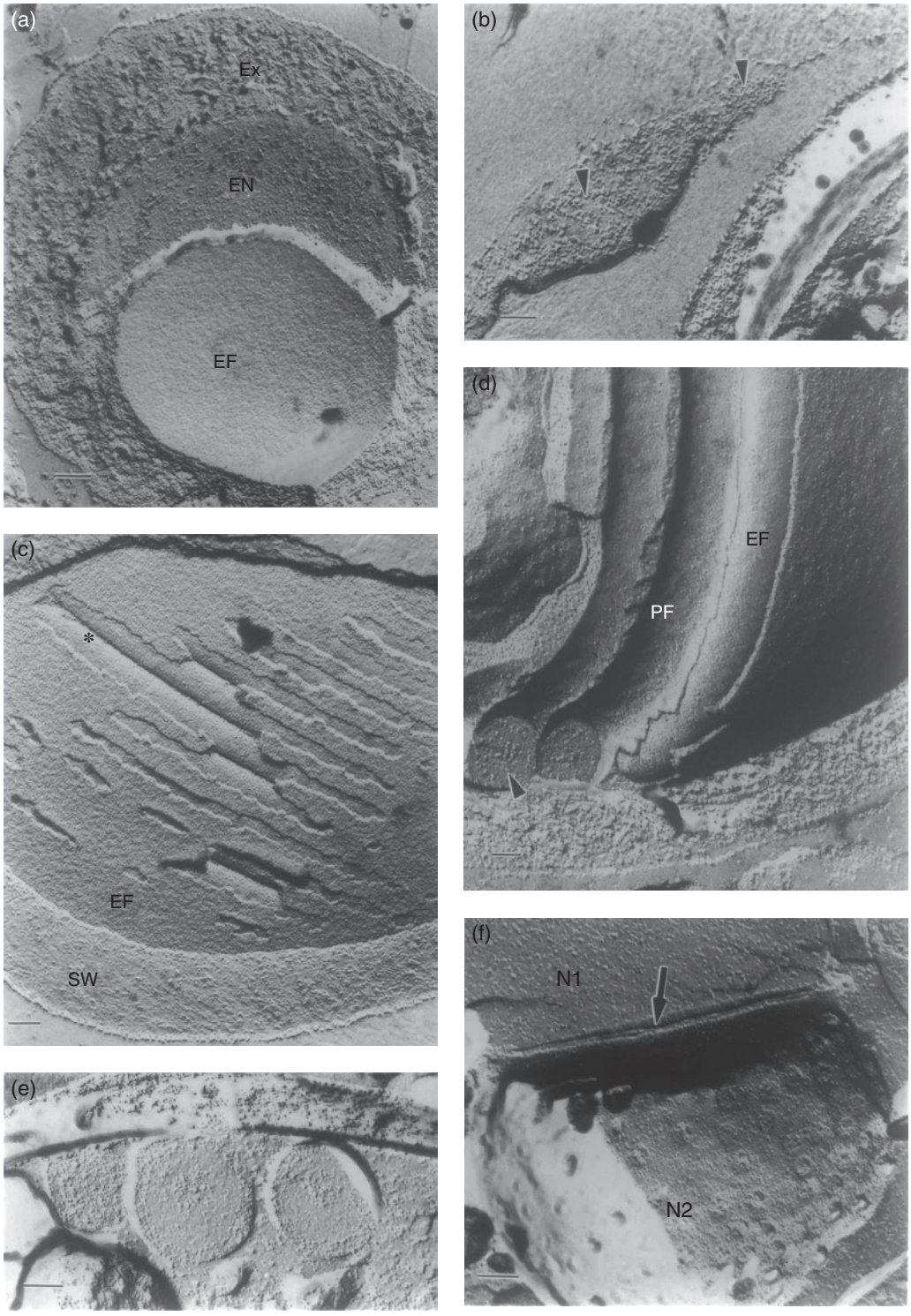

Figure 1.10 Freeze-fracture images of microsporidian spores. (a) Tangentially fractured spore wall of *Amblyospora opacita*, showing the ectoplasmic face of the plasma membrane, the endospore with fibers, and the exospore with coarse fibers and granules. (b) Fracture through the SPOV membrane of *A. opacita* (arrowheads), showing irregular granular structure demonstrating that it is not a cytomembrane. (c) Tangential fracture through an immature spore of a *Tuzetia* species, showing the ectoplasmic face of the plasma membrane covered with intramembranous particles (IP) and intramembranous particles on the ectoplasmic face of the unit membrane enveloping the polar filament (asterisk). (d) Fractured spore of *Amblyospora varians*, showing cross-fractured polar filament coils (arrowhead) and the protoplasmic and ectoplasmic faces of the unit membrane ensheathing the polar filament. In mature spores, the hemimembranes of the filament are nearly devoid of intramembranous particles. (e) Cross-fractured polar filament. Note that it appears to be solid with an outer ring and a central spot of fine particles. (f) Fractured diplokaryon of *Ambylospora bracteata*. One nucleus (N1) is cross-fractured. The second nucleus (N2) shows pores in the nuclear membrane. Arrow indicates the apposed nuclear membranes. Scale bars = 100 nm. EN, endospore; Ex, exospore; N, nucleus, SW, spore wall; BF and PF, ectoplasmic and protoplasmic faces of a split unit membrane. Reprinted from Wittner, M., Weiss, L. M. (eds.) 1999. *The Microsporidia and Microsporidiosis*. ASM Press, Washington, DC.

presence of a multilayered exospore was one of the arguments for the differentiation of *Nosema locustae* from other *Nosema* species, and the creation of a new genus *Antonospora* (now *Paranosema*) (Slamovits et al. 2004). The chemical composition of the exospore is proteinaceous, and a number of microsporidia-specific proteins were recently characterized in exospores of various microsporidia (Vávra & Lukeš 2013) (see Chapter 10 of the present volume).

The exospore of some microsporidia differentiates rapidly, while in others, it becomes more complex through a series of stages to attain its final structure in the mature spore. The sequence of layers is a useful tool in the identification of microsporidia (Larsson 1986b). A number of genera have exospores of a unique type, such as *Napamichum* (Fig. 1.9c) and *Episeptum* (Fig. 1.4a) (Larsson 1986e, 1996). The ultrastructure of the exospore is probably an indicator of relationships. For example, in the genera of Thelohaniidae and Amblyosporidae, the exospore of one of the spores types (the octospore) typically has a basic sequence of layers, one of the intermediate layers resembling a double membrane. In addition, each genus might have more or less complex specific layering (Fig. 1.9b and c). The genera of the family Mrazekiidae share an exospore having a wide, uniform basal layer and an external double-membrane-like stratum (Fig. 1.11 and Fig. 1.20a–c). In microsporidia from aquatic hosts, the exospore frequently forms ornamentations in the form of appendages, fibers, spore tails, etc. (Vávra 1963), resulting in exospores of a unique type for the genus. The exospore of *Caudospora* spp. is enormously hypertrophied and forms a winglike and a taillike expansion, giving the spore the appearance of a human sperm, visible in light microscopic preparations (Fig. 1.1h). The often long tails of *Jirovecia* spp. are also distinct using light microscopy (Lom 1953; Larsson 1989b, 1990b). Tubular exospore projections make the spores of the genera *Hirsutosporos* and *Inodosporus* easy to identify. In *Hirsutosporos*, the tubular projections form a girdle and a posterior tuft (Batson 1983), whereas in *Inodosporus*, they are arranged as a small anterior fork and three or four long posterior appendages (Overstreet & Weidner 1974). The filamentous spore projections of *Trichoctosporea pygopellita* are visible using interference phase-contrast optics but are invisible with other light microscopic techniques (Fig. 1.9f–h). They are best observed by TEM, as are the tubular exospore projections of *Janacekia* spores (Vávra 1965; Loubès & Maurand 1976; Rausch & Grunewald 1980) (Fig. 1.9d and e). To this category belong the mucus-like envelopes which are present on the spores of some aquatic microsporidia. When the spore comes in contact with water, the mucus-like material swells making the spores buoyant (Lom & Vávra 1963b). The presence of a mucous layer is revealed under the light microscope by mixing spores in a suspension with India ink (see Section 1.11.3.5) (Fig. 1.1m). In negative-stained TEM preparations, the mucus has a fine, fibrous structure (Vávra 1976a).

1.6.3.2 The Endospore

The endospore is electron transparent and hence appears as a structureless layer below the exospore (Fig. 1.4 and Fig. 1.9). This layer is up to 100 nm thick. The thickness is uniform except at the apex of the spore, where it is considerably narrower, often half the size or less. In freeze-fracture preparations, the endospore of *Amblyospora* species is granulofibrillar with short fibers most commonly oriented parallel to the spore surface (Vávra et al. 1986) (Fig. 1.10a). The material of the endospore is α-chitin, confirmed by staining reactions and physical analyses using infrared spectroscopy and X-ray diffraction (reviewed in Vávra 1976a). The presence of chitin can be utilized for fluorescent detection of microsporidia (Vávra & Chalupský 1982; Van Gool et al. 1993; Vávra et al. 1993a) (for details, see Section 1.11.2.3).

The endospore is formed late during spore maturation, and the layer grows until the spore is completely mature. The late completion of the endospore is probably a consequence of the fact that it seals the spore, separating the microsporidium from the surrounding host cytoplasm on which it is metabolically dependent until the spore matures.

1.6.4 The Plasma Membrane

The internal surface of the endospore is lined with the plasma membrane (Fig. 1.4 and Fig. 1.9a–c). This membrane delimits the cytoplasmic contents of the spore against the wall and is usually considered part of it because it remains in situ in the emptied spore (Lom 1972; Weidner 1972; Undeen & Frixione 1991). The sporoplasm acquires a new plasma membrane (believed to be derived from the polaroplast) when it leaves the spore.

Freeze fracture reveals the plasma membrane to be a classical cytomembrane containing intramembranous particles (Vávra et al. 1986; Bigliardi et al. 1996). These particles are very numerous in young spores but have nearly disappeared in mature spores. The intramembranous particles are interpreted as transport proteins which can be expected to decrease during spore maturation (Vávra et al. 1986) (Fig. 1.10a and c; Fig. 1.14d).

It must be stressed that the microsporidian spore is a single cell. The only plasma membrane present in the spore is the membrane that delimits the spore cytoplasm from the spore wall. There is no membrane-delimited "germ" inside the spore.

1.6.5 The Nucleus

One or two typical eukaryotic nuclei are found in the center of the spore (Fig. 1.4 and Fig. 1.15a). In spores with double nuclei, they are coupled as diplokarya (Fig. 1.11) with one exception. In the binucleate spores of *Binucleospora elongata*, each nucleus is enveloped in multiple membranes, disturbing the normal diplokaryotic association

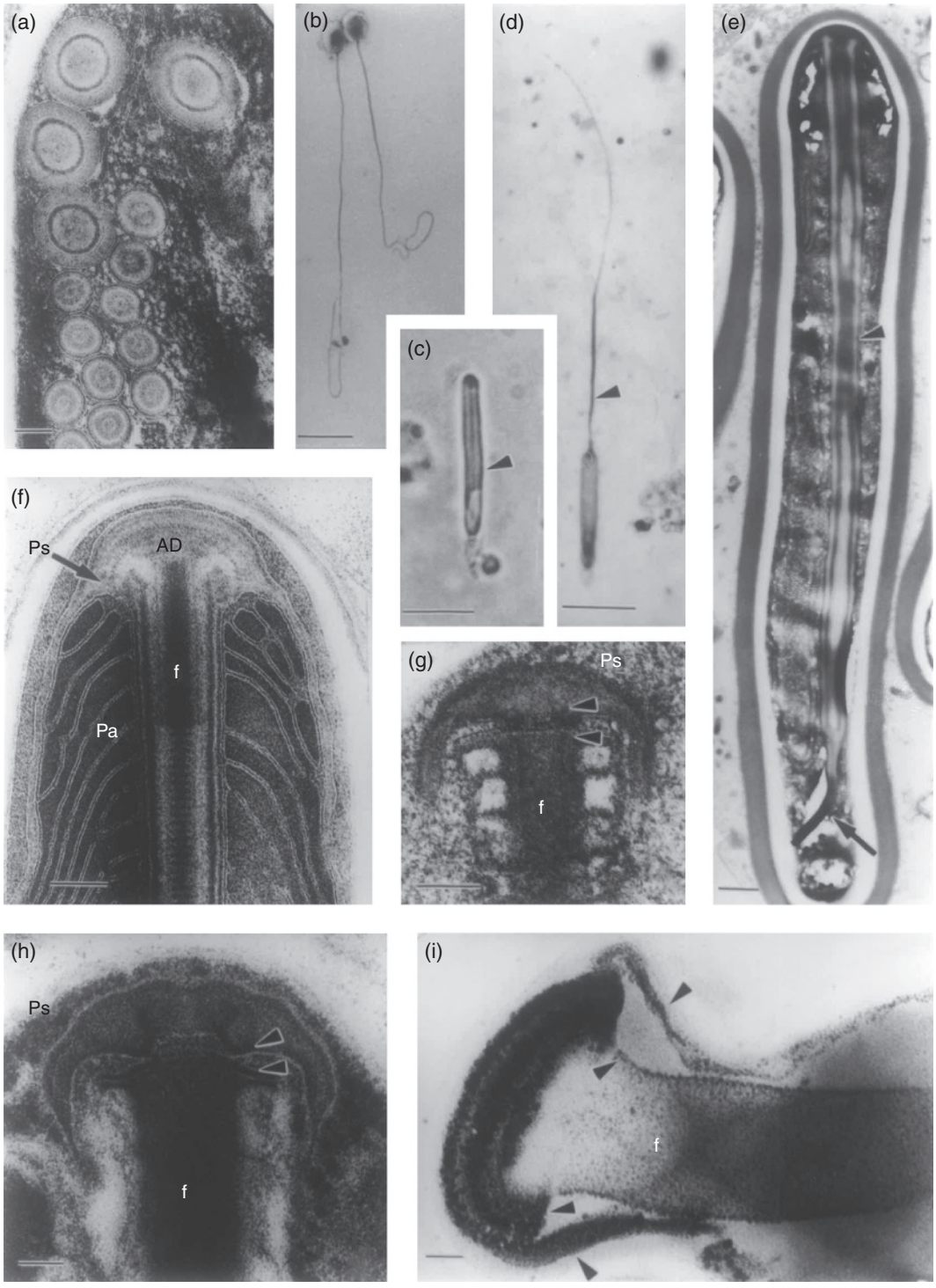

Figure 1.11 Gross morphology of the polar filament and anchoring apparatus. (a) Anisofilar filament (*Amblyospora* sp.). (b) Ejected anisofilar filament (polar tube) (*Trichoctosporea pygopellita*). (c–e) Spores with straight (manubroid) filament, visible in living spores (c) (*Jirovecia involuta*), ejected (d) (arrowhead indicates the straight, wide part) (*J. involuta*), and longitudinally sectioned (e) (arrowhead indicates the wide part and arrow indicates the narrow posterior part) (*Bacillidium strictum*). (f) Common type of filament anchoring, with a wide polar sac, layered anchoring disk, and all layers of the filament (except for the unit membrane cover) united with the anchoring disk (*Paraepiseptum* (formerly *Cougourdella*) *polycentropi*). (g, h) Cap-like polar sac, no visible anchoring disk, and collar-to-socket attachment of the filament (arrowheads) (g) (*Chytridiopsis trichopterae*) and (h) (*Intexta acarivora*). (i) Presence of carbohydrates with α-glycol groups revealed by Thiéry's reaction (arrowheads) (*Mrazekia cyclopis*). TEM (a, e–h), Giemsa stain (b), phase contrast (c), hematoxylin stain (d), PAS technique, TEM (i). Scale bars = 100 nm (a, f, g), 10 µm (b, c, d), 50 nm (h, i), 0.5 µm (e). (h). AD, anchoring disk; f, polar filament; Pa, anterior part of the polaroplast; Ps, polar sac. Reprinted from Wittner, M., Weiss, L. M. (eds.) 1999. *The Microsporidia and Microsporidiosis*. ASM Press, Washington, DC.

(Bronnvall & Larsson 1995a). The shape of the nuclei is spherical to ovoid. Exceptionally, it is horseshoe-shaped like the nucleus of *Metchnikovella hovassei* (Vivier & Schrével 1973).

1.6.6 Cytoplasmic Organelles

In the cytoplasm of the spore, the ER is often seen as strands of polyribosomes, especially prominent around the nucleus in young spores. Polyribosomes either look like double rows of ribosomes sandwiched between membranes (Fig. 1.4a and b) or no membranes at all are visible. Usually there are no prominent differences between transversely and longitudinally sectioned polyribosomes. However, it has occasionally been seen, for example, in *Heterosporis finki* (Schubert 1969), *Trachipleistophora anthropophthera* (Vávra et al. 1998), and *Hamiltosporidium* (formerly *Flabelliforma*) *magnivora* (Larsson et al. 1998) (Fig. 1.4c) that the components of transversely sectioned polyribosomes are arranged in circular configurations with nine ribosomes in each circle. In this arrangement, no membranes are visible.

The Golgi reticulum is prominent in young spores as long as the infection apparatus still has not attained its final shape. It has to be mentioned, however, that although defined Golgi membranes seem to be absent in fully mature spores (while Golgi-like posterosome appears in immature spores), membranes with enzymatic Golgi activity are found in freshly extruded sporoplasms (Takvorian et al. 2013) (see Section 1.4.6) (Fig. 1.32e). So far, mitosomes have not been identified in spores.

1.6.7 The Polar Filament

The polar filament is the most conspicuous structure in the mature spore. Chapter 10 of the present volume covers its biochemical and functional aspects, while data on its mode of formation, structure, and diversity are presented here.

1.6.7.1 Polar Filament Types

In most microsporidia, the filament is threadlike and usually much longer than the spore. Commonly, three regions are visible: a straight anterior part (sometimes called the manubrial portion of the filament) usually about one-third of the spore length, a section where the filament bends to the side and almost touches the spore wall, and finally one or more filament coils (Fig. 1.4 and Fig. 1.5a). With few exceptions, the greatest part of the filament is coiled in the posterior half of the spore. There are several modifications, however, in the polar filament arrangement inside the spore.

A small number of microsporidia (*Chytridiopsis* and related genera) have a short polar filament (Fig. 1.15c). There is no straight part, which means that the complete filament is arranged in a few coils at one pole of the spore.

Exceptionally, the polar filament is shorter than the spore in length, appearing as a straight rod. Such filaments are characteristic of a small number of genera such as *Baculea* (Loubès & Akbarieh 1978), *Cylindrospora* (Fig. 1.15a), *Helmichia* (Larsson 1982), and *Scipionospora* (Bylén & Larsson 1996). These filaments are of the usual construction, and the only difference to filaments of related genera is the shorter length.

Some microsporidia have a thickened filament. The degree of thickening is variable and can involve only the straight, apical part of the filament or also some filament coils. In some genera, the thickened filaments have a very reduced coiled portion. (For details, see Section 1.6.7.2, item 4.)

1.6.7.2 Polar Filament Descriptors

Despite a basic uniform structure, there are several features of the polar filament that vary and thus are useful for the characterization of individual microsporidia.

When evaluating the polar filament, it is necessary to study mature spores. The filament grows in length until the spore is completely mature, new coils are added up to that time, and immature coils are narrower than mature ones. In a nearly mature spore, the last one or two coils, which are the most immature, are often narrower than the mature coils and their internal organization is less complex.

1. Polar filament types are basic characters used in the characterization of microsporidia at the genus or even the suprageneric level.
2. Number and arrangement of coils. Depending on the length of the filament, coils are packed in one or more layers (Fig. 1.4 and Fig. 1.5a). They are usually arranged regularly and close to each other as a single layer of coils or form a more or less distinct double layer (Fig. 1.11a), as in *Enterocytozoon bieneusi* (Fig. 1.24c). If the filament is long, the layers might appear as an irregular stack of coils, like in *Systenostrema corethrae* (Larsson 1986a, 1988a), or be arranged as in posterior direction increasing numbers of layers like in *Pleistophora hyphessobryconis* (Lom & Corliss 1967). The number of coils of a certain species usually tends to vary in a quite narrow limit. The number of coils should be counted in nearly mature or mature spores because the number increases as long as the spore matures.

3. Tilt of polar filament coils. The coils of the polar filament are frequently tilted in relation to the longitudinal axis of the spore. The angle of tilt has been used in discriminating species (Burges et al. 1974). The angle of tilt is difficult to measure because it depends on the plane of sectioning. The spores must be sectioned longitudinally, and the most anterior and the most posterior points of the anterior filament coil must be cut. Most species exhibit an angle of tilt between 40° and 60°, with an individual variation of 5–10° between different spores of the same species. Sometimes the variation is probably a result of erroneous measurements. In the plane perpendicular to the correct plane for measuring, the angle of tilt appears to be 90°.
4. Width of the polar filament. Two basic types of polar filaments can be identified (Weiser 1977). One type has the same, or nearly the same, thickness along its entire length, the isofilar filament (Fig. 1.5a and Fig. 1.16c). In the other type, the anisofilar filament, the anterior part is thicker (Fig. 1.4a, Fig. 1.11a, and Fig. 1.13e). An abrupt constriction located in the coiled section separates the wide and narrow parts. The anisofilar condition is visible in the ejected polar filament and can be observed with light microscopy (Fig. 1.11b). The most proximal zone, close to the anchoring site, is usually somewhat wider in both types of filaments (Larsson 1986c). A new term, "heterofilar," was introduced to describe a polar filament in which one or a few intermediate coils differ in size from the anterior and posterior coils (Voronin 1989a).

   A slightly different type of filament thickening is characteristic of genera of the family Mrazekiidae and apparently also of *Microfilum lutjani* (Faye et al. 1991), in which the anterior part appears as a wide, stiff, rodlike structure (Fig. 1.8i and Fig. 1.11c–e). Léger and Hesse (1916) introduced the term "manubrium" for this handle-like part of the filament. The straight section is often followed by a thin, distal part (Fig. 1.11e) forming one half coil, as in *B. filiferum* (Larsson 1989c), or more commonly a few coils. Polar filaments of microsporidia having a manubrium instead of a coiled filament resemble anisofilar filaments. However, in contrast to the situation in a typical anisofilar filament, there is no abrupt constriction between the wide and narrow parts. Instead, there is a zone with a successive reduction of the diameter, and the differences in width between the wide and narrow parts are greater than in normal cases of anisofilarity.

   The term "manubrium" has also been used for the wide filament of the family Metchnikovellidae (Fig. 1.15b and f) (Hildebrand & Vivier 1971; Vivier 1975; Desportes & Théodoridès 1979; Ormières et al. 1981; Sprague et al. 1992). However, this filament is of a unique type, and therefore this term should be avoided.

   The anisofilar/isofilar construction of the filament and the presence of the manubrium are characteristic features at the generic level.
5. The length of the filament is a character that must be interpreted with caution. The length calculated from electron micrographs of spores is different from the values obtained by measuring extruded filaments. Weidner (1972) calculated that the length of the polar filament in *Ameson michaelis* was 20–30 times the spore length when inside the spore and 60–100 times the spore length as an ejected tube. The diameter of 100–120 nm remained unchanged.
6. Internal structure of the polar filament is dealt with in detail in the Section "Usual Polar Filament Structure." It is recommended to describe the polar filament structure, including the sequence of layers, when describing a new species.
7. Mode of polar filament–polar sac connection. This character divides microsporidia into two structural and probably evolutionary groups (see Section 1.6.7.3 and Fig. 1.12a and b).

1.6.7.3 The Polar Sac–Anchoring Disk Complex

In the mature spore, the polar filament terminates in a bell-shaped structure, the polar sac–anchoring disk complex, situated close to the apex of the spore (Fig. 1.4a, Fig. 1.8b–d, and Fig. 1.11f–i). At this point, the spore wall is thinnest, and the rupture through which the filament emerges during spore germination is formed here. In microsporidia with oval, pyriform, or rodlike spores, the polar sac–anchoring disk complex is usually located terminally, and the filament exits as a prolongation of the longitudinal axis of the spore (Fig. 1.4a and Fig. 1.11c–e). It is more unusual for the filament anchoring site to be subapical and for the filament to emerge slightly sideways (Fig. 1.5, 1.27d and Fig. 1.29c).

The polar sac–anchoring disk complex has two components. In mature spores, the polar sac surrounds the proximal part of the polaroplast in a bell-like fashion (Fig. 1.4a, Fig. 1.5a and b, and Fig. 1.11f). The sac is a unit membrane fold filled with an electron-dense substance. The polar filament enters the polar sac and terminates in its center. The disk is a biconvex, often layered body which can be interpreted as a modified terminal, flattened part of the filament (Fig. 1.5b and Fig. 1.8b–d and f). In cross section, the disk shows several alternating layers of more or less dense material. The polar sac and the anchoring disk contain carbohydrates in the form of mannose-rich glycoproteins (Taupin et al. 2007) as shown by the PAS staining for light microscopy (Fig. 1.1n) and its modification for electron microscopy (Thiéry 1972) (Fig. 1.1n and Fig. 1.11i) (Vávra 1972). Demonstration of this material by staining spores in smears or sections is a diagnostic method for microsporidia (see Section 1.11.2.2).

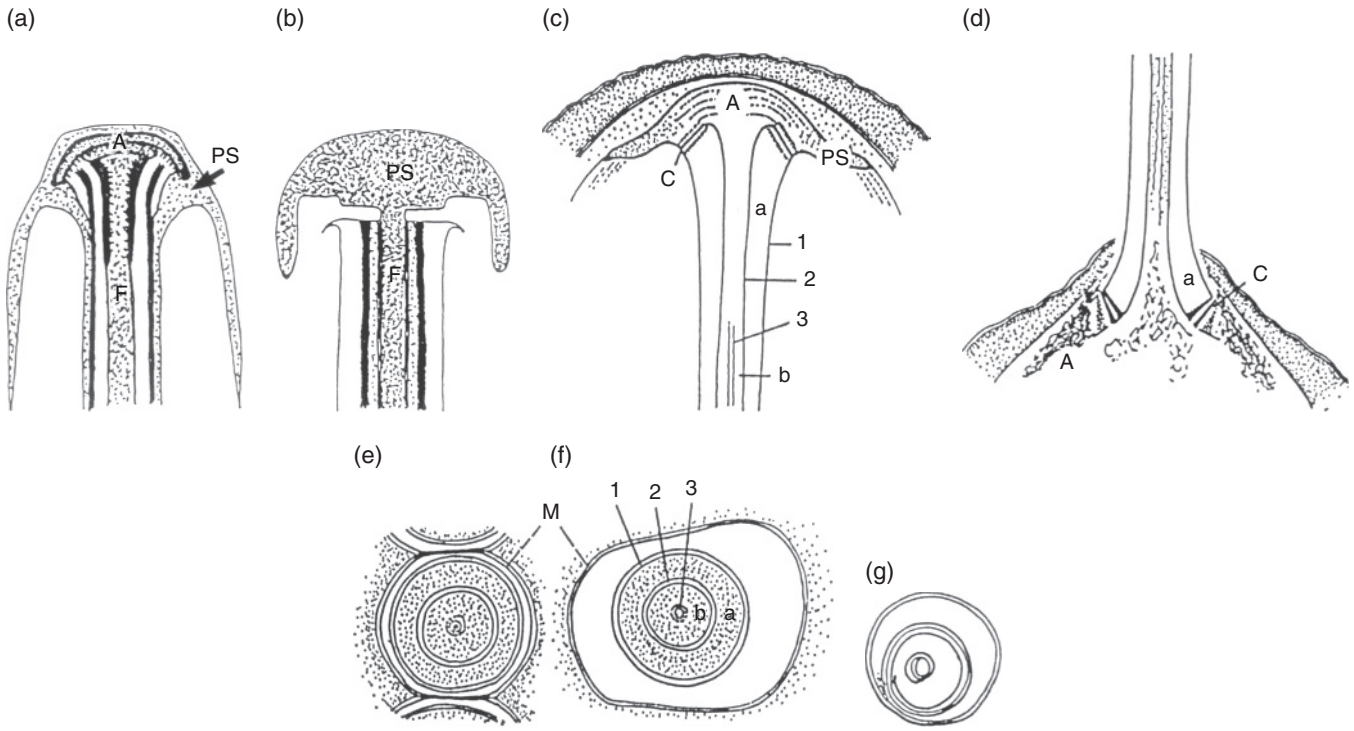

Figure 1.12 (a, b) Schematic representation of polar filament–polar sac connection in microsporidia from typical microsporidia (a) and *Chytridiopsis*-like microsporidia (b). (c–e) Schematic representation of polar filament evagination; (c) shows the tip of the extrusion apparatus in a dormant spore; (d) the polar sac–polar filament relationship in an extruded spore. Note that the structure labeled c serves as a hinge for the evaginating filament. (e) Cross section of the filament in a dormant spore. (f) Filament in an activated spore. (g) Cross section of the extruded filament. A, anchoring disk; a, polar filament wall; b, polar filament lumen; c, hinges; M, membrane ensheathing the polar filament; PS, polar sac; 1, 2, and 3, layers (not unit membranes!) seen in the filament. Reprinted from Wittner, M., Weiss, L. M. (eds.) 1999. *The Microsporidia and Microsporidiosis*. ASM Press, Washington, DC.

1.6.7.4 Polar Filament–Polar Sac Relationship

Microsporidia exhibit two modes of polar filament–polar sac connections:

1. In the majority of microsporidia, the polar filament in its entire width enters the polar sac, and all layers of the filament connect with the disk (Fig. 1.8d, Fig. 1.4a, and Fig. 1.11f). The external layers of the filament widen in a funnel-like fashion inside the sac, increasing the filament width to the same width as the anchoring disk. It has been observed in some microsporidia, for example, *Napamichum dispersus* (Larsson 1984) and *Amblyospora culicis* (Toguebaye & Marchand 1985, 1986), that fibrous material connects the external layers of the filament to the anchoring disk (Fig. 1.8f). This fibrous material serves as "hinges" around which the polar filament turns during eversion (Lom 1972) (see Section 1.6.7.6).
2. The polar sac of *Chytridiopsis*-like microsporidia (Larsson 1993) and Metchnikovellidae (Vivier & Schrével 1973) is a rather small, cuplike body (Fig. 1.11g and h, Fig. 1.12b, and Fig. 1.15b). This sac is also a folded unit membrane containing electron-dense material. However, there is no visible anchoring disk and no proofs of the filament entering the sac. In the *Chytridiopsis*-like microsporidia, the posterior center of the polar sac is shaped like a socket (Fig. 1.11g and h). The external layers of the polar filament widen anteriorly to a collar-like structure with approximately the same width as the socket (Fig. 1.11g and h). The unit membrane of the polar sac is continuous with the surface layer of the filament. However, the socket and collar are separated by a distinct gap. Only the center of the polar filament enters the polar sac (Fig. 1.12b).

1.6.7.5 Fine Structure of the Polar Filament

During polar filament initiation, the transversely sectioned filament usually appears as a ring limited by a thick, electron-dense border and containing a fibrogranular electron-lucent matrix and a dark, circular central spot (Fig. 1.8a). Longitudinal sections reveal that the limiting border of the filament is continuous with the polar sac and that the dark material in the center of the filament penetrates for some distance into the sac (Fig. 1.8c and d). The electron-dense material inside the polar sac is the first sign of the future anchoring disk. During morphogenesis of the spore, the original structure of the filament is extensively reorganized, and the filament in its final form is a complex, multilayered structure. The construction of the

mature polar filament is best evaluated in transverse sections, in which a number of concentric layers of different electron density and thickness are visible (Fig. 1.13).

Usual Polar Filament Structure

A basic filament organization is shared by the majority of microsporidian species. However, the appearance of individual layers is influenced both by the visualization techniques used and by the degree of maturity of the spore. For these reasons, all layers are not always distinct, and the thickness of the respective layers varies among species. The following sequence of layers is usually discernible in the transversely sectioned filament (from the outside inward) (Fig. 1.13a–c): an external unit membrane (i); three layers often of approximately the same thickness, electron dense (ii), translucent (iii), and dense (iv); a layer resembling transversely sectioned translucent fibrils embedded in a moderately dense matrix (v); and the center (vi). The center is subdivided, but the layers are often not distinct. For example, species of the genera *Episeptum* (Larsson 1996), *Systenostrema* (Larsson 1988a), and *Vavraia* (Larsson 1986d) possess this kind of polar filament. Normally, the wide and narrow coils of an anisofilar filament exhibit the same sequence of layers, and the differences in diameter are mainly due to a different width at the center (layer 6) as in *Vavraia holocentropi* (Larsson 1986d) and in *Episeptum* spp. (Larsson 1996) (Fig. 1.4a). However, even external layers can be considerably wider in the wide part like in *Trichoctosporea pygopellita* (Larsson 1994b).

Vávra (1976a) monitored the filaments of several microsporidia from initiation to maturation, gave a more detailed account of the layering, and expressed the idea that the filament is a thick-walled tube with composite outer and inner walls consisting of three (dense, transparent, dense) layers each. Between the outer and inner walls, there is a wide electron-transparent layer. During filament formation, the thick, dark outer zone of the immature filament splits into two electron-dense concentric rings separated by a lucent layer (layers 2–4). These three layers represent the outer wall of the filament tube. Another three, but less thick, layers (two dense rings separated by less opaque material and probably a subdivided layer 5) represent the inner filament wall. The inner tube seems to be built from fine fibers arranged helically along the filament length. These fibers can be seen both during polar filament formation and as a meshwork in negatively stained extruded filaments (Vávra 1976a) (Fig. 1.13f). In between the outer and inner composite walls is an electron-transparent layer into which extend, in cartwheel fashion, the fibers from the wall of the inner tube. These fibers react positively when stained by Thiéry's (1972) reaction for carbohydrates (Fig. 1.13g). The lumen of the inner tube (the center layer 6) contains granular material of two electron densities: a dense central spot surrounded by a less dense matrix. In freeze-fracture preparations, the filament looks like a solid rod (Fig. 1.10e). When a specimen is cross-fractured, an inconspicuous ring of granules close to its outer rim and another accumulation of granules in its center are revealed (Fig. 1.10d–e and Fig. 1.14a–c). The filament is enveloped by a unit-type membrane as shown by the freeze-fracture technique (Vinckier et al. 1993) (Fig. 1.10c and d and Fig. 1.14c). It has been argued that the filament-ensheathing membrane is not a part of the filament proper, but belongs to the polaroplast membrane system (Vávra 1976a). The carbohydrate (glycoprotein) material is located mainly in the inner filament wall and is much less dense than in the outer filament wall (Fig. 1.13h).

Polar Filaments of Unusual Structure

A minority of microsporidia have unusual types of polar filaments.

1. Microsporidia of the family Mrazekiidae produce rod-shaped spores possessing a thick polar filament of the manubrium type (Fig. 1.8i and Fig. 1.11e). The internal organization differs from the common type in that layer 5 in the straight portion is exceptionally wide and has a mottled structure (Fig. 1.13c). In the narrow part of the filament, it is reduced to a narrow, dense stratum (Larsson 1994a).
2. The *Chytridiopsis*-like microsporidia differ from other microsporidia in several ways. The spores are small and spherical, a normal polaroplast is absent, and the polar filament is mostly untilted. A smaller number of filament layers can be distinguished. The external dense layer of the filament is transformed into an alveolate layer in which expansions of the dense layer enclose small, round alveoli with electron-lucent content. In cross section, such a filament might have a stellate form (Fig. 1.15e and h). In tangential section, a honeycomb-like alveolar layer on the surface of the filament is seen in *Coccospora brachynema* (Richards & Sheffield 1970) (Fig. 1.15g and h), *Chytridiopsis* (Larsson 1993) (Fig. 1.15c), and *Nolleria* (Beard et al. 1990). These unusually constructed filaments are difficult to interpret. As none of the *Chytridiopsis*-like microsporidia has a polaroplast, it is believed that the lucent alveoli at the filament surface represent a special type of polaroplast vesicles and that the honeycomb-like layer is a primitive type of polaroplast (Vávra 1976a).

In *Intexta acarivora* (Larsson et al. 1997b), the unit membrane at the polar filament surface is a smooth layer below which is a zone with winding tubules of electron-lucent material (Fig. 1.15d). *Buxtehudea scaniae* (Larsson 1980) and *Burkea gatesi* (Puytorac & Tourret 1963) differ from the other microsporidia of this group by having a long polar filament with a

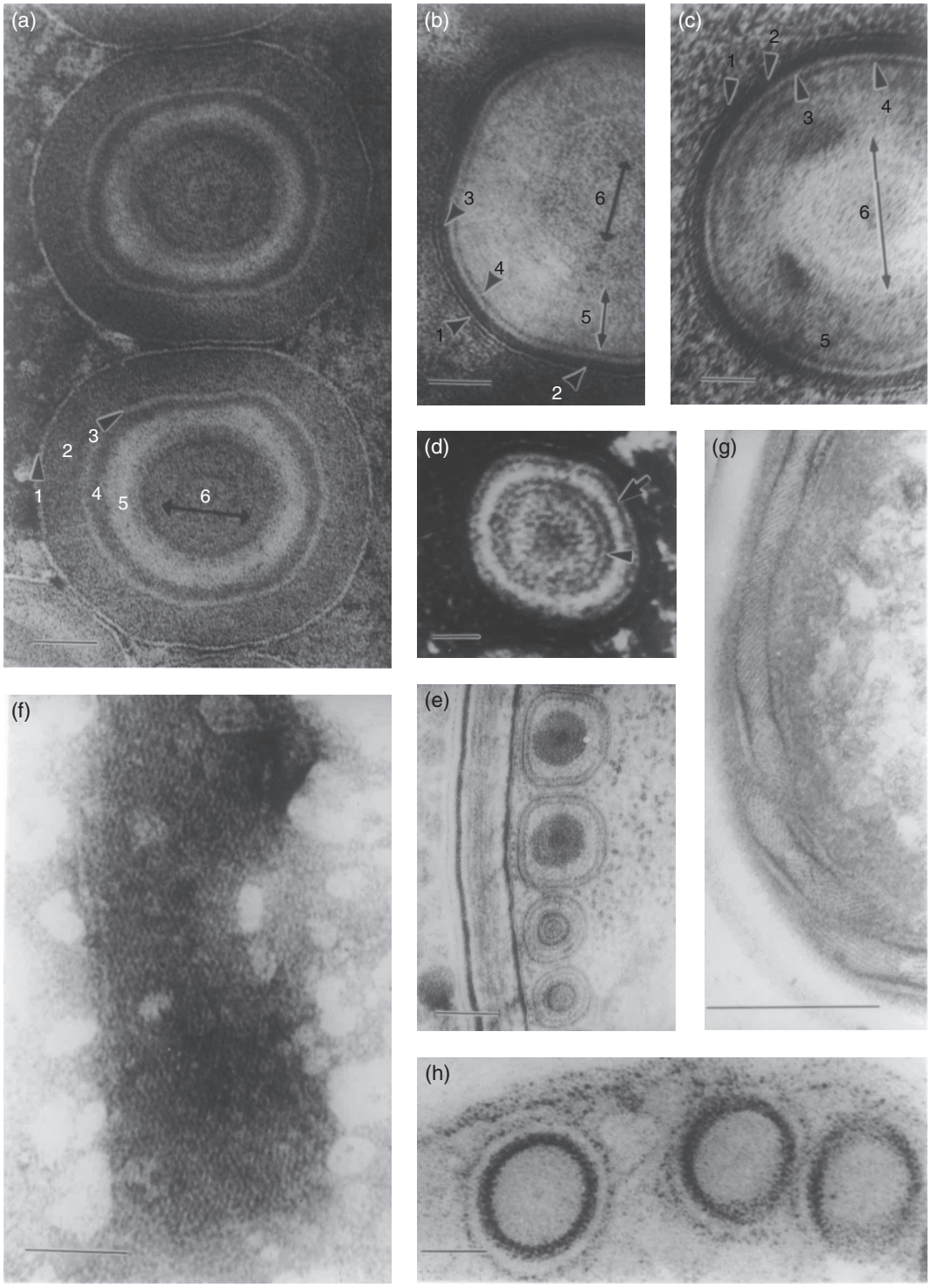

Figure 1.13 Fine structure of the polar filament. (a–c) Transversely sectioned filaments; the most easily observed layers are numbered 1–6 (*Trichoctosporea pygopellita)* (a), (*Janacekia adipophila*) (b), and (*Jirovecia involuta)* (c). (d) Layering of the filament, showing the double layers of the outer (arrow) and inner (arrowhead) filament walls (*Heterosporis finki*). (e) Layering seen in immature spores. Note the difference in polar filament layers in the anterior and posterior coils (*Amblyospora culicis*). (f, g) Fibrillar substructure of the polar filament: the filament of *Paranosema* (formerly *Nosema*) *whitei* after tryptic digestion (f) and the fibrillar substructure of one of the filament layers revealed by Thiéry's reaction for carbohydrates in *Microsporidium* sp. from *Artemia salina* (g). (h) Cross section of a filament stained by Thiéry's method (*Norlevinea daphniae*). All images TEM. Scale bars: 50 nm (a–c, f, h), 25 nm (d), 100 nm (e), 0.5 μm (g). Reprinted from Wittner, M., Weiss, L. M. (eds.) 1999. *The Microsporidia and Microsporidiosis*. ASM Press, Washington, DC.

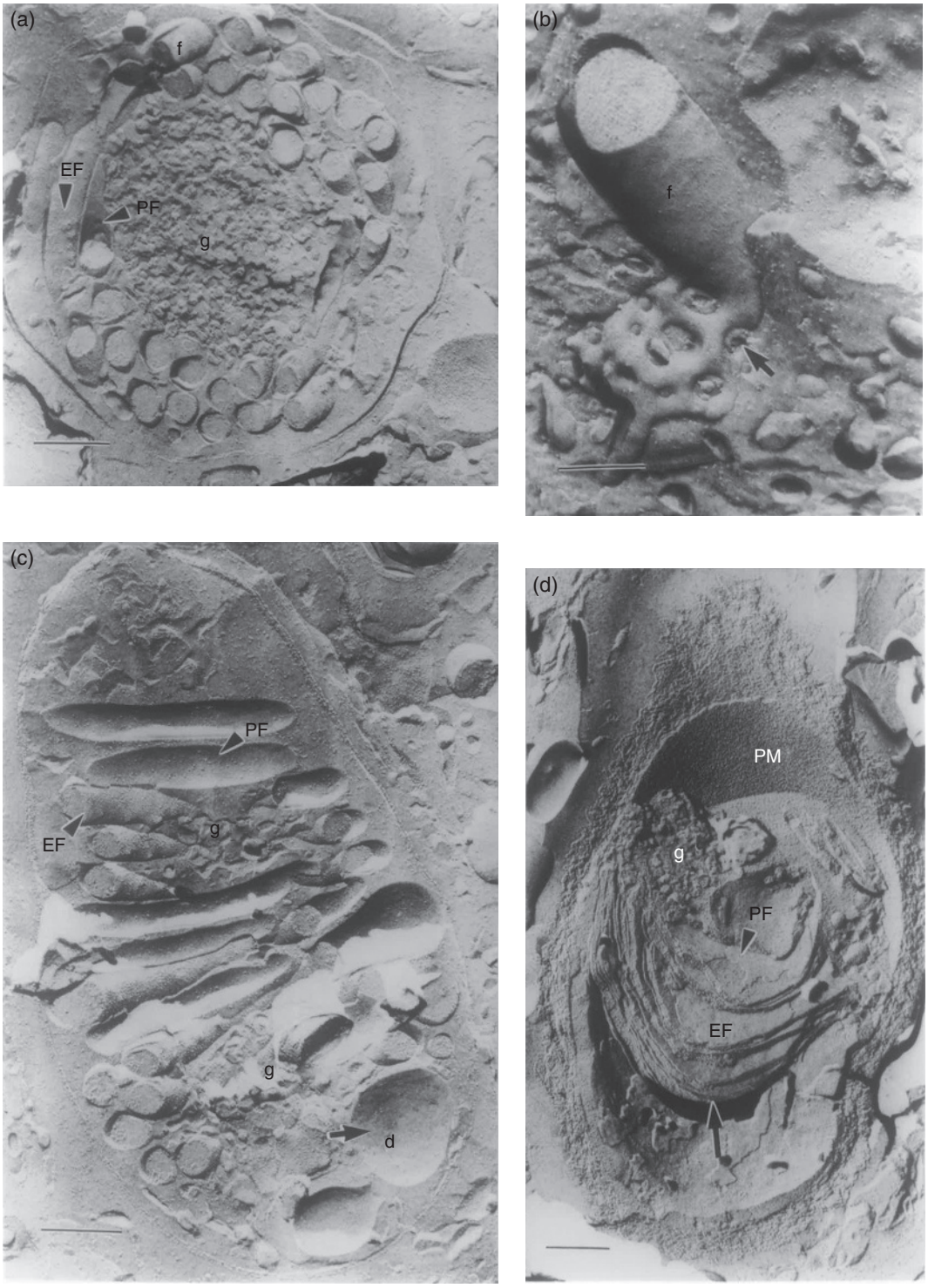

Figure 1.14 Freeze-fracture images of microsporidian spores. (a) Tangential fracture of a young spore of *Nosema apis*, showing the hypertrophied reticulum of the Golgi zone and cross and tangential fractures of several coils of the polar filament. Both faces (BF and PF) of the cytoplasmic membrane around the filament are shown. (b) Sporoblast of *Amblyospora varians*, showing the origin of the polar filament by coalescence of Golgi reticulum vesicles (arrow). (c) Longitudinal fracture through a young spore of *N. apis*, demonstrating that the polar filament is a solid cylinder enveloped by a cytoplasmic membrane with EF and PF faces; the EF face bears more numerous intramembranous particles; arrow indicates the posterior vacuole membrane with PF face. (d) The polaroplast (arrow) of *N. apis* is revealed as a stack of membranes bearing intramembranous particles on both hemimembrane faces. The ectoplasmic face (EF) of the spore plasma membrane (Pm) bears numerous intramembranous particles. Scale bars = 0.5 µm (a, c, d), 250 nm (b), 250 nm. g, Golgi zone; f, polar filament; EF and PF, ectoplasmic and protoplasmic faces of a split unit membrane; PM, plasma membrane (ectoplasmic face). Reprinted from Wittner, M., Weiss, L. M. (eds.) 1999. *The Microsporidia and Microsporidiosis*. ASM Press, Washington, DC.

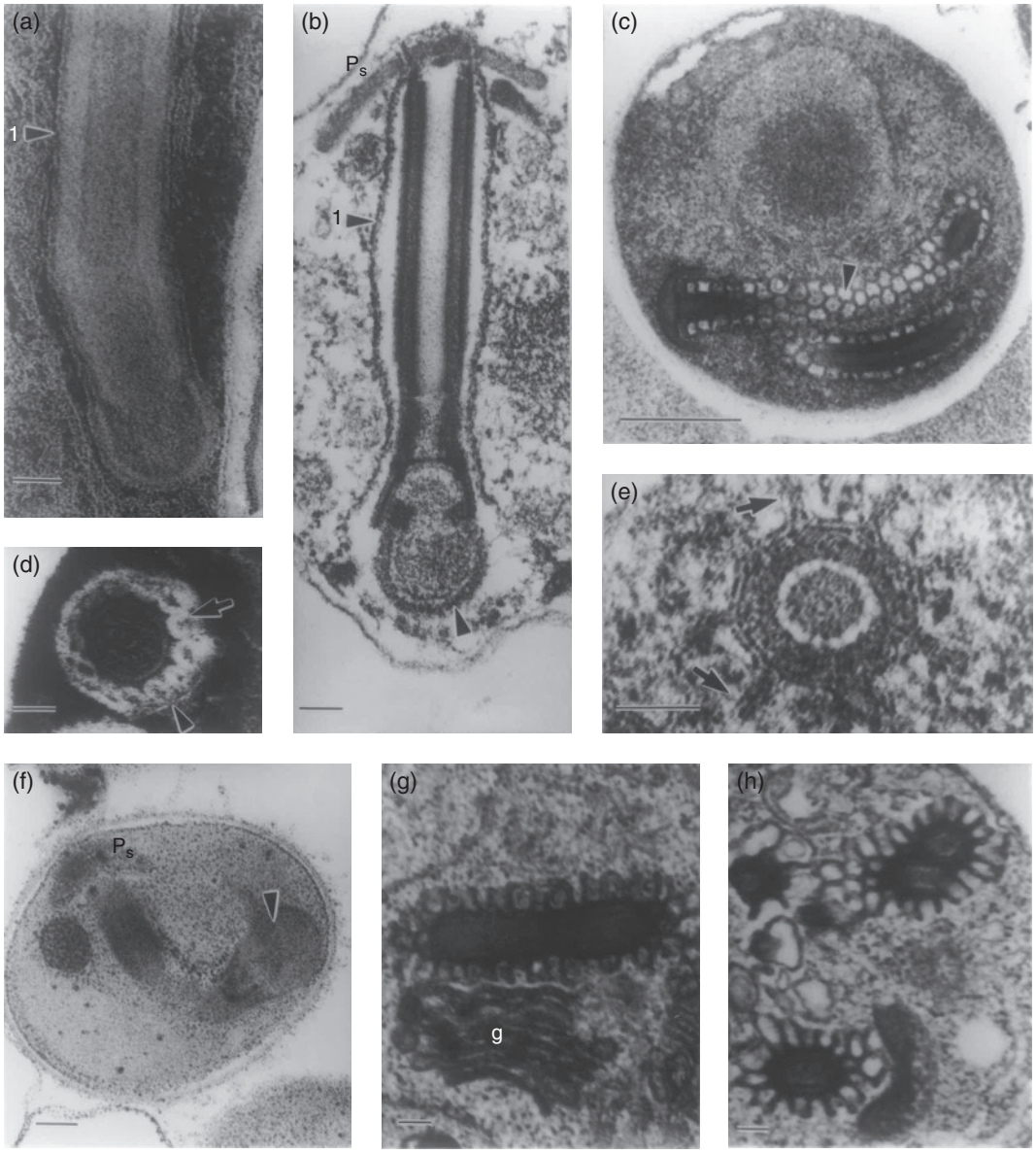

Figure 1.15 Unusual types of filaments. (a) Posterior part of a short, straight filament of normal cytology (*Cylindrospora fasciculata*). (b) Straight filament of Metchnikovellidae, ending with a "gland" (arrowhead) (*Amphiacantha* sp.). (c) Short and completely coiled filament of *Chytridiopsis trichopterae* covered by a honeycomb-like surface layer (arrowhead). (d) Transversely sectioned filament of *Intexta acarivora* (arrow indicates tubular material and arrowhead indicates the covering unit membrane). (e) Transversely sectioned filament of *Buxtehudea scaniae* (arrows indicate unit membrane folds). (f) Filament of *Metchnikovella hovassei* with the bulbous "gland" (arrowhead). (g, h) Longitudinal (g) and transversal (h) sections of a filament with a honeycomb layer (*Coccospora brachynema*). All images TEM. Scale bars = 50 nm (a, d, e), 0.5 µm (c, f), 100 nm (b, g, h). Nu, nucleus; Ps, polar sac, g, Golgi. Reprinted from Wittner, M., Weiss, L. M. (eds.) 1999. *The Microsporidia and Microsporidiosis*. ASM Press, Washington, DC.

distinct tilt, which gives the spores the same polarity as the normal microsporidian spore. The polar sac at one pole of the spore crowns the straight anterior part of the filament. The posterior section of the filament is arranged in numerous coils at the opposite pole. The unit membrane covering the filament of *B. scaniae* is folded, and the folds wind around the filament. The transversely sectioned filament resembles an eight-pointed star (Fig. 1.15e). The interior of the filament is similar to the interior of filaments of normal cytology, including the presence of a fibrous layer (layer 4 in the normal polar filament layering).

3. The polar filament of metchnikovellideans is a wide, stout structure ending with a posterior bulbous swelling (Fig. 1.15b and f). The filament is uncoiled in *Amphiamblys bhatiellae* (Ormiéres et al. 1981) and *Amphiamblys laubieri* (Desportes & Théodoridès 1979) and is bent in a half coil posteriorly in *Metchnikovella hovassei* (Vivier & Schrével 1973). The straight filament has been called a manubrium (see Section 1.6.7.2), and French authors have called the posterior swollen part a

"gland" from the similarity with an acorn (Vivier & Schrével 1973). The filament has a unit membrane cover, a zone of granular material, and a distinctly organized central axis with a sequence of layers similar to the normal stratification of a polar filament. The swollen part is separated from the manubrial part by a differently organized zone (Larsson 2000; Larsson & Køie 2006). A fold of the unit membrane projects, from the posterior swollen part, creating a lamellar, and partly tubular, structure filled with granular material similar to the material in the external zone of the filament.

1.6.7.6 The Polar Filament during Spore Germination

At present time, it remains unresolved whether the filament inside the spore is a final product or a pool of materials from which a tube is formed during spore germination. Indeed, it was proposed that the filament actually grows and forms a tube by polymerization of the material at the filament tip during eversion (Weidner 1982; Weidner et al. 1995). On the other hand, there is, however, no compelling reason not to believe that the filament simply turns inside out (as a finger of a glove does) during eversion as Lom and Vávra argued (1963a) and as corroborated by light microscope and ultrastructural observations (Lom 1972; Vávra 1976a). According to this model, the filament exit proceeds as follows. In the germinating spore, the polaroplast swells first and the regular arrangement of its membranes is disturbed while intermembrane spaces increase (see the following text). In the filament, the narrow space between the unit membrane ensheathing the filament and the filament proper increases first (Fig. 1.12e and f) concurrently with the swelling of the polaroplast. Later, the intrasporal pressure squeezes the base of the filament (at the site of its attachment to the anchoring disk) through the thin part of the spore wall (Fig. 1.5c). The filament turns inside out during the exit, its basal part turning around the "hinge-like" fibrous structure (Fig. 1.8f and Fig. 1.12d) fastening the wall of the everting tube to the anchoring disk (Fig. 1.12c and d). The extruded tube shows several concentric layers (Lom 1972) (Fig. 1.12g).

The "simple eversion model" is certainly more complex than presented earlier if one considers the complexity of the filament substructure. Unresolved also remains the elasticity of the filament material, which might explain the large discrepancy between the length of the filament measured inside the spore and the length of the extruded state. The difference is as great as 100–120 µm versus 300–500 µm in a fish microsporidium (Lom & Corliss 1967). See section 1.6.7.2, item 5.

1.6.8 The Polaroplast

The polaroplast is a system of membrane-limited cavities in the anterior part of the spore (Fig. 1.4a, Fig. 1.5a and b, and Fig. 1.16). In most microsporidia, it is a voluminous structure surrounding the straight part of the polar filament and ending at the level of the anterior filament coils. One-third to one-half of the spore volume is occupied by the polaroplast, and only rarely is it rudimentary or nonexistent. In immature spores, the developing polaroplast has an irregular texture, while the polaroplast of mature spores is a distinctly organized structure with compartments that vary in shape, but most commonly, they are lamellar.

1.6.8.1 Conditions for Evaluating Polaroplast Structure

When evaluating the construction of the polaroplast, it is necessary to study the polaroplast of mature spores. All members of a genus share a polaroplast of nearly identical construction, and the construction is thus a useful classification character. As an organelle built from membranous compartments, the polaroplast is sensitive to fixation and embedding procedures. Because of this sensitivity, its structure is easily influenced by the handling of the spores during preparation. In well-preserved specimens and in spores fixed in hypertonic fixatives, the polaroplast lamellae are tightly packed and regularly spaced. Hypotonic fixatives cause the polaroplast to swell (Vávra 1976a; Vinckier et al. 1993). Good preservation of unit membranes, both of the polaroplast and the polar filament, which shows their trilaminar nature, is a prerequisite for correct interpretation of polaroplast structure. Further, it is important to note how the polaroplast has been sectioned. A perfect longitudinal section gives a different picture of the polaroplast than an oblique section. The images also differ when a longitudinal section taken close to the midline of the spore is compared to a section taken at the periphery. Some of the aberrant polaroplast types described are only illustrated by oblique sections, and there are reasons to doubt some of the interpretations. Even if two lamellar polaroplasts look identical when sectioned longitudinally, transverse sections might reveal a difference, because the lamellae might be arranged in two ways. Either the lamellae are radially complete, which means that each one surrounds the polar filament completely (Fig. 1.16e), or they are more narrow, arranged like the petals of a flower (Fig. 1.16f).

1.6.8.2 Fine Structure of the Polaroplast

The compartments of the polaroplast are shaped like lamellae, chambers, or tubules delimited by approximately 5 nm thick unit membranes. The unit membrane character of the polaroplast was confirmed by the freeze-fracture technique which revealed the presence of intramembranous particles on the faces of split polaroplast membranes (Vinckier et al. 1993)

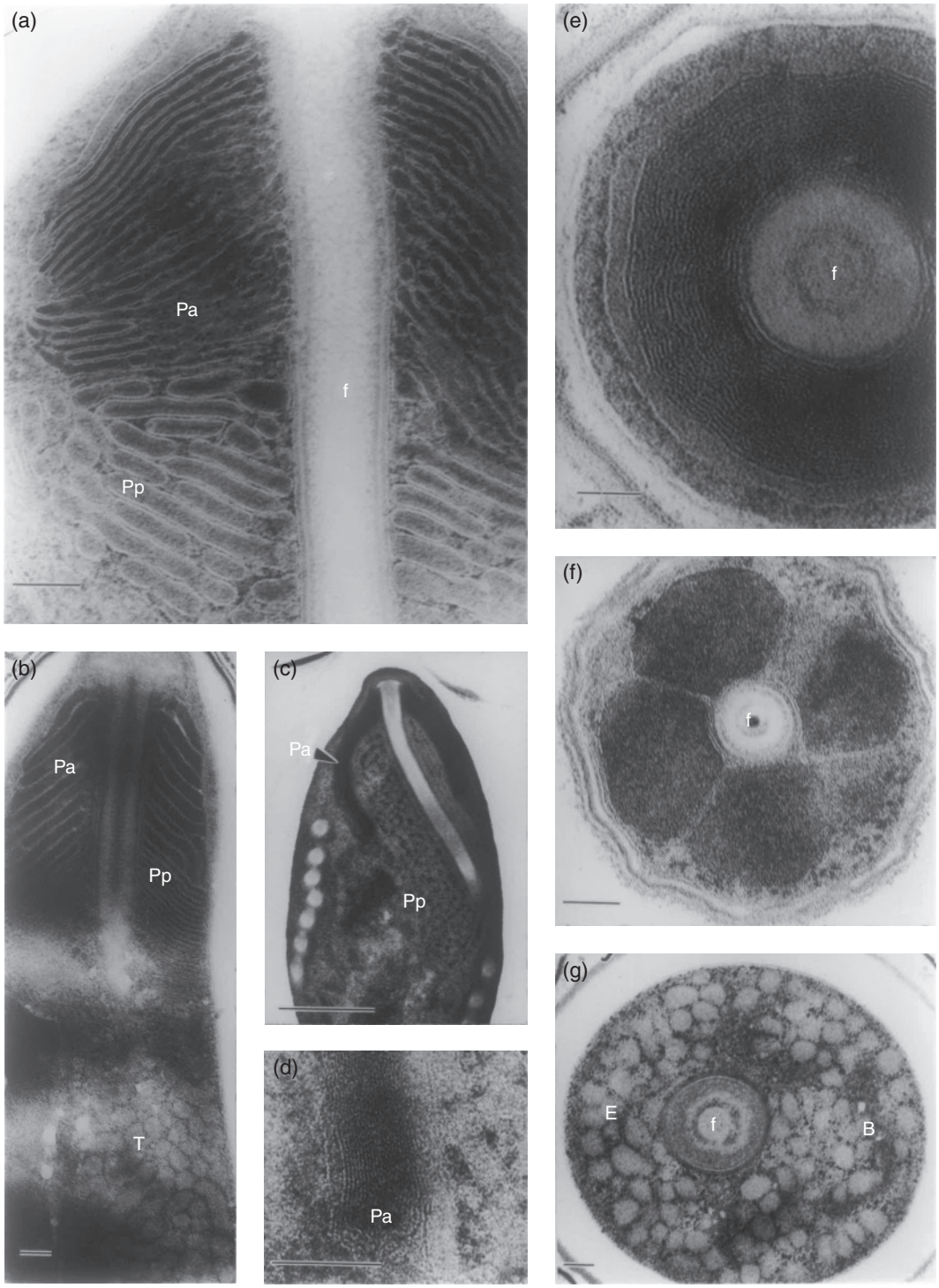

Figure 1.16 Fine structure of the polaroplast. (a) The most common type of bilaminar polaroplast, with more closely packed anterior lamellae (*Vavraia holocentropi*). (b) Polaroplast with three regions (wide lamellae, narrow lamellae, and tubules) (*Agglomerata sidae*). (c, d) Bilamellar polaroplast with exceptionally closely packed anterior lamellae ("cavum") (*Nosema artemiae*). (e–g) Three aspects of the transversely sectioned polaroplast, (e) concentric lamellae (*Cylindrospora fasciculata*), (f) petallike arrangement (*Paraepiseptum* (formerly *Cougourdella*) *polycentropi*), and (g) tubules (*Jirovecia involuta*). All images TEM. Scale bars = 100 nm (a, b, d, f, g), 50 nm (e), 0.5 µm (c). (f, g). Pa, anterior polaroplast; Pp, posterior polaroplast; T, tubules, f, polar filament. Reprinted from Wittner, M., Weiss, L. M. (eds.) 1999. *The Microsporidia and Microsporidiosis*. ASM Press, Washington, DC.

(Fig. 1.14d). The polar sac, the compartments of the polaroplast, and the unit membrane covering the polar filament belong to the same membrane system, and the membranes of the polaroplast form anastomoses to the unit membrane of the polar filament. The polaroplast is most commonly divided into a shorter anterior part and a more voluminous posterior section, but there are several variations on the theme, including subdivision into up to four different regions.

1. The most commonly observed type of polaroplast has two lamellar parts. Anterior lamellae are closely packed and regularly arranged, while posterior lamellae are wider and less regularly organized (Fig. 1.5a and b and Fig. 1.16a). This polaroplast is typical of *Encephalitozoon* (Barker 1975), *Pleistophora* (Canning & Nicholas 1980), and numerous other genera. The two regions are referred to as the lamellar polaroplast and the vesicular polaroplast, respectively. A polaroplast with inverted construction, with two regions of regularly arranged lamellae, where the anterior lamellae are wide and the posterior ones narrow, is characteristic of the genera *Episeptum* (Fig. 1.4a) and *Trichotuzetia* (Vávra et al. 1997).
2. Certain microsporidia, for example, *Ameson michaelis* (Sprague et al. 1968), *Spraguea lophii* (Loubès et al. 1979), and *Helmichia aggregata* (Larsson 1982), have a zone of compressed and unusually electron-dense lamellae anteriorly to the uniform lamellar polaroplast (Fig. 1.16c and d). Originally, this zone was believed to be a cavity, not a lamellar organelle, and the term "cavum" was used to denote such a region (Sprague et al. 1968).
3. Variations in the posterior part of the two-region lamellar polaroplast are not unusual. The posterior lamellae of some *Amblyospora* species (Andreadis 1983; Dickson & Barr 1990) are so wide and irregularly shaped that they are best described as chambers. In *Napamichum cellatum*, the posterior compartments are almost tubular (Bylén & Larsson 1994).
4. Two variations of a polaroplast with three regions have been described. One type has narrow lamellae anteriorly, a median section of wide lamellae, and a posterior region with tubules. This is the polaroplast of *Binucleospora elongata* (Bronnvall & Larsson 1995a). In the second type of three-region polaroplast, a section with wide lamellae is followed by one with narrow, closely packed lamellae and a final portion with tubules. This type of polaroplast was originally observed in the genus *Agglomerata* (Fig. 1.16b), but is also known to occur in *Lanatospora tubulifera* (Bronnvall & Larsson 1995b).
5. A polaroplast with four regions was observed in *Microsporidium fluviatilis* (Voronin 1994). In posterior direction, the following regions are visible: loosely arranged chambers, closely packed chambers, large globular compartments, and posterior lamellae.
6. A few genera have uniform lamellar polaroplasts. The polaroplast of *Cystosporogenes deliaradicae* is lamellar in the normal way, protruding sideward from the polar filament (Larsson et al. 1995). The lamellae of the polaroplasts of *Cylindrospora fasciculata* (Larsson 1986c) and *Ordospora colligata* (Larsson et al. 1997a) are folded, one outside the other.
7. In the trimorphic *Amblyospora* species, which alternate between mosquitoes and copepods, the elongate type of spore produced in the copepod exhibits a different type of uniform polaroplast, composed entirely of globular sacs (Sweeney et al. 1985; Becnel & Sweeney 1990). It was originally considered unique to *Amblyospora*, but new studies have revealed that a similar spore morph with a polaroplast of the same type is also produced by the mosquito parasites of the genera *Culicospora* (Becnel et al. 1987), *Culicosporella* (Becnel & Fukuda 1991), and *Edhazardia* (Becnel et al. 1989).
8. *Bohuslavia asterias* has a polaroplast lacking distinct regions (Larsson 1985). The shape of the compartments changes successively from wide, irregular chambers anteriorly to closely packed lamellae posteriorly.
9. A minority of microsporidia have membranous or tubular elements different from a normal polaroplast in their spores. These structures are sometimes interpreted as being primitive or rudimentary polaroplasts. *Baculea daphniae* has such a rudimentary polaroplast in the form of a vacuole with membranous septa (Loubès & Akbarieh 1978). *Chytridiopsis*- and *Metchnikovella*-like microsporidia lack a distinct polaroplast (Fig. 1.15b, c, and f). The surface structures of the uniquely constructed polar filaments have been interpreted as being homologous to a polaroplast (Vávra 1976a).

1.6.9 The Posterior Vacuole

The posterior vacuole is the third component of the extrusion apparatus of the spore (Fig. 1.4a and Fig. 1.5a). It is a membrane-lined area with a clear or spongy content located in the posterior part of the spore. It looks like an empty vacuole when observed in the light microscope, and the size and shape are quite variable. At one extreme, some microsporidia apparently do not have a posterior vacuole, and in other cases, it looks like an inconspicuous slit. Typically, however, the vacuole is readily visible, and in some species, it is large and occupies more than half of the spore volume. Fish microsporidia frequently have such large vacuoles.

The vacuole is enclosed by a unit-type membrane as shown by the freeze-fracture technique (Vinckier et al. 1993) (Fig. 1.14c). Like other parts of the extrusion apparatus, the vacuole is evidently a product of the Golgi vesicles. This is corroborated by the presence of a spongy reticulum of electron-dense vesicles in the posterior vacuole of immature spores. It is similar, or probably identical, to the Golgi reticulum forming the polar filament. This structure was called a posterosome by Weiser and Žižka (1974, 1975), a term replacing earlier names such as "posterior body" and "inclusion body."

The mutual spatial relationship between the polar filament and the posterior vacuole is not well known. There are divergent opinions as to whether the filament enters the vacuole and terminates there. Weidner (1972) postulated that the polar filament enters the vacuole but it is separated from it by a membrane. However, freeze-fracture technique has failed to prove

that the filament enters the vacuole (Vinckier et al. 1993). On the other hand, Lom and Vávra (1963a, and unpublished data) have noticed that during spore germination and polar filament unwinding, the posterosome vigorously spins inside the vacuole. This observation is interpreted as proving that the filament ends inside the vacuole and that in immature spores the posterosome is identical to the Golgi material at the distal end of the filament. One can also speculate if the posterosome material is identical with the membrane reticulum ("MIN") described to occur in freshly discharged sporoplasms by Cali et al. (2002) and Takvorian et al. (2013) (Fig. 1.32d).

1.7 ENVELOPES OF MICROSPORIDIAN ORIGIN

The whole development of microsporidia takes place in intimate relationship with the host cell cytoplasm. This contact is maintained until the moment the spores are nearly mature and reflects the fact that the microsporidia are fully dependent on the metabolism of the host cell.

The sporoplasm is inoculated into the host cell, which ensures that the microsporidium enters the host cell unrecognized and protected from host defense reactions. The parasite plasma (PP) membrane (together with its eventual glycocalyx material) is in direct contact with the host cell cytoplasmic matrix during merogony and in many microsporidia also during the sporogony. The host cell envelopes the microsporidium with a cisterna of ER with ribosomes. Many microsporidia are separated from the host cell by a boundary of parasite (see the following text) or of presumed host cell origin (see Section 1.9.2). Microsporidia separated from the host cell cytoplasm by a parasite-formed boundary are said to have a closed type of sporogony (see Section 1.5.3). They produce various vesicle-like structures inside which the spores are formed: SPOVs of two kinds, exospore-derived envelopes, and cyst-like structures. The various types of envelopes provide a barrier between the host fluids and the spores. If envelopes are used as taxonomical criteria, it is crucial to discriminate between those produced by the host cell in reaction to a microsporidian infection and those derived from microsporidia, as well as to determine the manner in which the microsporidia-derived envelopes are produced.

1.7.1 Sporophorous Vesicles

The SPOV (Fig. 1.17, Fig. 1.33b and c) is known as a pansporoblast in older literature, an obsolete and not recommended term for microsporidia (Vávra & Sprague 1976; Canning & Nicholas 1980).

The SPOV originates as a layer of secretions generated by the organism. It loses contact with the plasma membrane and forms an envelope. The volume of the SPOV between the envelope and the microsporidian cell is called the episporontal space (Vávra 1984). A vesicle produced by the sporont is called a sporontogenetic SPOV, and when produced by the meront (which is a rare case), a merontogenetic SPOV (Canning & Hazard 1982). In some microsporidia, the vesicle is a transient structure: it remains until the spores mature, and then rapid degeneration ensues. Other microsporidia sporulate in more or less persistent vesicles. As most envelopes are delicate structures, light microscopy is rarely sufficient to confirm the presence of SPOVs, but spore groups with a regular number of spores are indicative.

SPOVs are normally spherical or ovoid, as in *Amblyospora*, *Thelohania*, *Parathelohania*, *Vavraia*, and *Trachipleistophora* (Fig. 1.17a, Fig. 1.28c, and Fig. 1.29b) (Hazard & Oldacre 1975; Vávra et al. 1981, 1998). Microsporidia belonging to the genera *Chapmanium* (Hazard & Oldacre 1975), *Napamichum* (Larsson 1984), and *Ormieresia* (Vivarès et al. 1977) sporulate in fusiform SPOVs.

The spherical SPOVs of *Trichoduboscqia epeori*, a parasite of mayflies, are ornamented with usually four, more than 20 µm long, needlelike appendages (Batson 1982). They have an internal core of material similar to collagen. The number of projections varies from two to four, correlated with the number of spores enclosed (Léger 1926; Weiser 1961; Batson 1982). SPOVs are released into water from dead hosts, and the projections are likely to be floatation devices.

The SPOV of *Telomyxa glugeiformis* is an oval body (Fig. 1.17g–j) in which two spores are embedded in an electron-dense material (Léger & Hesse 1910; Codreanu & Vávra 1970; Larsson 1981a). Its shape resembles that of a microsporidian spore, and it was originally believed to be a single spore (Léger & Hesse 1910).

1.7.1.1 The Sporontogenetic Sporophorous Vesicle

The first deposited layer of electron-dense secretions on the surface of the sporont produced the vesicle, usually as a thin, electron-dense structure which progressively detaches from the plasma membrane, forming an envelope (Fig. 1.18a–c). Two kinds of sporontogenetic SPOVs exist:

1. A multicell SPOV, the most frequently occurring type, collects all sporoblasts inside a common envelope. Multicell vesicles are found in many microsporidia, such as the genera *Amblyospora* (Hazard & Oldacre 1975) and *Episeptum* (Larsson 1996). Multicell vesicles are usually prominent under the light microscope, appearing as more or less well-defined

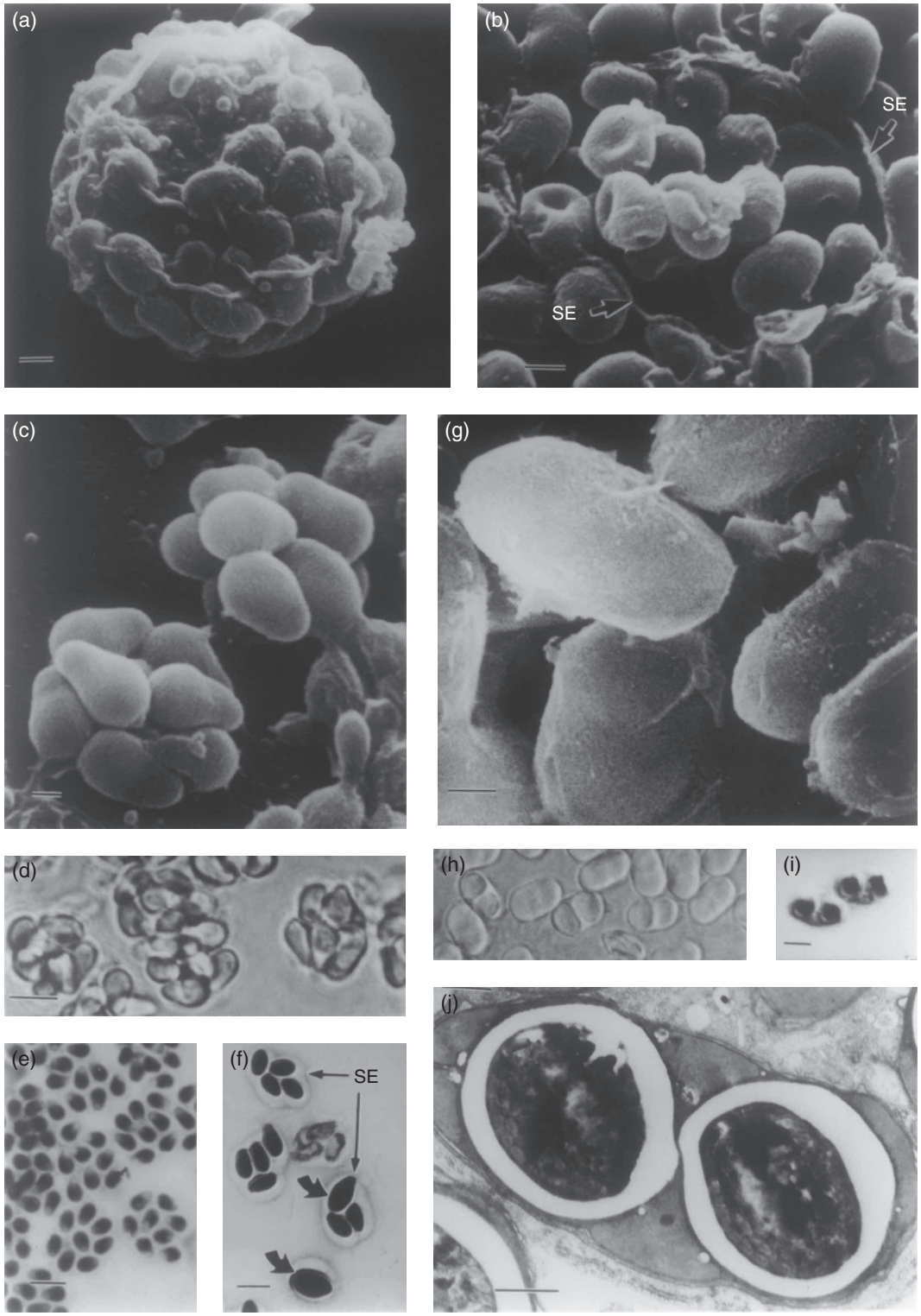

Figure 1.17 Gross morphology of the SPOV. (a, b) The merontogenetic SPOV of *Vavraia holocentropi*, complete and sectioned. (c–e) Three aspects of the octosporous SPOV of *Systenostrema candida*. (f) Tetrasporous SPOVs of *Gurleya dorisae* with two vesicles exhibiting macrospores (large arrows) and a reduced number of spores. (g–j) Four aspects of the disporous vesicle of *Telomyxa glugeiformis*. SEM (a–c, g), phase contrast (d, h); hematoxylin stain (e, f), Giemsa stain (i), TEM (j). Scale bars = 1 µm (a–c), 5 µm (d–f, h), 1 µm (g, i), 0.5 µm (j). SE, sporophorous vesicle envelope. Reprinted from Wittner, M., Weiss, L. M. (eds.) 1999. *The Microsporidia and Microsporidiosis*. ASM Press, Washington, DC.

packets of spores (Fig. 1.1b, d, and f, Fig. 1.17c–f, and Fig. 1.29e). In well-preserved samples, SPOVs are also visible by scanning electron microscopy (Fig. 1.28c). The number of spores in such vesicles can vary between two and many. In some microsporidian genera, the number is constant, and in others, it is variable. The number of spores per vesicle is a useful character for the identification of microsporidia at levels above the species. It is necessary to be careful when SPOVs with many spores are seen in the intestinal tissues of a host. Spore-loaded intestinal epithelium cells shed into the gut lumen can easily be mistaken for multisporous SPOVs (Fig. 1.21a and b).

2. If the SPOV envelope divides simultaneously with the plasmodium inside, finally enclosing each spore in a vesicle of its own, single-cell SPOVs are formed (Fig. 1.18d and e). Single-cell vesicles are characteristic of a small number of genera, *Tuzetia*, *Janacekia*, *Alfvenia*, *Nelliemelba* (Maurand et al. 1971; Larsson 1983d), and *Lanatospora* (Bronnvall & Larsson 1995b), and can normally only be seen using TEM. The individual SPOVs of *Janacekia adipophila* are visible around sporoblasts and immature spores in stained smears, due to stained inclusions of the episporontal space (Fig. 1.14 in Larsson 1992).

Structure of the Sporontogenetic Sporophorous Vesicle

The primordium of a SPOV either develops simultaneously all over the sporont and a complete envelope is released, as in the genus *Cystosporogenes* (Fig. 1.18a and b), or vesicle primordia appear spotwise over the surface of the sporont (Fig. 1.6e). The latter appears to be the more common occurrence. The envelope of the future SPOV is then released as blisters (Fig. 1.18c) which later join together to form a complete vesicle. This initiation is typical of *Tuzetia*-like microsporidia. These blisters are filled with electron-dense material (Fig. 1.6e) easily stained with hematoxylin stains, which makes the sporogonial stages appear spotted in stained smears (Fig. 1.18e).

The envelope of a SPOV is normally a thin layer, measuring only a few nanometers, as in *Cystosporogenes deliaradicae* (Fig. 1.18a). The layer sometimes has the appearance of a two-layered membrane, but in other species, it is clearly a uniform layer. Freeze-fracture studies of vesicles of *Tuzetia* and *Amblyospora* spp. have revealed that it is not a unit-type membrane (Vávra et al. 1986) (Fig. 1.10b).

Aberrant Types of Sporontogenetic Sporophorous Vesice

Only a few genera produce aberrant types of sporontogenetic SPOVs. Spores of the genus *Berwaldia* are enclosed in individual vesicle envelopes composed of a membrane-like coat supported by tubules. The SPOV appears folded and is attached at intervals to the exospore (Larsson 1981b; Vávra & Larsson 1994). The envelopes of *Telomyxa glugeiformis* (Fig. 1.18h), *Cryptosporina brachyfila* (Fig. 1.18i), and *Pegmatheca lamellata* (Larsson 1987) are thicker structures measuring up to about 30 nm. The envelope of *T. glugeiformis* has a layered texture different from that of the electron-dense exospore of the mature spore (Codreanu & Vávra 1970; Larsson 1981a), while the layered envelope of *C. brachyfila* is constructed like the exospore (Hazard & Oldacre 1975). In this species, stratified exospore material is produced twice, the first layer of secretions yielding the SPOV and the second the exospore (Fig. 1.18i). The vesicles of *Pegmatheca* spp. are even more unusual in that all sporonts generated by the last merogonic division remain together and their SPOVs adhere, even when containing mature spores (Hazard & Oldacre 1975; Larsson 1987) (Fig. 1.18j and k). Another unusual condition is seen in *Polydispyrenia* (Canning & Hazard 1982). The multinucleate meront does not release merozoites but remains undivided when it enters sporogony. A SPOV is formed at the onset of sporogony originating as a typical sporontogenetic SPOV but functioning as a merontogenetic vesicle in collecting all daughter cells produced by the meront.

1.7.1.2 The Merontogenetic Sporophorous Vesicle

In a small number of microsporidia, the dense material building the SPOV appears already during merogony (Canning & Hazard 1982). Great quantities of electron-dense material are deposited on the external surface of the plasma membrane of the meront (Fig. 1.18g and Fig. 1.28a). The result is an up to 165 nm-thick (*Vavraia culicis*), often amorphous cell wall (Fig. 1.18f), permeated by membranous channels and forming a surface labyrinth intermeshed with the host cell cytoplasm. At the time of sporogony, the sporogonial plasmodium retracts and membranous channels and labyrinth-like protrusions disappear, leaving the amorphous layer as a persistent envelope collecting all daughter cells originating from the meront. Finally, it is filled with mature spores (Fig. 1.17a and b). Characteristically, the envelope of a merontogenetic SPOV remains thick. This kind of envelope is produced by microsporidia of the genera *Pleistophora*, *Vavraia*, and *Trachipleistophora* (Fig. 1.18f and g and Fig. 1.28b and c). Each genus builds envelopes of characteristic structure: two or three layers of different electron density in *Pleistophora* (Canning & Nicholas 1980) and two thick, dense strata separated by a thin layer of lucent material in *Vavraia* (Canning & Hazard 1982) and *Trachipleistophora anthropophthera* (Vávra et al. 1998) (Fig. 1.18f). There is a uniformly dense layer in *Trachipleistophora hominis* (Hollister et al. 1996). In the genus *Trachipleistophora*, the envelope forms a tuft of 25–40 nm-wide fibers or tubules extending into the host cell cytoplasm (Weidner et al. 1997; Vávra et al. 1998) (see also Section 1.10.3).

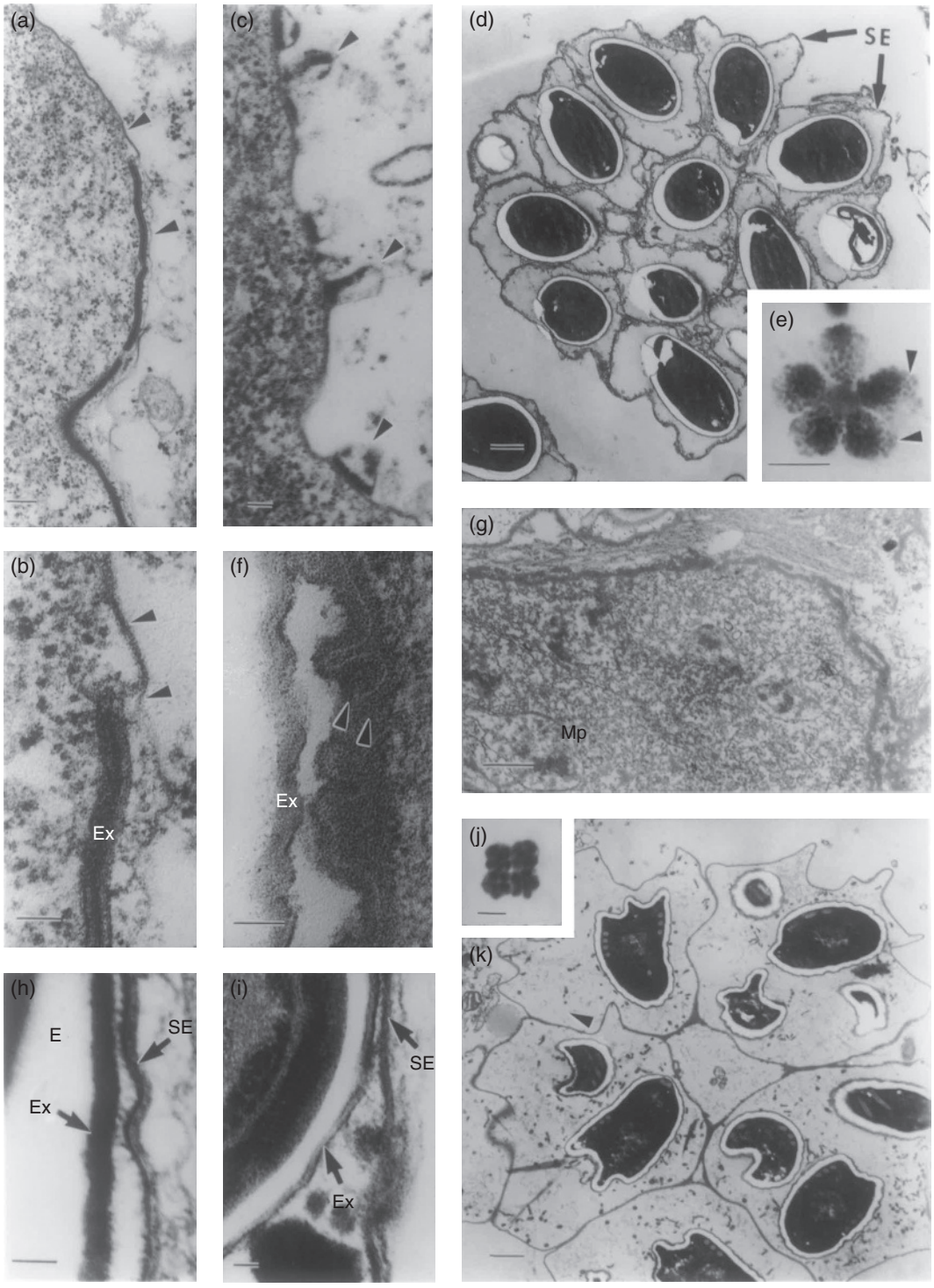

Figure 1.18 Ultrastructure of the SPOV. (a, b) Initiation over wide areas of the sporont surface (arrowheads indicate envelope) (*Cystosporogenes deliaradicae*). (c) Blister-like initiation (arrowheads) (*Tardivesicula duplicata*). (d) Mature spores enclosed in individual SPOVs (*Janacekia undinarum*). (e) Blister-like protuberances (arrowheads) of the individual vesicles stain darkly on the rosette-like dividing sporont (*Janacekia adipophila*). (f, g) Layered (arrowheads) merontogenetic SPOV of *Vavraia holocentropi* surrounding mature spores (f) and during initiation (g). (h, i) Unusual types of thick SPOVs from *Telomyxa glugeiformis* (h) and *Cryptosporina brachyfila* (i), the envelope of this species is identical to the exospore. (i, k) Connected SPOVs (*Pegmatheca lamellata*). TEM (a–d, f–i, k), hematoxylin stain (e, j). Scale bars = 100 nm (a), 50 nm (b, c, f, h, i), 1 µm (d), 10 µm (e), 0.5 µm (g, k), 5 µm (j). (j–k). E, endospore; Ex, exospore; Mp, merogonial plasmodium; SE, sporophorous vesicle envelope. Reprinted from Wittner, M., Weiss, L. M. (eds.) 1999. *The Microsporidia and Microsporidiosis*. ASM Press, Washington, DC.

1.7.1.3 The Episporontal Space and Inclusions

The episporontal space is defined as the cavity between the envelope of the SPOV and the sporont wall (Vávra, 1984). At the onset of sporogony, the episporontal space is small and may not even be continuous over the whole surface of the parasite. The episporontal space, however, becomes important as the primordial envelope of the SPOV detaches more and more from the sporont, or its daughter cells, and the volume of the vesicle increases.

The episporontal space is not an empty space because it contains a variety of electron-dense inclusions. These structures are more numerous in the early phase of sporogony, with a peak when sporoblasts are released. Simultaneously with the maturation of the spores, the quantity of inclusions decreases, and SPOVs with ripe spores usually have only remnants of this material. Exceptionally, this material disappears almost completely, as in *Hyalinocysta* spp. (Hazard & Oldacre 1975; Larsson 1989a).

The inclusions are of three kinds: fibrous, tubular, or crystalline (granular). In many cases, the individual forms are combined. Inclusions are also dynamic structures changing in quantity and appearance during SPOV maturation.

Thin, fibrous material is a regular component of SPOVs, as in *Amblyospora capillata* (see Larsson 1983a) and *Thelohania maenadis* (Vivarès 1980). The fibrils often traverse the episporontal space from the surface of the sporont to the envelope of the SPOV. The fibrils of *Trichotuzetia guttata* have a distinct substructure and are arranged in a regular manner (Fig. 1.19a and b).

In *Trichoctosporea pygopellita*, fibrous material, persisting as exospore projections from the mature spore (Fig. 1.9f–h), occurs together with a unique type of inclusion appearing as arrays of globular chambers (Larsson 1994b).

The episporontal space of *Tuzetia*-like microsporidia is traversed by nonseptate tubules, which are narrow in *Tuzetia* and *Lanatospora* (Voronin 1989b) and wide in *Janacekia* (Fig. 1.9d and e and Fig. 1.19c) (Weiser & Žižka 1975; Loubès & Maurand 1976). In *Berwaldia* spp., tubular material is so closely associated with the envelope of the SPOV that it appears two-layered (Larsson 1981b). *Thelohania*-like microsporidia have tubular inclusions of two different kinds. The lumen of the narrow tubules is often filled with electron-dense material, and the tubular nature is not always obvious. The wide tubules, which are projections from the sporoblast wall, are septate and have a wall constructed like the exospore layer (Fig. 1.19e and f). *Cystosporogenes deliaradicae* (Larsson et al. 1995) shares characteristic tubules with *Agmasoma penaei* (Fig. 1.19e) (Hazard & Oldacre 1975). In *Glugea stephani*, three different kinds of tubular structures have been defined, and a numbered system was proposed (Takvorian & Cali 1983).

Inclusions in the form of parallel thick-walled tubules forming a kind of labyrinth within the episporontal space are characteristic of SPOVs of the genus *Vairimorpha* (Weiser & Purrini 1985; Moore & Brooks 1992, 1994) but occur also in some other microsporidia as, for example, in *Toxoglugea* (Fig. 1.19d).

Crystalline or granular material is a prominent feature of newly formed SPOVs of *Amblyospora* spp., also visible in light microscopic preparations (Fig. 1.19g). The crystals are successively reduced during maturation of the spores, but a small number of crystals are normally also present in old vesicles. Still greater production of crystalline material is seen in *Cryptosporina brachyfila*, in which spores are more or less obscured by the crystals (Hazard & Oldacre 1975). At the ultrastructural level, crystals are composed either of a uniform electron-dense material, as in *Amblyospora* (Fig. 1.19g) (Hazard & Oldacre 1975) and *C. brachyfila* (Fig. 1.21i), or of material of variable electron density and texture, as in *Napamichum* spp. (Fig. 1.19h and i).

Little is known about the chemical nature of the secretory material of the episporontal space, but the close connection, and sometimes structural similarity, to the exospore suggests that the exospore and the inclusions have the same or similar chemical composition. Weidner and collaborators identified protein fibers in the episporontal space of an unidentified *Thelohania* species as cytokeratin intermediates and desmosomal analogs (Weidner et al. 1990).

Various functions have been attributed to episporontal secretions. An older term for these structures, "metabolic granules," vaguely suggested some role in the metabolism of the organism (Hazard & Oldacre 1975). More specifically, it has been proposed that the secretions are surplus material from the production of sporoblasts which is more or less used up during the formation of spores (Larsson 1986b). The observation that some types of secretory material are structurally identical to exospore material (Fig. 1.19e) supports this idea. The other interpretation is based on the tendency of this material to form tubules, channels, or strands sometimes connecting the outer layer of sporoblasts or immature spores with the wall of the SPOV, for example, as in *Chapmanium cirritus* (Hazard & Oldacre 1975), *Trichotuzetia guttata*, and *Janacekia debaisieuxi* (Fig. 1.19a–c). This finding suggests a conductive function, which was experimentally demonstrated by Overstreet and Weidner (1974) in *Inodosporus spraguei*. For more information on different kinds of SPOVs and secretory inclusions, see Larsson (1986b).

1.7.2 Exospore-Derived Envelopes

Some members of the families Mrazekiidae and Tuzetiidae enclose their spores in exospore-derived envelopes which can be mistaken for individual SPOVs of the *Tuzetia* type.

1. *Mrazekiidae*. The sporoblasts of Mrazekiidae generate a thick, stratified exospore in which the basal layer is wide and uniform and the surface layer resembles a double membrane. The two-layered exospore remains unchanged in mature spores of *Bacillidium strictum* (Larsson 1992), *Jirovecia caudata* (Larsson 1990b), and probably also *Hrabyeia*

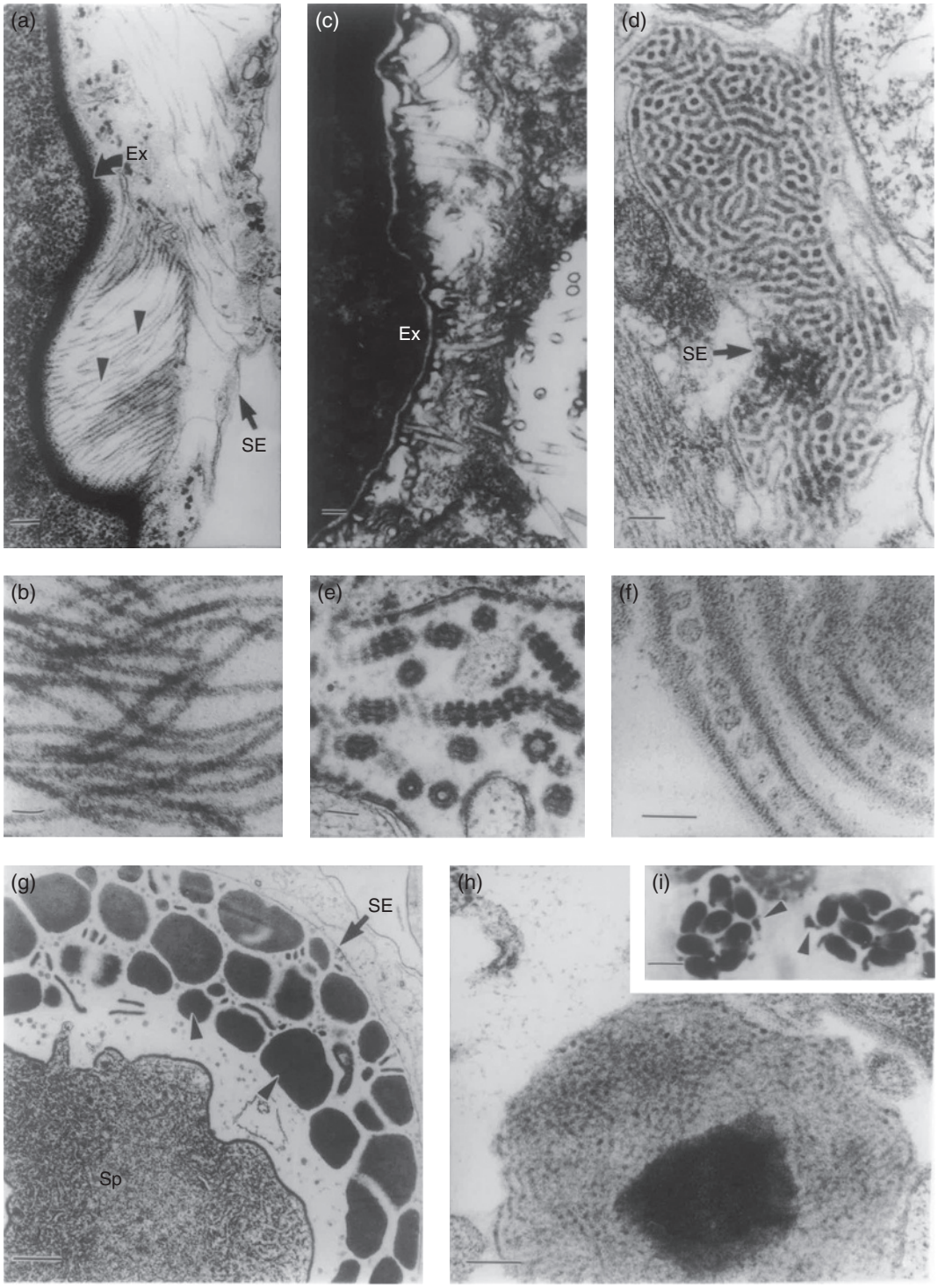

Figure 1.19 Exospore projections and inclusions of the episporontal space. (a, b) Fibrous material (arrowheads) connecting the exospore with the envelope (*Trichotuzetia guttata*). (c) Wide tubules from exospore to envelope (*Janacekia debaisieuxi*). (d) Labyrinth-like tubular material (arrowheads) (*Toxoglugea variabilis*). (e) Tubular exospore-derived material (*Agmasoma penaei*). (f) Septate, exospore-derived tubules (*Systenostrema candida*). (g) Uniform amorphous crystal-like material (arrowheads) (*Amblyospora* sp.). (h, i) Two-layered crystals (arrowheads) (*Napamichum dispersus*). TEM (a–h), hematoxylin stain (i). Scale bars = 100 nm (a, c–e, h), 50 µm (b, f), 0.5 µm (g), 5 µm (i). Ex, exospore; SE, sporophorous vesicle envelope; Sp, sporont. Reprinted from Wittner, M., Weiss, L. M. (eds.) 1999. *The Microsporidia and Microsporidiosis*. ASM Press, Washington, DC.

xerkophora (Lom & Dyková 1990). In *Bacillidium filiferum*, the surface layer is released in the shape of filiform projections (Larsson 1989c), while in *Jirovecia brevicauda*, the surface layer is transformed into tubular projections (Larsson & Götz 1996). In both species, only the wide basal layer remains as the exospore of the mature spore. In *Bacillidium criodrili* (Larsson 1994a), *Jirovecia involuta* (Larsson 1989b), and *Rectispora reticulata* (Larsson 1990d), the surface component of the exospore of the sporoblast is completely released from the basal layer, which remains as the exospore

of the mature spore. The surface layer forms a complete sac around the mature spore (Fig. 1.20a–c), making it indistinguishable from an individual SPOV.

2. *Tuzetiidae*. Spores of microsporidia of the family Tuzetiidae are enclosed in individual SPOVs generated by the sporont (Fig. 1.18d). In two of the species, *Alfvenia nuda* (Larsson 1983d, 1986b) and *Nelliemelba boeckella* (Milner & Mayer 1982), a second envelope is formed internally to the SPOV when surface material from the layered exospore of the sporoblast is released. At least in *A. nuda*, a part of the sporoblasts retains the complete exospore, with the result that spores with double and single envelopes occur together.

1.7.3 Sporont-Derived Sacs

The dense material remains as a cover on the plasma membrane of the sporont and together with it forms a persistent cyst-like sac which collects the spores (Fig. 1.20d–g). This is typical of *Chytridiopsis*- and *Metchnikovella*-like microsporidia, the spores of which are produced endogenously (Desportes & Théodoridès 1979; Purrini & Weiser 1984; Beard et al. 1990; Larsson et al. 1997b). In this process, vacuoles appear within the sporogonial plasmodium, separating each nucleus with a surrounding zone of cytoplasm from each other. Each of these units matures into a sporoblast, and the vacuole membranes are incorporated as the plasma membrane of the sporoblast. Thus, the plasma membrane of the sporogonial plasmodium is not incorporated into the spore wall but remains as the internal layer of a complex envelope (Fig. 1.20e). In both *Metchnikovella*- and *Chytridiopsis*-like microsporidia, enveloped sporogony in sporont-derived sacs occurs together with a sporogony in which spores may be collected in a parasitophorous vacuole of host cell origin (Fig. 1.20f and h) (Vivier & Schrével 1973; Larsson 1993).

The sporont-derived sacs of *Metchnikovella*-like microsporidia are long, fusiform, or nearly cylindrical structures with blunt or threadlike poles (Fig. 1.20h) (Vivier & Schrével 1973; Desportes & Théodoridès 1979; Ormières et al. 1981). *Chytridiopsis*-like microsporidia sporulate in spherical sacs (Fig. 1.20f and g).

1.7.4 Parasitophorous Vacuole as Envelope of Parasite Origin?

Several microsporidian genera develop in the host cell in a vacuolar space limited by a thin membrane. This membrane appears already on the sporoplasm and adheres tightly to its plasma membrane. During development, the outer membrane detaches progressively, and a vacuolar space called parasitophorous vacuole develops in which the developmental stages and later spores are collected. There are divergent opinions whether the vacuole is of host or parasite origin. The first opinion is presently prevailing, but the parasite origin cannot be completely ruled out (see Section 1.9.2 for more details).

1.8 CYTOLOGICAL ANOMALIES IN MICROSPORIDIA

Cytological anomalies, reported or visible in micrographs, are not unusual in microsporidia. Many of them are obviously artifacts caused by the techniques used or can be explained by external influences on the host. Others stem from internal conditions within the microsporidium itself. A third kind of anomaly involves the presence of foreign inclusions in the microsporidian cell.

1. *External influences*. Teratological development of microsporidia is, for example, known to be caused by drugs administered to the host (Liu & Myrick 1989; Ditrich et al. 1994). Contact with another microorganism is the probable explanation for a number of anomalies seen in *Cystosporogenes deliaradicae* (Larsson et al. 1995). The anomalies were observed in host specimens simultaneously infected by the fungus *Strongwellsea castrans*, and teratological spores were especially frequent in the proximity of hyphae.
2. *Internal conditions*. Frequent anomalies include incompletely separated sporoblasts, which are especially common in microsporidia with rod-shaped spores, and disorganization of the polar filament of mature spores (Vávra 1962; Becnel et al. 1989; Larsson 1989c, 1990d, 1995). Anomalies in the polar filament are visible as disturbed coiling, supernumerary and undifferentiated polar filament coils, or coils with an increased number of centers. There are also frequent reports of abortive sporogony, e. g. in *Edhazardia aedis* (Becnel et al. 1989) and *Hyalinocysta expilatoria* (Larsson 1983c), in which a number of sporoblasts fail to mature to spores.

Some observations of aberrant cytology can probably be explained as reductions. At least two species of microsporidia, *Amblyospora capillata* (Larsson 1983a) and *Napamichum aequifilum* (Larsson 1990a), have polar filaments that appear to be isofilar. However, it is more likely that the filaments are anisofilar but with the posterior narrow part reduced. Both species belong to genera with distinct cytological characteristics and anisofilar polar filaments. The absence of SPOVs in the sporogony of *Nudispora biformis* is probably another example of reduction (Larsson 1990c). This microsporidium is

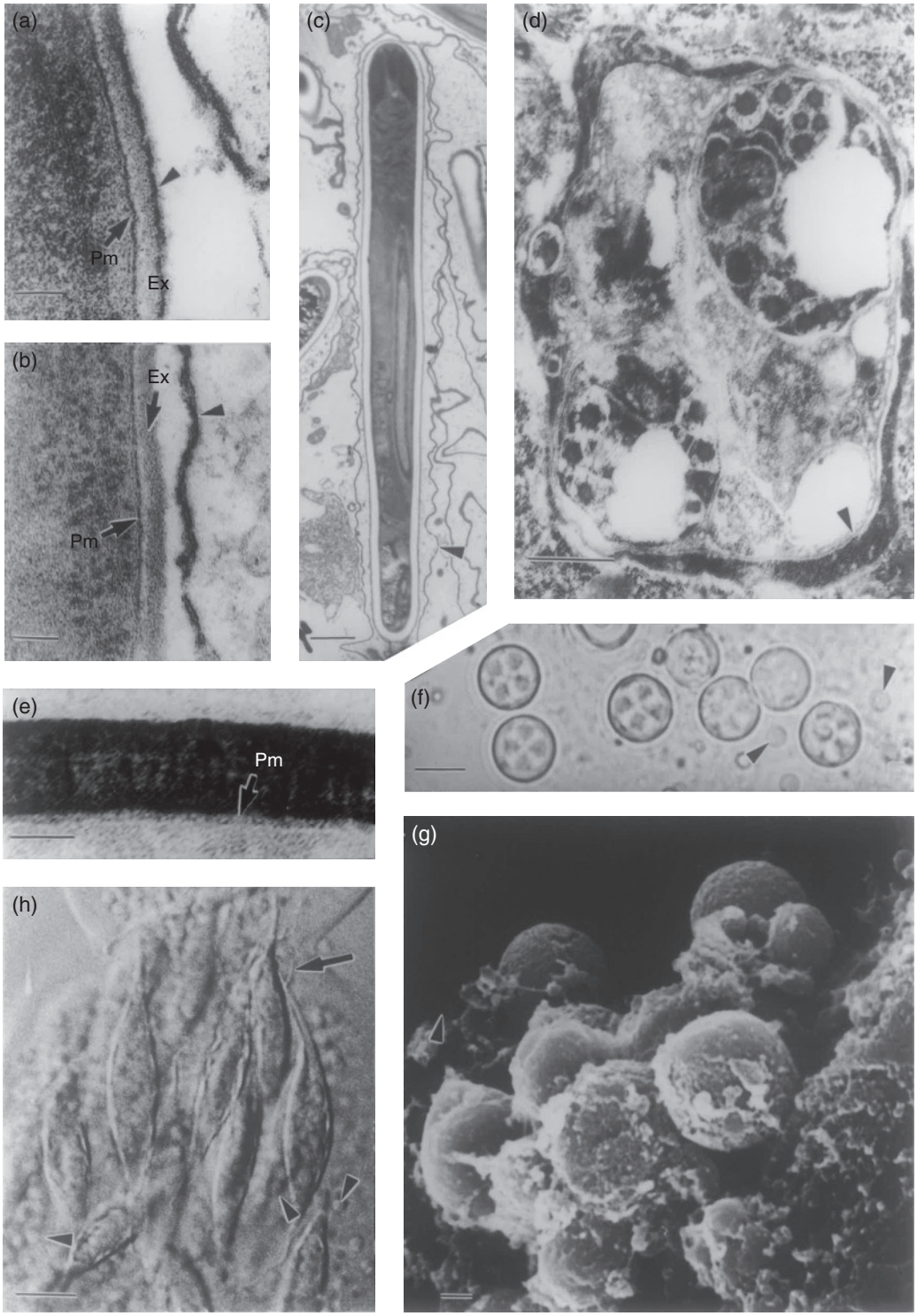

Figure 1.20 Exospore-derived envelopes and sporont-derived sacs. (a–c) Two steps in the initiation of an exospore-derived envelope. Arrowheads indicate the surface layer of the exospore that forms the envelope and the released envelope surrounding a mature spore (*Jirovecia involuta*). (d) External part of a sporont which is transformed into an envelope (arrowheads) (*Intexta acarivora*). (e–g) Thick-walled cyst-like sacs of *Chytridiopsis trichopterae*: (e) showing the mature envelope; (f) living cysts enclosing spores, arrowheads indicate spores of the unenveloped sporogony; and (g) mature cysts. (h) Live fusiform sacs of an *Amphiacantha* species (arrows indicate threadlike projections, arrowheads spores in sacs and free in the cytoplasm). TEM (a–e), phase contrast (f, h), SEM (g). Scale bars = 50 nm (a, b, e), 1 µm (c, g), 0.5 µm (d), 5 µm (f, h). Ex, exospore; Pm, plasma membrane. Reprinted from Wittner, M., Weiss, L. M. (eds.) 1999. *The Microsporidia and Microsporidiosis*. ASM Press, Washington, DC.

cytologically similar to *Thelohania*-like microsporidia, which sporulate in SPOVs, and it behaves identically in both merogony and sporogony, producing episporontal space inclusions of the *Thelohania* type.

3. A different kind of anomaly is the presence of cytological inclusions of foreign origin. Three reports classified the foreign bodies as virus particles. The earliest observation was made by Liu (1984), who described particles resembling bee viruses in the cytoplasm of lysed spores of the honeybee parasite *Nosema apis*. Others have described intranuclear particles, which were spherical and aggregated, having a lucent periphery and an electron-dense center and measuring 20–25 nm in diameter. The first observation was from two unidentified species of the family Thelohaniidae (Larsson 1988b), and the second from *Trichotuzetia guttata* (Vávra et al. 1997).

1.9 MICROSPORIDIA-INDUCED EFFECTS ON HOST CYTOLOGY

The host cell is more or less visibly affected by the development of a parasite, but a clear pathogenic effect caused by a microsporidium is apparent only during the sporogony of the parasite (Fig. 1.21). In earlier stages, the microsporidium behaves more like a cellular symbiont with whom the host cell is cooperating. The following paragraphs mention general effects of microsporidia on the cytology of the host cell. The topic was reviewed by Weissenberg (1976), but much new information has appeared after that.

1.9.1 Association with Host Cell Organelles

On rare occasions, microsporidia establish close associations with specific organelles of the host cell. *Chytridiopsis* species develop in such close association with the host nucleus that the sporulating microsporidium rests in an invagination of the nuclear envelope (Fig. 1.21e) (Sprague et al. 1972). Similarly, *Enterocytozoon bieneusi* is usually abutted to the enterocyte nucleus (Desportes-Livage et al. 1996) (Fig. 1.22f). A location close to the host nucleus is also frequent in *Encephalitozoon hellem*, as is the association of microsporidia with host cell mitochondria (Fig. 1.22d and Fig. 1.23b). *Buxtehudea scaniae*, another example, provokes the mitochondria of the host cell to aggregate closely around sporulating microsporidia, creating a frame-like structure (Fig. 1.21d). *Nucleospora salmonis* is found within the host cell nucleus. Other microsporidia, such as *Janacekia debaisieuxi*, induce lysis (Maurand 1973; Weiser 1976a; Larsson 1983d), whereby the walls of infected cells are destroyed and the infected tissue is transformed into a syncytium, a cell soup in which thousands of microsporidian cells are dispersed among nuclei and organelles of the host cells.

1.9.2 The Parasitophorous Vacuole as Host Cell Product?

Some microsporidia, such as *Encephalitozoon* spp. and *Glugoides intestinalis* (Larsson et al. 1996), are known to be separated from the host cell cytoplasm not only by their plasma membrane, but by another membrane, which forms an additional boundary, separating the microsporidium from the cytoplasm of the host cell. This boundary membrane is seen already on the sporoplasm and early meronts and is tightly applied to the outer face of the PP membrane (Fig. 1.25a and b). During development, this membrane progressively detaches from the meront surface, first visible as a kind of vacuolar blebs between the plasma membrane of the parasite and the vacuolar membrane (Fig. 1.26e). These blebs progressively merge (Fig. 1.25c). Finally, a large vacuole is formed in which the dividing meronts partly adhere to the vacuolar membrane in a tight junction manner (Weidner 1976b) (Fig. 1.27f). Sporoblasts and spores detach from the membrane and lie freely in the center of the vacuole (Fig. 1.27e). The membrane-lined cavity thus formed around the microsporidium and its developmental stages is called a parasitophorous vacuole (Barker 1975). The membrane bordering the vacuole forms a rich canopy of blebs protruding into the vacuolar lumen (Weidner 1976b) (Fig. 1.27a). The parasitophorous vacuole is generally considered to be of host cell origin, although the way in which it is formed has not been explained satisfactorily (Bohne et al. 2011; Fasshauer et al. 2005). A system of a branching network of proteinaceous filaments within the parasitophorous vacuole of *Encephalitozoon* was described (Canning et al. 1994; Ghosh et al. 2011). Similarly, an intravacuolar material forms septa in the parasitophorous vacuole of *E. intestinalis* (Cali et al. 1993) (Fig. 1.25e and d). However, the presence of such intravacuolar materials seems to favor the hypothesis that the parasitophorous vacuole of *Encephalitozoon* actually is a special kind of a SPOV and that the intravacuolar filaments and other materials are the homologs of the secretory material in SPOVs of other microsporidia (Vávra, unpublished).

1.9.3 Host Cell Hypertrophy

A common effect of microsporidiosis is hypertrophic enlargement of the host cell, including the nucleus (Weissenberg 1976). In insects infected by microsporidia, the effects are especially visible on the nuclei of the fat cells (Liu 1972; Martins & Perondini 1974). Not only the number of nuclei but also the volume of chromosomes is increased (Pavan et al. 1969). It is

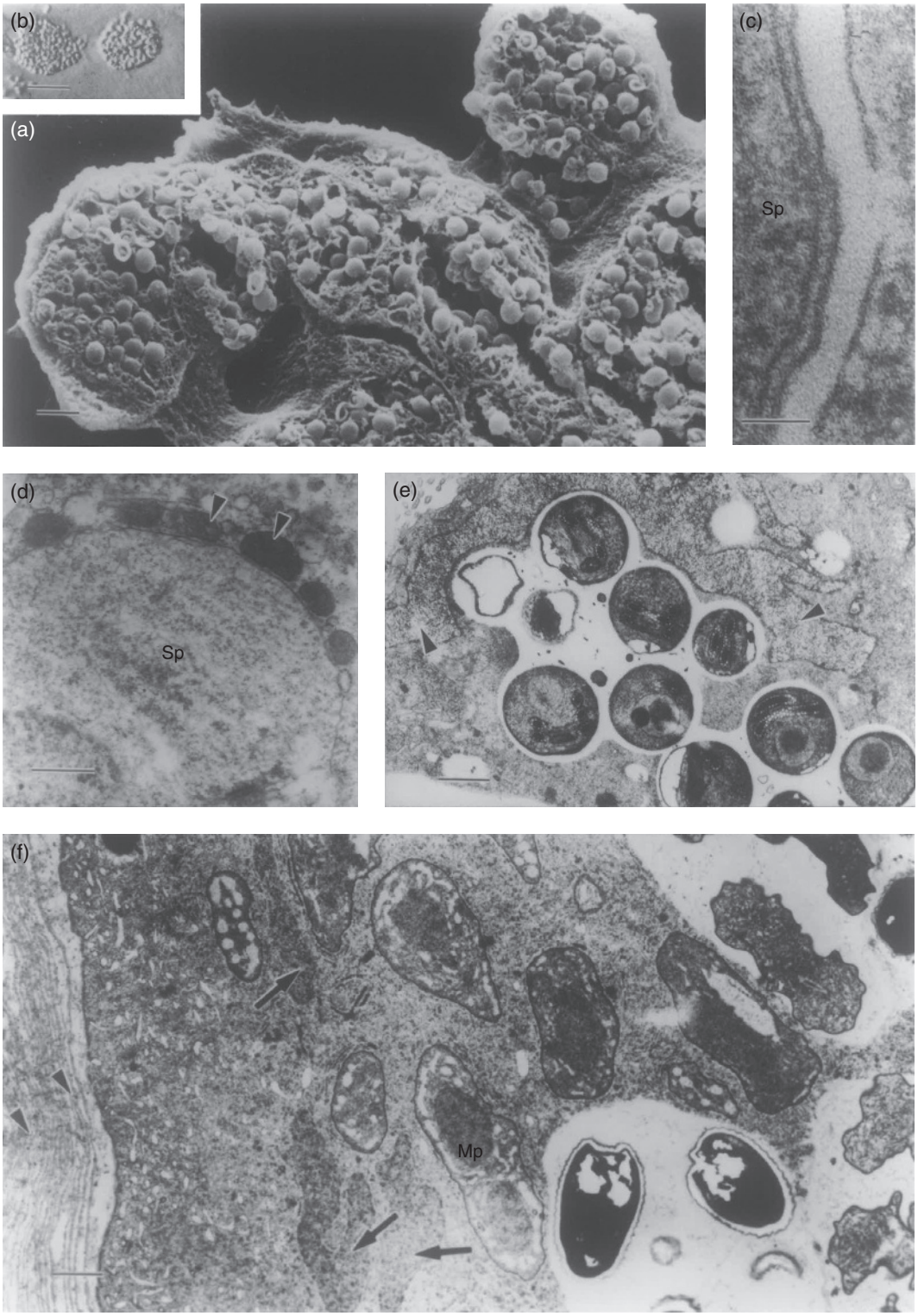

Figure 1.21 Microsporidian-induced effects on the host cytology. (a) Gut epithelium cells filled with microsporidian spores (*N. apis*). (b) Epithelium cells released into the gut lumen which can be mistaken for multisporous SPOVs (*N. apis*). (c) A parasitophorous vacuole (*Glugoides intestinalis*). (d) Host cell mitochondria (arrowheads) accumulated at the surface of a sporont (*Buxtehudea scaniae*). (e) Host nucleus (arrowheads) enveloping spores of *Chytridiopsis trichopterae*. (f) The *Glugea* xenoma with multilayered wall (arrowheads) and with the most immature stages of the microsporidian at the periphery (arrows indicate host nuclei) (*Glugea anomala*). SEM (a), interference phase contrast (b), TEM (c–f). Scale bars = 5 µm (a), 25 µm (b), 50 nm (c), 0.5 µm (d), 1 µm (e, f). MP, merogonial plasmodium; PM, plasma membrane; S, spore; SN, sporont; Sp, sporogonial plasmodium. Reprinted from Wittner, M., Weiss, L. M. (eds.) 1999. *The Microsporidia and Microsporidiosis*. ASM Press, Washington, DC.

unusual for the nuclei of host cells to be accidentally invaded, as in infections caused by *Nosema bombycis* (Takizawa et al. 1973) and *Nosemoides simocephali* (Loubès & Akbarieh 1977). Some microsporidia, however, specifically infect the nuclei of host cells as, for example, *Nucleospora salmonis* (Hedrick et al. 1991) and *Enterospora* species (Stentiford & Bateman 2007; Stentiford et al. 2007).

The most striking example of hypertrophic growth is the formation of giant cells filled with microsporidian spores (a xenoma). It is frequently encountered in fish but also in other hosts (Lom & Dyková 2005). The classical example is the infection by *Glugea anomala* (Canning et al. 1982), a common parasite of epidermal cells of sticklebacks (*Gasterosteus* and *Pungitius* spp.), provoking a complex host–parasite association. The invaded cell is ruled by the parasite, and the host nucleus is forced to divide. The result is a xenoma, a giant epithelial cell containing thousands of host nuclei and millions of microsporidia (Fig. 1.21a and b). It is stratified, with mature spores in the center and immature stages at the periphery (Fig. 1.21f). The xenoma is externally covered by a multilayered coat into which fibroblasts and epithelial fragments are incorporated.

1.9.4 Infections of the Digestive Tract Epithelium

In the epithelium of the digestive tract, the high regenerative capacity compensates to some extent for destruction, and microsporidia-filled epithelial cells are shed into the gut lumen (Fig. 1.21b). Such spore-filled cells can easily be mistaken for multisporous SPOVs.

1.10 COMMENTS ON THE STRUCTURE OF SOME HUMAN OPPORTUNISTIC MICROSPORIDIA

Only human microsporidia with enough structural data to allow comparison with other microsporidia are considered here. The review is only covering the cytology. Information on the biology of the respective microsporidia considered here can be found in Chapter 15 of the present volume.

1.10.1 *Enterocytozoon bieneusi*

Enterocytozoon bieneusi Desportes, Le Charpentier, Galian, Bernard, Cochand-Priollet, Laverne, Ravisse, and Modigliani, 1985, occurs relatively frequently in enterocytes of the small intestine of many mammals and birds, and it is probably the most frequent microsporidian parasite of humans (Vávra & Lukeš 2013). The ultrastructure was described by Desportes et al. (1985), Cali and Owen (1990), Desportes-Livage et al. (1991, 1996), Hilmarsdottir et al. (1993), and Orenstein (1991).

All data on the fine structure of the organism have been based on biopsy materials. The organism is apparently sensitive to fixation procedures, and some of its recognized ultrastructural characters (the rare presence of membranes, the paleness of the cytoplasm in early stages, and the extremely dilated perinuclear cisternae) may be due to the handling of the material prior to fixation. When ferriosmium fixation is used, better preservation of cytoplasmic elements is achieved (Hilmarsdottir et al. 1993; Desportes-Livage et al. 1996).

Enterocytozoon bieneusi is monomorphic and has isolated nuclei throughout its life cycle (Cali & Owen 1990). The nuclei in diplokaryotic arrangement reported in the original description were probably closely adjacent nuclei following karyokinesis. The sausage-like nuclei encountered in early plasmodia are evidently nuclei ready for rapid sequential mitoses (Fig. 1.22d), a prerequisite for an organism living in short-lived enterocytes. Spindle plaques were seen positioned across the short axis of the nucleus, suggesting that splitting of chromosome chromatids occurs first without physical separation into individual nuclei (Cali & Owen 1990). Nuclear divisions evidently take place in rapid sequence, as deeply lobed nuclei, the transition between long, sausage-like nuclei and round nuclei, are rarely seen (Orenstein, unpublished data). Actual karyokinesis, however, was observed only once, with the spindle plaques positioned across the short axis of the sausage-like nucleus in an invagination of the nuclear membrane, giving the elongate nucleus a dumbbell form (Spycher, unpublished data) (Fig. 1.22e). Synaptonemal complexes were not seen in *E. bieneusi* nuclei. All stages occur in direct contact with the cytoplasm of the enterocytes in the zone between the host cell nucleus and the brush border. The parasites are often wedged into a shallow depression of the enterocyte nucleus (Fig. 1.22f) and surrounded by host cell mitochondria adhering to the PP membrane (Fig. 1.22d and Fig. 1.23b). Merogony in its classical sense (as a multiplicative stage) probably does not occur in *Enterocytozoon* or is very limited. Two adjacent parasite cells abutted without intervening host cell cytoplasm were seen (Cali & Owen 1990; Orenstein, unpublished data), but the actual division was not observed. The isolated locations of individual *Enterocytozoon* cells in enterocytes indicate that the infection starts as a single, uninucleate cell (Fig. 1.22c) which develops into a multinucleate plasmodium, in which organelles of future spores differentiate (Fig. 1.23b). The only cell division observed so far was that taking place during sporoblast formation (Fig. 1.24a).

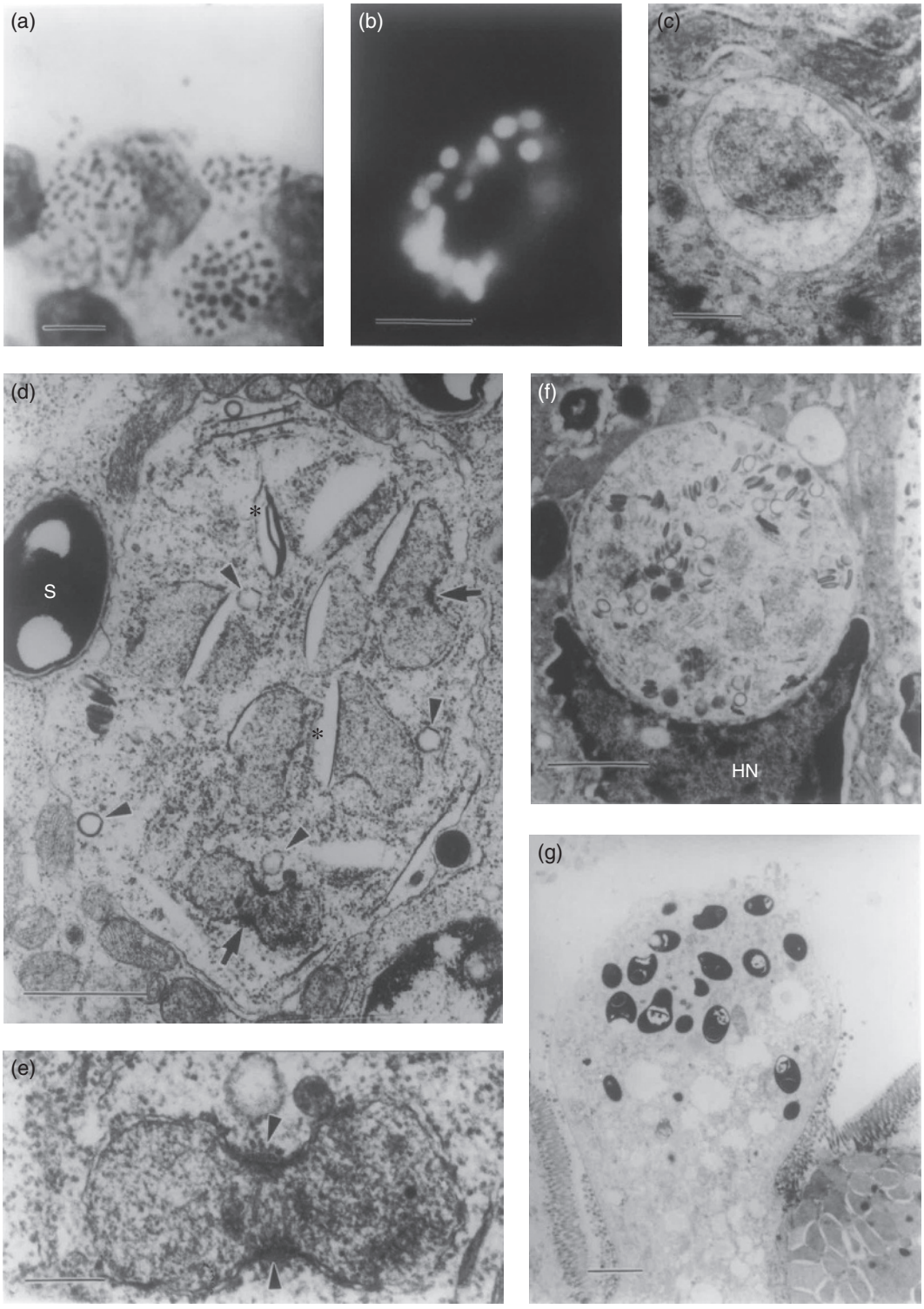

Figure 1.22 *Enterocytozoon bieneusi*. (a) Groups of spores originating from an individual plasmodium (Giemsa stain). (b) Spores of a sporogonial plasmodium in intestinal biopsy (fluorescence, Calcofluor staining). (c) Uninucleate, initial stage. (d) Multinucleate plasmodium with elongate nuclei, some of which are dividing (arrows). Expanded perinuclear cisternae contain dense material (asterisks). First primordia of the extrusion apparatus (possible polar sac) appear as dense rings (arrowheads). (e) Dividing nucleus as in (d). Spindle plaques (arrowheads) and the spindle are situated across the shorter axis of the nucleus. (f) Association of a multinucleate plasmodium with the nucleus of the host enterocyte. (g) Infected enterocyte with spores is released into the intestine lumen. Scale bars = 5 µm (a, b), 0.5 µm (c), 1 µm (d), 250 nm (e), 2 µm (f, g). All images TEM (c–g). HN, host cell nucleus; S, spore. Reprinted from Wittner, M. and Weiss, L. M. (eds.) 1999. *The Microsporidia and Microsporidiosis*. ASM Press, Washington, DC.

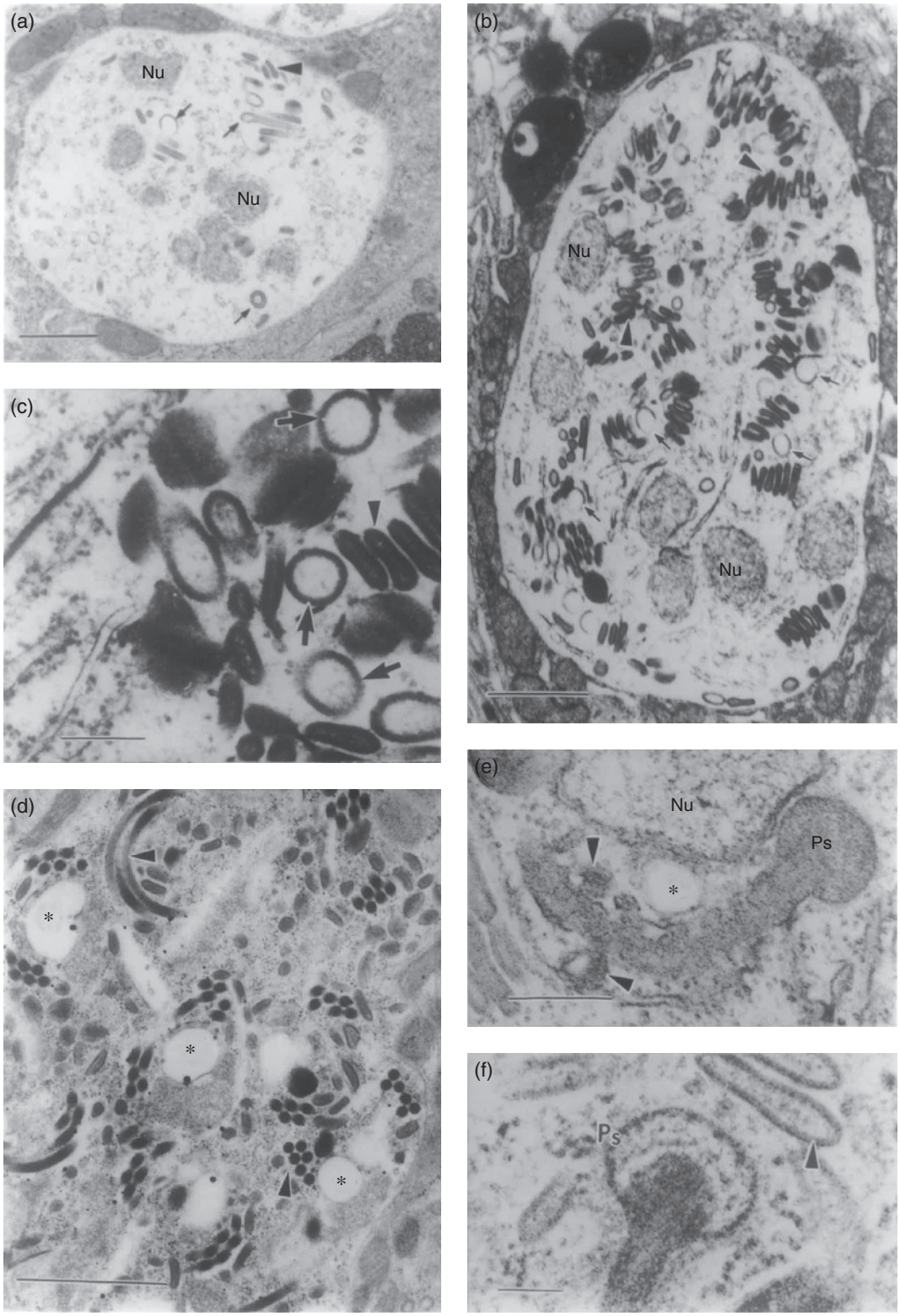

Figure 1.23 Formation of extrusion apparatus elements in multinucleate plasmodia of *E. bieneusi*. Polar sac (?) primordia are shown by arrows, polar filament primordia by arrowheads. (a) Initial stage. (b) Advanced sporogonial plasmodium. (c) Detail at high magnification. (d) More advanced plasmodium. A vacuole representing the primordium of the polaroplast and of the future posterior vacuole is associated with each nucleus (*). (e) Both the polar sac and the vacuole (*) are associated with the nucleus. Vesicular outgrowth of the polar filament probably represents the formation of the polaroplast (arrowheads). (f) Detail of the polar sac. All images TEM. Scale bars = 1 µm (a, b, d), 250 nm (c, e), 100 nm (f). Nu, nucleus; Ps, polar sac. Reprinted from Wittner, M., Weiss, L. M. (eds.) 1999. *The Microsporidia and Microsporidiosis*. ASM Press, Washington, DC.

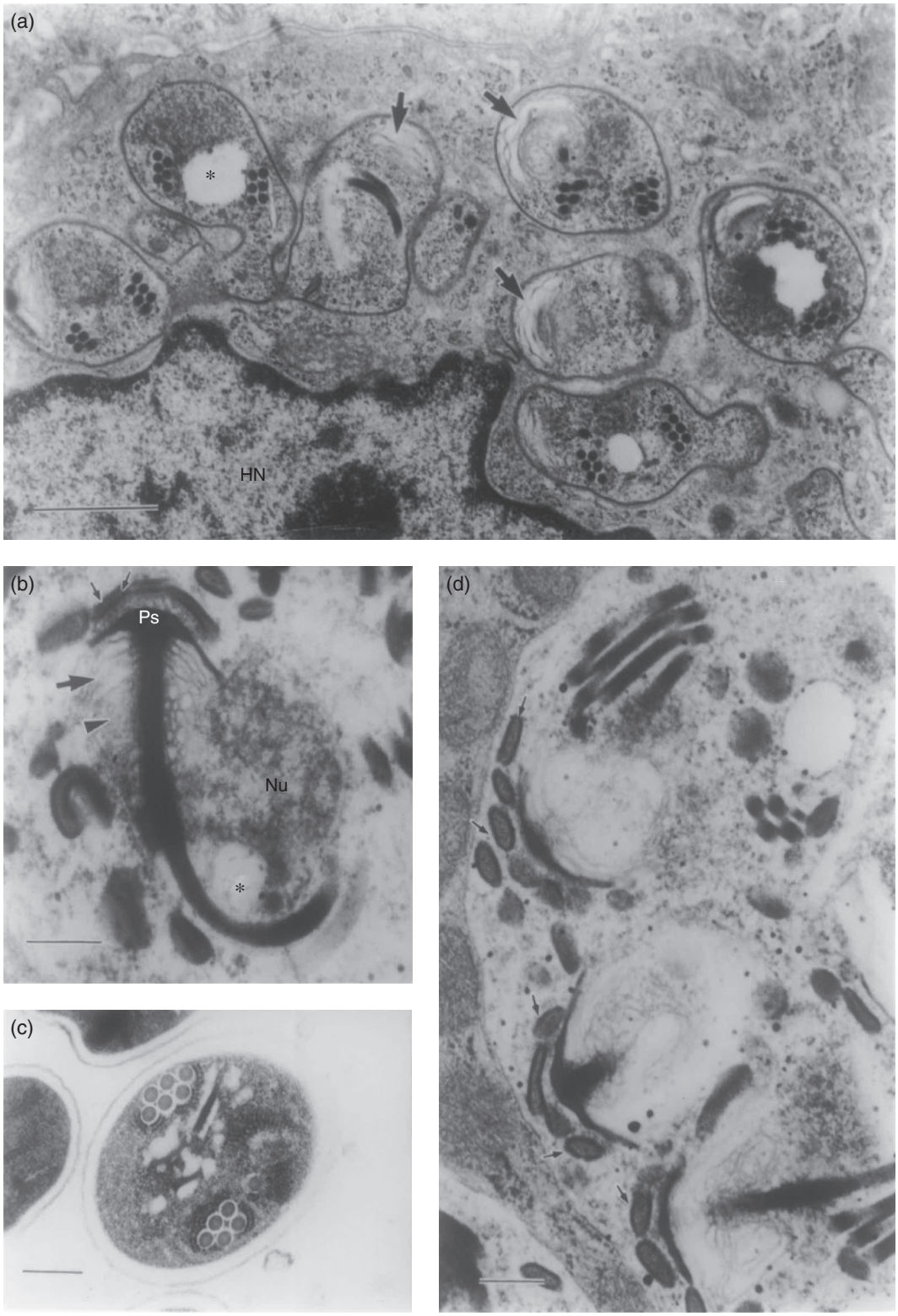

Figure 1.24 Spore formation in *Enterocytozoon bieneusi*. (a) Origin of the sporoblasts. In the sporoblast, a lamellar polaroplast is formed (arrows) and the future posterior vacuole (*) starts to appear. Polar filament coils are already organized in the final form. (b) Detailed view of the polar sac, polar filament, lamellar polaroplast (large arrow), vesicular polaroplast (arrowhead), nucleus, and future posterior vacuole (*). Note several dense vesicular structures above the polar sac and the opaque material between these vesicles and the polar sac (small arrows). (c) Nearly mature spore with a very thin exospore, relatively thick endospore, and characteristically coiled polar filament forming two rows. (d) Beginning of sporoblast formation. The anterior parts of the extrusion apparatus assemble near the plasmodium surface. Note that each polar sac is exteriorly lined with elongated vesicles (small arrows). All images TEM. Scale bars = 1 µm (A), 250 nm (b–d). Nu, nucleus; HN, host cell nucleus; Ps, polar sac. Reprinted from Wittner, M., Weiss, L. M. (eds.) 1999. *The Microsporidia and Microsporidiosis*. ASM Press, Washington, DC.

Conventional splitting of the microsporidian life cycle into merogony and sporogony on the basis of secretion of electron-dense material on the cell plasma membrane cannot be applied to *Enterocytozoon*. The PP membrane remains as a naked unit membrane until the sporoblast stage, a long time after the extrusion apparatus elements have been formed in the plasmodium. Because this formation starts very early, it is impossible to define what stage is a meront or a sporont. Terms such as "early uninucleate stages," "early plasmodia," "advanced plasmodia," "sporoblasts," and "spores" seem to describe the *E. bieneusi* developmental stages in the best way.

Early uninucleate stages are small cells (about 1 µm) enveloped by a unit membrane, having a single nucleus and a cytoplasm with ribosomes and traces of ER (Fig. 1.22c). Early plasmodia are round or oval cells with several elongate, sausage-like nuclei and a few lamellae of ER. Expanded regions of the nuclear envelope (expanded perinuclear cisternae) or of rough ER form the electron-lucent clefts with a dense border consisting of a multilamellar material of phospholipid composition (Desportes-Livage et al. 1993) (Fig. 1.22d). Small aggregates of Golgi vesicles are located at the distal ends of some ER lamellae and are identical with the "vesicular precursors of the polaroplast" described by Desportes-Livage et al. (1991) and Hilmarsdottir et al. (1993).

Advanced plasmodia are identified by the presence of many round nuclei and of several structures indicating the entry of the microsporidium into the sporogony. Although these structures are described separately, they are probably parts of the same vesiculomembranous system forming the extrusion apparatus.

1. First to appear in the cytoplasm are several ovoid or spherical "empty-looking vesicles" (ELVs), about 200–250 nm in diameter and limited by a thick, dense, but sometimes incomplete border (Fig. 1.23a and c). These structures are identical with the "polar tube precursors" of Hilmarsdottir et al. (1993) and of Desportes-Livage et al. (1996). These vesicles originate in association with the ER and are often seen lining the edges of ER cisternae and in contact with the electron-dense lamellar inclusions in the ER (Cali & Owen 1990) (Fig. 1.22d). The destiny of these vesicles is not clear. They remain identifiable until the time the electron-dense disks (see item 2) begin to organize into stacks representing future polar filament coils. Each stack of disks, which will form a polar filament of one future spore, assembles around an ELV (Spycher, unpublished data) (Fig. 1.23b). It is hypothesized here that the ELVs are primordia of polar sacs.
2. The second structure is represented by "electron-dense disklike (EDD) structures" (Cali & Owen 1990) appearing in sections as sausage-like formations with very dense borders and less dense centers (Fig. 1.23b and c). Ferriosmium fixation and higher resolution show that the borders of EDD structures are limited by a membrane and are multilayered (Hilmarsdottir et al. 1993; Desportes-Livage et al. 1996). Individual EDD structures seem to be bound together by membrane bridges (Ditrich et al. 1994). In addition to the ELVs, EDD structures appear in the cytoplasm at the borders of the electron-lucent clefts (expanded ER lamella) and in the vicinity of Golgi vesicles. The disks accumulate first in stacks and are reported to fuse later to form arcs and complete coils of the polar filament (Fig. 1.23b and d).
3. Each nucleus becomes associated with a membrane-bound lucent vacuole (perinuclear vacuole, PNV) (150–200 nm) situated in a shallow depression of the nucleus (Fig. 1.23d and e). The PNV is probably identical with the "electron-lucent inclusions" seen in Figure 3 of Cali and Owen (1990). The PNV increases in size during development and is often seen either incompletely or completely divided into two compartments (Fig. 1.23d). During this period, the vacuole is about 400–500 nm in size. It is hypothesized here that one of the compartments gives rise to the polaroplast and the other to the posterior vacuole.
4. The polar sac is formed as a dense vesicle with a membranous border, and it is closely associated with the nucleus and partly invaginated in its membrane. The sac is located close to the PNV, and at this site, the perinuclear cisterna contains electron-dense material (Fig. 1.23e). The polar filament appears as a filamentous extension of the polar sac (Fig. 1.23e). It has a dark core surrounded by a less dense layer bounded externally by a double membrane, the same membrane that encloses the polar sac. The dense core material penetrates for a certain distance into the sac and inside the sac forms a cupola-like heap of dense material (Fig. 1.23f). During the advanced stage of sporogenesis, the polar sac flattens, the coils form a continuous thread, and small vesicles of the vesicular polaroplast appear as outgrowths of the membrane enclosing the straight part of the filament (Fig. 1.23e).
5. Finally, the complete set of extrusion apparatus organelles belonging to each nucleus is formed in the plasmodium (Fig. 1.24d). The individual polar sacs, each with its extrusion apparatus complement, assemble close to the plasma membrane of the plasmodium (Orenstein 1991) (Fig. 1.24d). Invagination of the plasma membrane, concurrently thickened by addition of the surface coat (future exospore layer of the spore), separates the uninucleate sporoblasts, each with a complete set of spore organelles (Fig. 1.24a). Sporogony is thus polysporoblastic (up to about 60 spores arising from one sporogonial plasmodium) (Vávra, unpublished data) (Fig. 1.22a and b) with precocious spore organelle formation. Spore maturation involves formation of the posterior vacuole and of the endospore layer beneath the thin exospore.

Spores, 1.5 by 0.9 µm, are ellipsoid and have a single nucleus. Despite many observations, their fine structure is poorly known, as most observed spores were not completely mature. Fully mature spores have a relatively thick (40 nm) endospore and a thin (l3 nm) single-layer exospore (Orenstein 1991). The polaroplast has a compressed anterior lamellar part and a pos-

terior vesicular part. Five to six isofilar coils of the polar filament are arranged in two rows (Fig. 1.24d). Teratological sporogenesis probably caused by the AIDS drug azidothymidine was described by Ditrich et al. (1994). It included the formation of large, deeply lobed sporogonial plasmodia, incompletely separated sporoblasts, and unusually large spores (2.5 µm) with 10 coils of the polar filament.

The unique nature of this microsporidium resides primarily in the precocious development of spore organelles within the plasmodium and the late initiation of the electron-dense coat of the sporogonial plasmodium. This order of events is probably due to the necessity for the organism to complete its life cycle within an enterocyte living only for 4–5 days (Desportes-Livage et al. 1991), after which the spores are shed into the intestinal lumen (Orenstein 1991) (Fig. 1.22g). The dense, multilamellar phospholipid material occurring early in the ER lamellae evidently serves as a pool of material for the polar filament and membranous structures of the future spore. The outer coat of dense material is formed late, probably because the relatively large plasmodium, with its many nuclei, synthesizing extrusion apparatus organelles, must have a very high metabolic rate and transmembrane transport must not be hindered.

If the development and structure of *E. bieneusi* are compared with that of other microsporidia, its closest counterparts are *Nucleospora salmonis* (previously classified in the genus *Enterocytozoon*), a parasite of nuclei of immature blood cells of salmonid fish (Hedrick et al. 1991), and *Enterospora* species, parasites of nuclei of hepatopancreatocytes of crabs (Stentiford et al. 2007). In these microsporidia, the extrusion apparatus develops early, before fission of the sporogonial plasmodium into sporoblasts.

1.10.2 *Encephalitozoon* Species

Three species of the genus *Encephalitozoon*, *E. cuniculi* Levaditi, Nicolau, and Schoen, 1923; *E. hellem* Didier, Didier, Friedberg, Stenson, Orenstein, Yee, Tio, Davis, Vossbrinck, Millichamp, and Shadduck, 1991; and *E.* (formerly *Septata*) *intestinalis* Cali, Kotler, and Orenstein, 1993, are known to infect humans. These species are morphologically similar, and only *E. intestinalis* can be distinguished from the other two species by the presence of a loose intravacuolar material among parasite cells (Cali et al. 1996b) (see the following text). The genus *Encephalitozoon* is monomorphic, having isolated nuclei in all life cycle stages. Development typically takes place in a parasitophorous vacuole believed to be of host origin (Bohne et al. 2011) (see below and Section 1.9.2). The limiting membrane of the parasitophorous vacuole appears first as a unit membrane so closely applied to the plasma membrane that the meront seems to have two unit membranes at its surface (Barker 1975) (Fig. 1.25a and b). Later, the outer membrane surrounding the parasite starts to detach, and small electron-lucent areas appear between the PP membrane and the vacuolar membrane (Fig. 1.25c and Fig. 1.26e). As the parasite grows and divides, a single vacuolar space develops in which parasite cells are situated (Fig. 1.25d, Fig. 1.26b and c, and Fig. 1.27e and f). The vacuolar space contains meronts adhering to the vacuolar membrane (Fig. 1.26c and f) by an attachment resembling a tight junction (Weidner 1975, 1976b). Meronts divide by repeated binary fission, and because of delayed cytokinesis, small chains of meronts are formed (Fig. 1.26c). Sporonts are characterized by a layer of dense material on their plasma membrane, first deposited in strands and later as a homogeneous layer (Barker 1975). Sporonts detach from the vacuole membrane (Fig. 1.26f). Sporogony takes place in the lumen of the vacuole (Fig. 1.26c and f) and is thought to be disporoblastic and occasionally tetrasporoblastic (see the following text). The border of the parasitophorous vacuole that is not in direct contact with parasite cells forms a canopy of blebs extending into the vacuolar space (Weidner 1975, 1976b) (Fig. 1.27a).

The parasitophorous vacuole of *E. intestinalis* has a special character, being prominently lobed and containing septa consisting of a granular material (Fig. 1.25c). The septa form incomplete chambers enclosing individual parasites within the vacuole, and the material forming the septa is believed to be secreted by the parasites (Cali et al. 1993). Canning et al. (1994) believe that the septa originate from the compression of slightly electron-opaque, loosely dispersed reticulate material present in *Encephalitozoon* species parasitophorous vacuoles. This material (reported also by Ghosh et al. 2011) disappears during the sporogony of the other two species, *E. cuniculi* and *E. hellem*. Evidently, the interior of the parasitophorous vacuoles in *Encephalitozoon* is more structured than the loose contents seem to indicate. The fact that the sporoblasts and spores of *E. intestinalis* have a seemingly loose halo of a rather constant width (about 0.3 µm), separating them from the septa (Fig. 1.25e), favors this idea. The lobed appearance of the parasitophorous vacuole of *E. intestinalis* is a result of the fusion of vacuoles surrounding individual parasitic cells accompanied by host cell cytoplasmic debris caught as vacuoles coalesce (Fig. 1.25d). The fusion of several larger vacuoles was also described (Canning et al. 1994).

Spores, 2.5 by 1.5 µm, are ellipsoid and uninucleate (Fig. 1.26a and b) with a rugose exospore and a moderately thick endospore (Fig. 1.25d and Fig. 1.27g). At low magnifications, the exospore looks like a single layer about 30 nm thick, but high-resolution TEM shows that it has three layers: an outer electron-dense "spiny layer" (12 nm), an intermediate electron-lucent lamina (3 nm), and an inner dense fibrous layer (15 nm) (Bigliardi et al. 1996). The polaroplast is lamellar, and the polar filament is isofilar with three to eight coils in a single row, the number possibly being related to spore maturity (Fig. 1.26g and Fig. 1.27b, c, and g). A posterior vacuole is sometimes present (Fig. 1.26g and Fig. 1.27g). When released from the parasitophorous vacuole, the spores frequently extrude their polar filaments (Fig. 1.27d), a prerequisite for efficient intertissue transmission of the parasite.

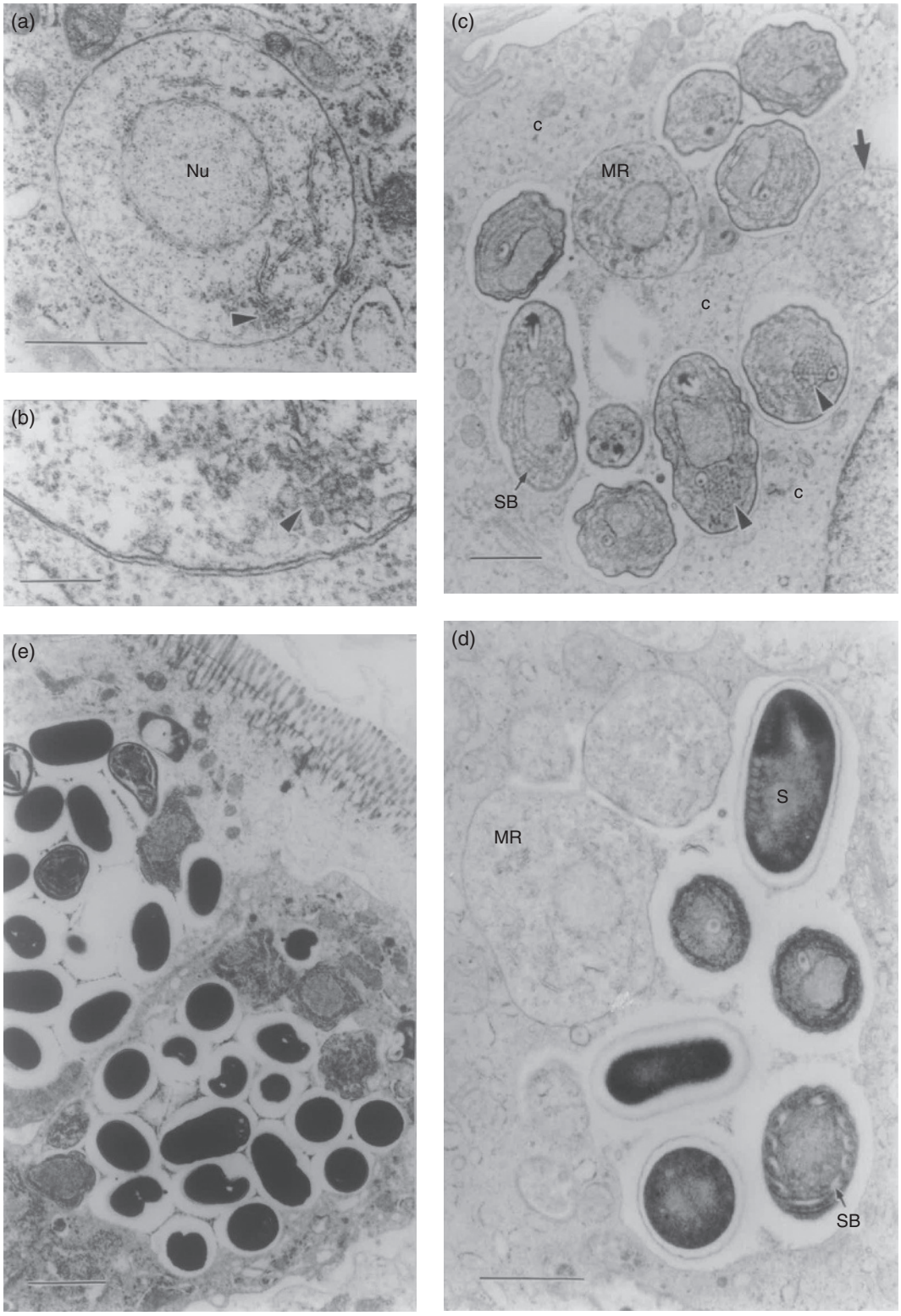

Figure 1.25 *Encephalitozoon* (syn. *Septata*) *intestinalis* (Golgi is indicated by arrowheads). (a) Initial meront surrounded by closely adhering membrane of the future parasitophorous vacuole. (b) Detailed view of the membranous complex of the meront in (a). (c, d) A large parasitophorous vacuole originates by progressive confluence of individual vacuoles around dividing parasites. A meront (arrow) is fully embedded in the host cell cytoplasm. (e) Fully formed vacuole with septa forming incomplete chambers around individual spores. All images TEM. Scale bars = 1.0 µm (a, c, d), 250 nm (b), 2 µm (e). c, host cell cytoplasm; MR, meronts; Nu, nucleus; SB, sporoblasts; S, spore. Reprinted from Wittner, M., Weiss, L. M. (eds.) 1999. *The Microsporidia and Microsporidiosis*. ASM Press, Washington, DC.

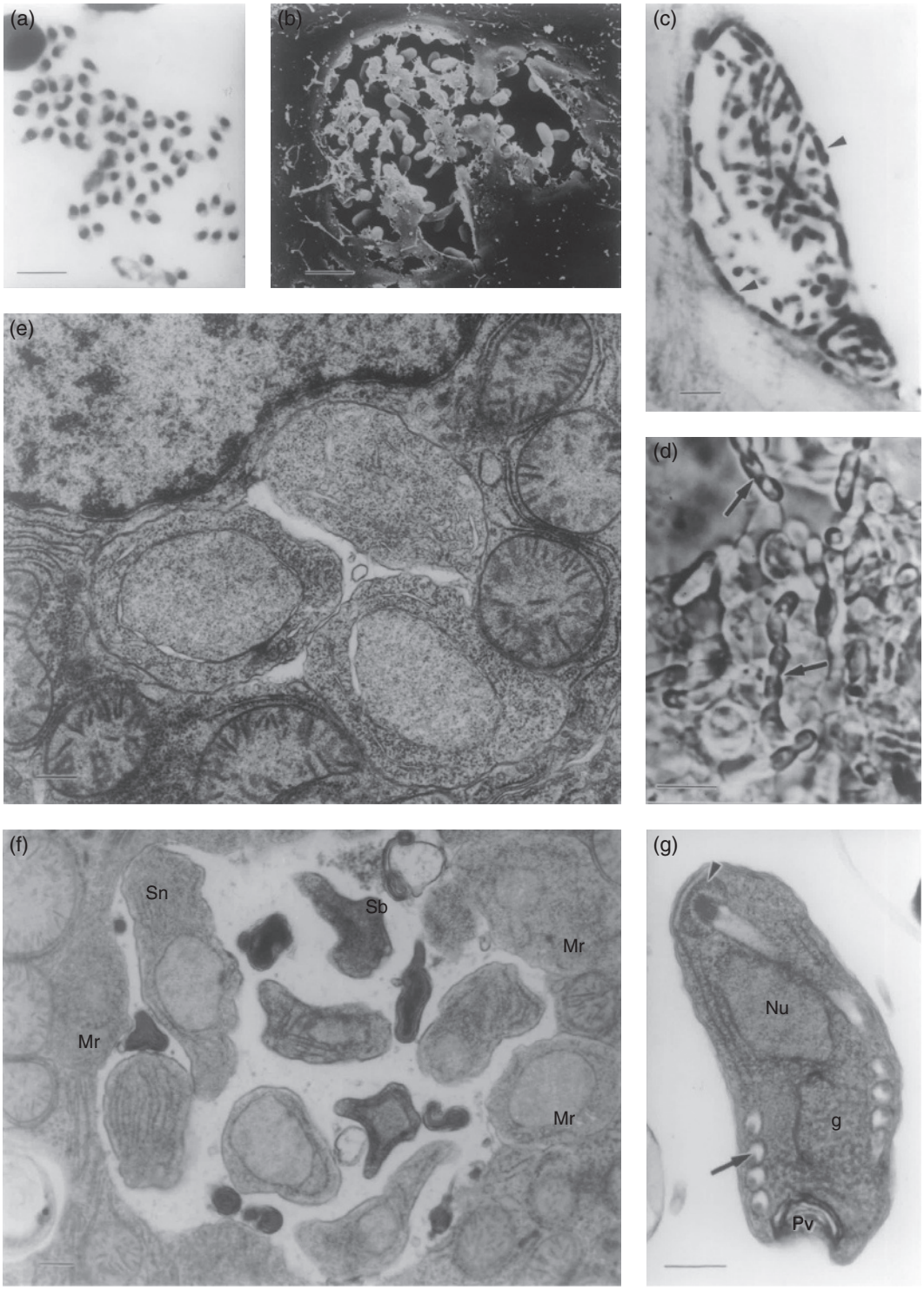

Figure 1.26 *Encephalitozoon cuniculi.* (a) Spores in a smear (Giemsa stain). (b) SEM view of a broken parasitophorous vacuole with spores. (c) Parasitophorous vacuole with meronts lining the vacuole borders (arrowheads) and sporogonial stages and spores in the center of the vacuole (Giemsa stain). (d) Chains of sporoblasts inside the parasitophorous vacuole (arrows) (phase contrast). (e) Early parasitophorous vacuole originating around three meronts. (f) Fully formed parasitophorous vacuole with meronts adhering to vacuole border, sporonts, and sporoblasts detached to the vacuole interior. (g) Young spore with organelles; arrow indicates early form of the polar filament; arrowhead polar sac. Mouse peritoneal exudate (a), liver of SCID mouse (b, e–g), rabbit chorioid plexus cell tissue culture (c, d). TEM (e–g). Scale bars = 5 µm (a–d), 0.5 µm (e–g). g, Golgi reticulum; Mr, meront; Nu, nucleus; Sb, sporoblast; Sn, sporont; Pv, posterior vacuole (collapsed). Reprinted from Wittner, M., Weiss, L. M. (eds.) 1999. *The Microsporidia and Microsporidiosis*. ASM Press, Washington, DC.

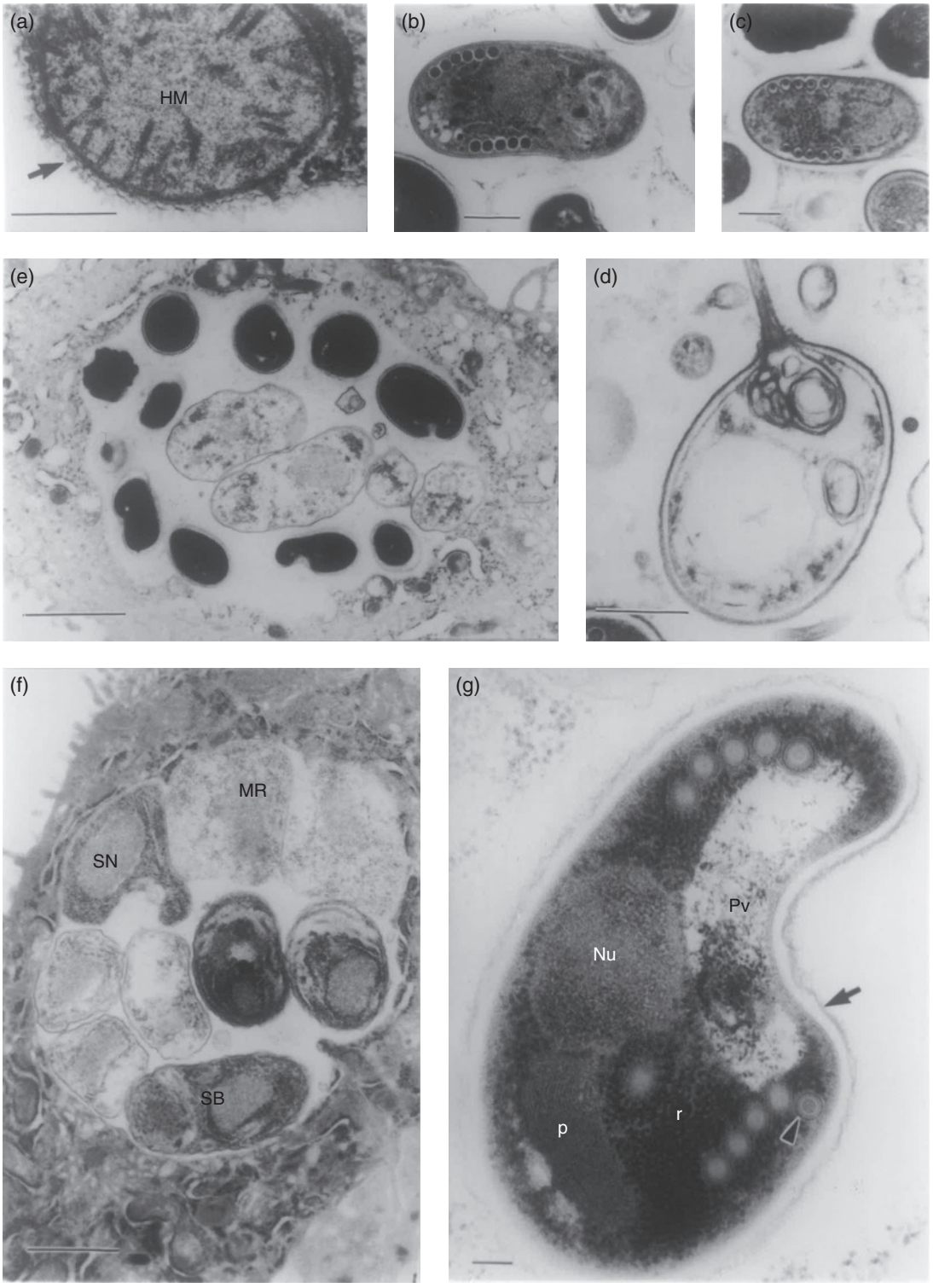

Figure 1.27 *Encephalitozoon* species: *E. intestinalis* (a–d), *E. hellem* (e–g). (a) Border of a parasitophorous vacuole. The canopy of blebs protruding into the vacuole is shown by the arrow. (b, c) Young spores with five filament coils. (d) Extruded spore. (e) Fully formed parasitophorous vacuole. (f) Earlier vacuole with meronts, sporont, and sporoblasts transforming into spores. (g) Spore with organelles. A polar filament with a substructure of concentric rings is shown by the arrowhead. The three layers of the spore wall, the plasma membrane, and the endo- and exospore layers are indicated by the arrow. All images. Scale bars = 0.5 µm (a–d), 2 µm (e), 1 µm (f), 100 nm (g). HM, host cell mitochondrion; MR, meront; Nu, nucleus; P, polaroplast lamellae; r, area with polyribosomes; SB, sporoblast; SN, sporont; Pv, posterior vacuole (distorted). Reprinted from Wittner, M., Weiss, L. M. (eds.) 1999. *The Microsporidia and Microsporidiosis*. ASM Press, Washington, DC.

Despite a number of reports on the subject, all details of the cytology of the *Encephalitozoon* species are still not clear. The origin of the parasitophorous vacuole in which the parasite develops is intriguing. Although its origin from a host material has been proposed (Agaud et al. 1997, Bohne et al. 2011), the way it originates (as a membrane closely applied to the plasma membrane of the early meront) and its similar configuration in many types of infected cells do not seem to disclaim the idea that the vacuole is of parasite origin (Vávra, unpublished).

Whether *Encephalitozoon* sporogony is disporoblastic or tetrasporoblastic has been argued (Cali et al. 1993; Canning et al. 1994; Cali et al. 1996b). This feature may depend on the relationship of the speed of growth to the cytokinesis of individual cells and on conditions under which the parasite has been grown. In tissue culture, rather long chains of sporonts (Vávra et al. 1972; Desser et al. 1992) are formed (Fig. 1.26d).

1.10.3 *Trachipleistophora* Species

Two known species of the genus *Trachipleistophora*, *T. hominis* Hollister, Canning, Weidner, Field, Kench, and Marriott, 1996, and *T. anthropophthera* Vávra, Yachnis, Shadduck, and Orenstein, 1998, were found in corneal scrapings, in muscle biopsy specimens, and in systemic infections of AIDS patients. It cannot be excluded that *T. hominis* actually is an insect parasite as it was found to be infective for mosquito larvae (Weidner et al. 1999).

Trachipleistophora hominis, the type species of the genus, was described as monomorphic and having a single nucleus. The meronts have a dense coat on their plasma membrane, forming branched processes into the host cell cytoplasm (Fig. 1.28a). This coat is the precursor of the SPOV (of the merontogenetic type), and it divides with the body of the meront. Merogony is probably limited to binary fission, as no chains or multinucleate merogonic plasmodia were observed. Sporogony begins with retraction of the sporont plasma membrane within the surface coat, which becomes a rather thick-walled envelope of the SPOV (Fig. 1.28b). The sporont divides by a series of binary fissions into uninucleate sporoblasts and spores, 2–32 per vesicle (Fig. 1.29b). Spores are pyriform, 4.0 by 2.4 μm (fresh) (Fig. 1.29a–c), and have an anterolateral anchoring disk, a lamellar polaroplast with two different types of lamellar spacing, and about 11 polar filament coils in a single row. Observations demonstrate that the polar filament is anisofilar, usually with three thinner posterior coils (Canning, unpublished data; Vávra, unpublished data).

Trachipleistophora anthropophthera is similar to the type species of the genus but differs by being dimorphic. It forms two types of SPOVs, each enclosing spores of a different type. SPOVs of type I are similar to those of *T. hominis* and usually contain eight or more thick-walled spores (3.7 by 2.0 μm, fixed) (Fig. 1.28c and Fig. 1.29b, d, and g). Type I spores are similar in organization to those of *T. hominis* but have an anisofilar polar filament, usually with seven thicker and two thinner coils (Fig. 1.28d). SPOVs of type II are formed in the same tissues and sometimes even in the same cell as type I vesicles (Fig. 1.29f). Type II SPOVs are thin-walled and contain only two type II spores (Fig. 1.29h), which are small, nearly round (2.2–2.5 by 1.8–2.0 μm, fixed), and thin-walled and have four or five isofilar polar filament coils (Fig. 1.28e and f). It is believed that type II spores disseminate the infection within the host tissues as they are frequently found with their polar tubes extruded (Orenstein, unpublished data) (Fig. 1.29i and j).

1.10.4 *Vittaforma corneae*

Vittaforma corneae (Shadduck et al. 1990) Silveira and Canning (1995), was isolated from human corneal stroma. The organism was also found in urinary and pulmonary tracts of AIDS patients (Chapters 15 and 16 of the present volume). This parasite is a monomorphic species having diplokarya throughout its life cycle. Synaptonemal complexes were not observed in nuclei. The nuclear configuration was the reason why the organism was originally described as *Nosema*.

The microsporidium is unique in having a complex of three unit membranes covering the organism, where the external two are presumed to be of host origin. The membranous complex is persistent during the entire life cycle, including the spore stage, which suggests that also the membranes derived from host cell are transformed in some way by the microsporidium.

The membrane arrangement can be explained by the parasite being surrounded by the host ER cisterna: the internal membrane is the parasite plasma (PP) membrane, the median membrane (so closely applied that it appears to be a second parasite membrane) is presumed to be the ribosome-free component of the host cell ER membrane (HERM1), and the external membrane, studded with ribosomes, represents the other part of the host ER cisterna (HERM2). Merogony proceeds as binary fission of diplokaryotic stages, and both the HERM1 and the HERM2 divide with the meront. “Clefts” in the form of an enlarged part of the perinuclear cisterna in meronts have been described (Silveira & Canning 1995). Dark material, similar in appearance to that present in perinuclear clefts of *Enterocytozoon bieneusi*, was seen in clefts of *Vittaforma* meronts, but it is probable that these clefts were fixation artifacts.

During sporogony, elongate, ribbon-shaped sporonts (plasmodia) are formed as a result of delayed cytokinesis (Fig. 1.30f). The sporonts are marked by deposition of electron-dense material on the PP, first in small patches appearing as curved, lenticular structures which progressively form a uniform dense coat on the sporont. The division is affected by means of deep clefts perpendicular to the long axis of the ribbonlike sporogonial plasmodium. The PP, together with the

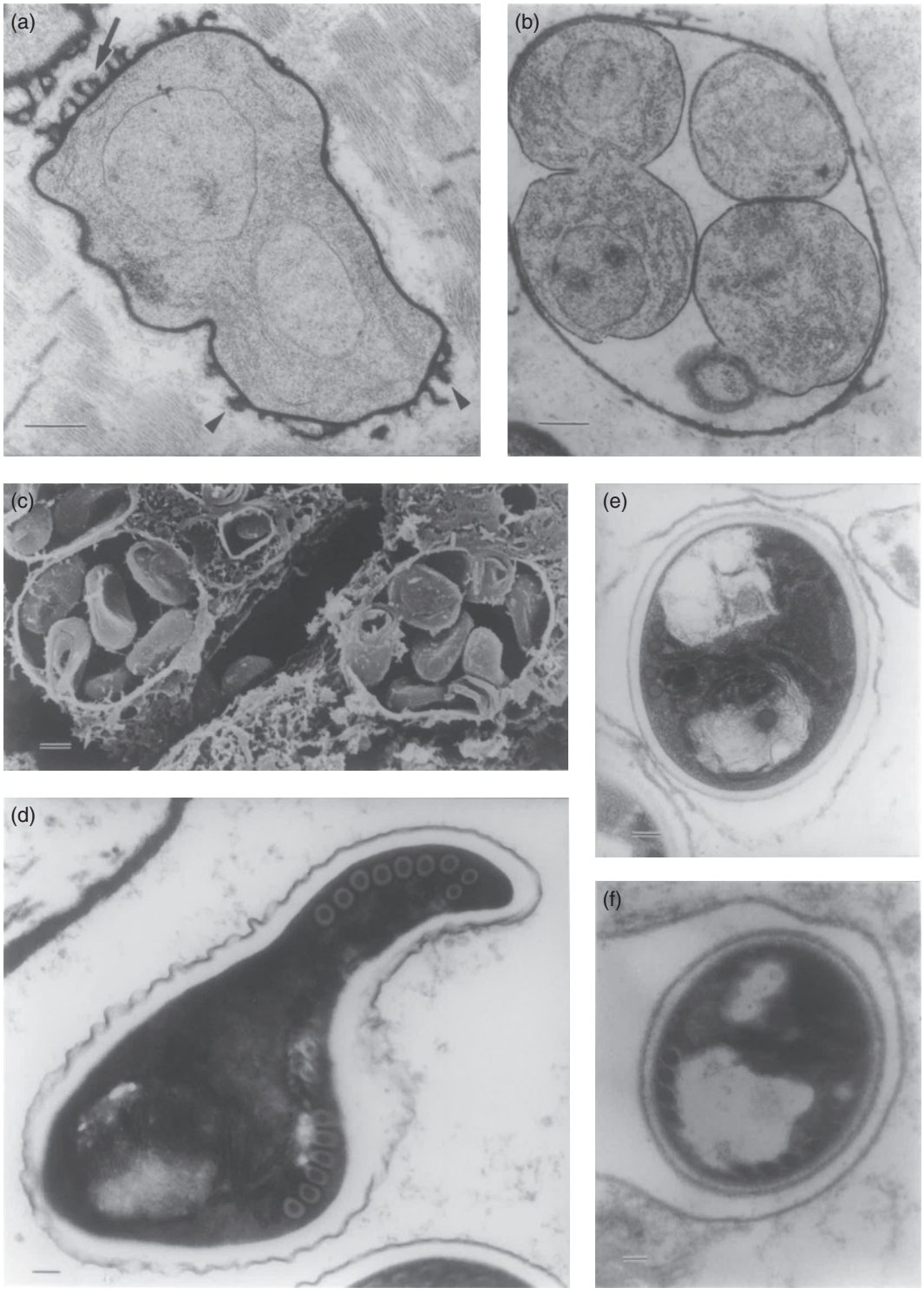

Figure 1.28 *Trachipleistophora* species. (a) Binucleate meront in skeletal muscle cell, showing the plasma membrane covered by dense material forming connections between meronts (arrow) and protuberances into the host cell cytoplasm (arrowheads). (b) SPOV with four presporoblast cells. (c) SPOVs with type I spores. (d) Thick-walled type I spore with seven thick and two thin coils. (e, f) Thin-walled type II spores with four isofilar coils. *T. hominis* in SCID mouse skeletal muscle (a) and RK-13 cell tissue culture (b), both images TEM. *T. anthropophthera* in human brain, SEM (c) and TEM (d–f). Scale bars = 0.5 µm (a), 1 µm (b, c), 100 nm (d–f). Reprinted from Wittner, M., Weiss, L. M. (eds.) 1999. *The Microsporidia and Microsporidiosis*. ASM Press, Washington, DC.

electron-dense coat and the inner face of the host ER (HERM1), invaginate and separate the plasmodial ribbon into up to eight linear arrays of sporoblasts. Membranous whorls resembling paramural bodies are formed at the bottom of the invaginating furrows. During sporoblast individualization, the HERM2 loses its close contact with the surface of the parasite, but still, it completely envelops each sporoblast and spore as a loose sheath (Silveira & Canning 1995).

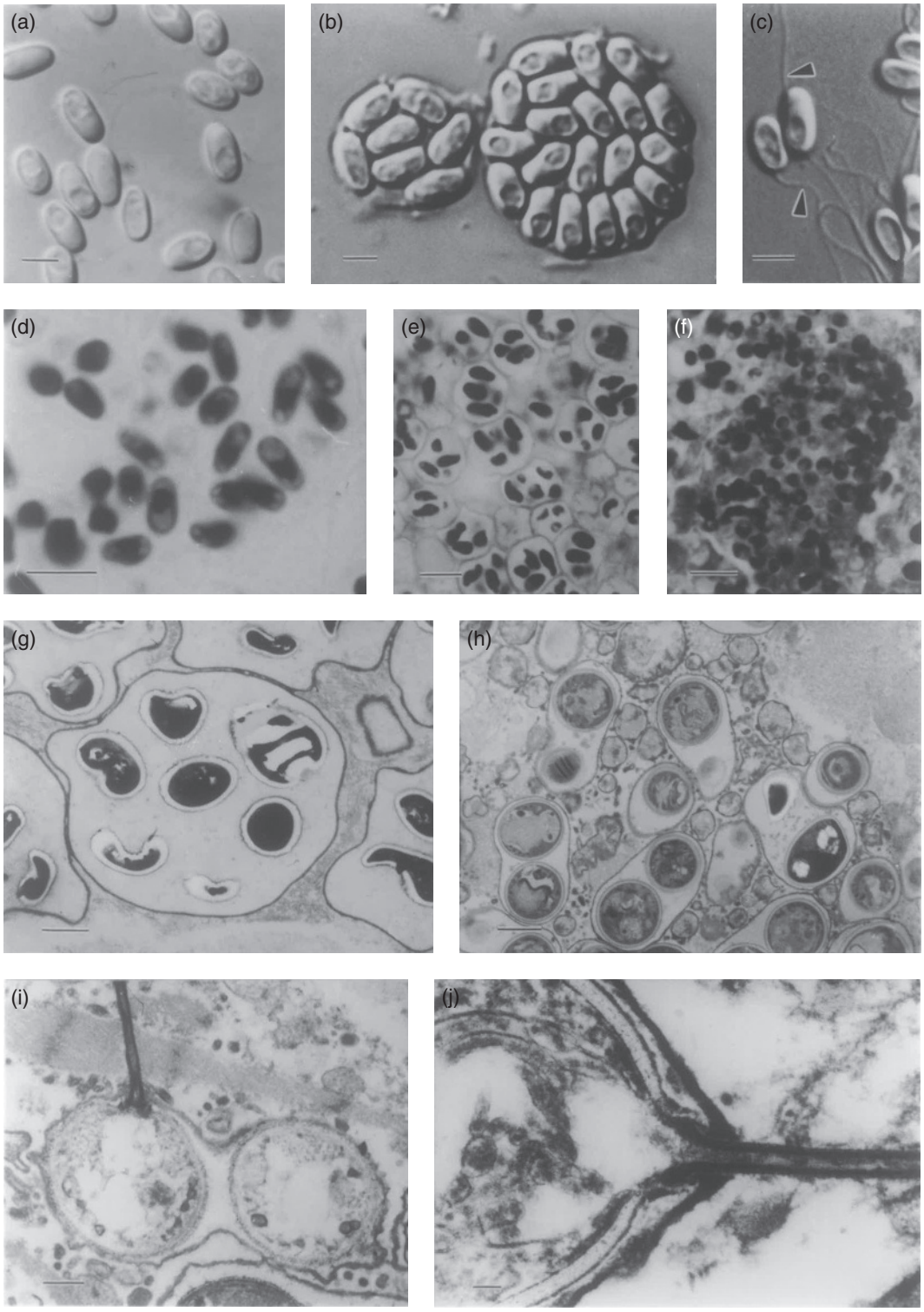

Figure 1.29 *Trachipleistophora* species. (a) Free spores (fresh). (b) Fresh spores in SPOVs. (c) Extruded spore, the polar tube extrudes subapically (arrowheads). (d) Stained free spores (Goodpasture's carbol-fuchsin stain). (e) Type I spores in SPOVs (semithin plastic section, methylene blue–azure II–basic fuchsin staining). (f) Aggregate of type II spores in histology section (hematoxylin and eosin stain). (g) Type I spores in a multisporous SPOV. (h) Type II spores in bisporous SPOVs. (i) Extruded type II spore. (j) Detail of the tip of an extruded type II spore, showing the tubular aspect of the polar tube. *T. hominis*, skeletal muscle homogenate of SCID mice (a–c). *T. anthropophthera*, human brain (d–h) and human heart muscle (i, j). Interference phase contrast (a–c), TEM (g–j). Scale bars = 5 µm (a–f), 1 µm (g, h), 0.5 µm (i), 100 nm (j). Reprinted from Wittner, M., Weiss, L. M. (eds.) 1999. *The Microsporidia and Microsporidiosis*. ASM Press, Washington, DC.

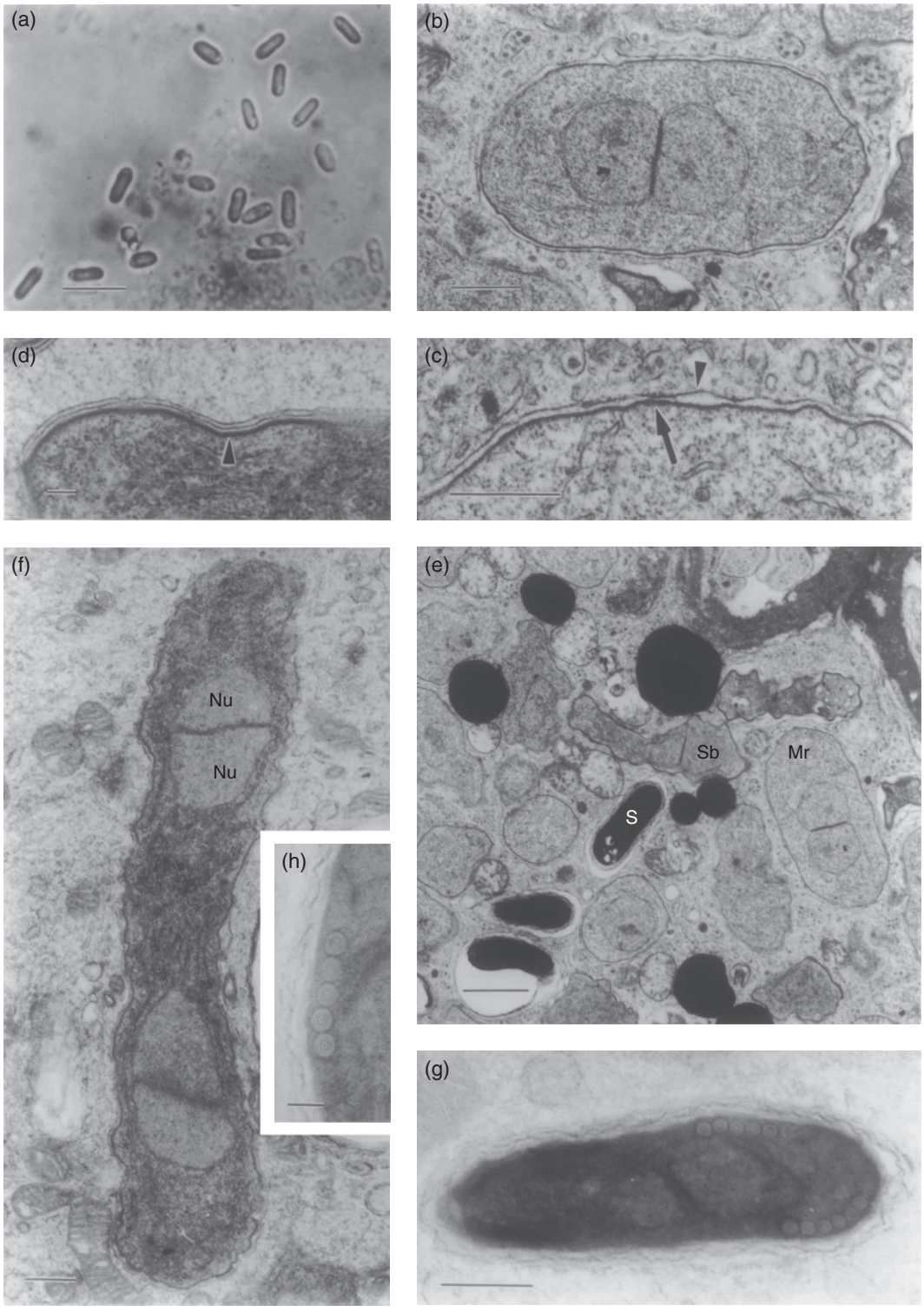

Figure 1.30 *Vittaforma corneae*. (a) Fresh spores (phase contrast). (b) Meront. (c) Meront enclosed by an inner membranous complex (arrow) of two adhering membranes (the inner one supposedly belonging to the parasite and the outer one belonging to the host) and one outer host membrane (arrowhead). (d) Cell boundary of the sporont, showing electron-dense material deposited on the internal (parasite) membrane (arrowhead). (e) Low-magnification view of infected mouse liver. (f) Dividing diplokaryotic sporont. (g) Mature spore enclosed in several membranous layers. (h) Polar filament coils with substructure. TEM (b–h). Scale bars = 5 µm (a), 0.5 µm (b, c, f, g), 100 nm (d, h), 1 µm (e). Reprinted with permission from J. A. Shadduck (D, F–H). Mt. meront; Nu. nucleus; Sb, sporoblast; S, spore. Reprinted from Wittner, M., Weiss, L. M. (eds.) 1999. *The Microsporidia and Microsporidiosis*. ASM Press, Washington, DC.

The spores (in tissue culture) are polymorphic, typically appearing as elongate cylinders (Fig. 1.30a). Small, ovoid spores or spores resembling long rods are also present. Spore size is reported to be 3.7–3.8 by 1.0 µm (Shadduck et al. 1990; Silveira & Canning 1995). The ovoid forms are half the indicated size, and long spores are twice as large as the typical form (image-splitting eyepiece measurements) (Vávra unpublished data). The spores are diplokaryotic. The polar filament is isofilar with about six coils (Fig. 1.30h). The exospore is about half as thick as the endospore, and it is surrounded by loose membranes (Fig. 1.30g). The polaroplast is composed of tightly packed lamellae, arranged around the straight portion of the polar filament, and a few posterior lamellae in groups of four (Silveira & Canning 1995).

The characteristic arrangement of membranes, which occurs in all stages including spores, represents the main distinguishing character of the genus *Vittaforma* (Fig. 1.30b–g). This is different from the situation in a number of other microsporidia that are encased in host cell ER cisternae, but only during the merogony. The arrangement in *Vittaforma* resembles that in *Endoreticulatus* spp. in which meronts are tightly enveloped by the host ER. However, in *Endoreticulatus*, sporogonic divisions occur in a vacuolar space bordered by the host ER, and in contrast to the arrangement in *Vittaforma*, the spores are not enclosed in individual sacs of host cell origin (Brooks et al. 1988; Cali & El Garhy 1991)

1.10.5 Human Pathogenic Microsporidia of the Family Tubulinosematidae

The family Tubulinosematidae was established by Franzen et al. (2005) for diplokaryotic microsporidia structurally similar to the genus *Nosema*. The main difference is found in meronts which have a glycocalyx-like layer of small tubuli and electron-dense vesiculotubular appendages on their plasma membrane. By these formations, the developmental stages of Tubulinosematidae interdigitate with the host cell cytoplasm. Spores of the family have a thick endospore and a thick, uniform exospore. The two genera, *Tubulinosema* and *Anncaliia* (formerly *Brachiola*), represent a family well supported by molecular phylogeny where both genera form sister clades. Tubulinosematidae are parasites of various insects, but several human infections involving representatives of both genera have been described.

1.10.5.1 Anncaliia algerae and Anncaliia vesicularum

Anncaliia algerae (syn. *Nosema algerae* Vávra & Undeen, 1970; and syn. *Brachiola algerae*) (Vávra & Undeen 1970; Lowman et al. 2000) and *A. vesicularum* (syn. *Brachiola vesicularum* Cali, Takvorian, Lewin, Rendel, Sian, Wittner, Tanowitz, Keohane, and Weiss, 1998). The first species, *A. algerae*, was originally described from insects (Vávra & Undeen 1970) but is presently known from a number of human infections (Coyle et al. 2004; Field et al. 2012). The second species, *A. vesicularum*, was described from a skeletal muscle biopsy specimen from an AIDS patient (Cali et al. 1996a, 1998). These microsporidia are monomorphic, diplokaryotic and develop in direct contact with the host cell cytoplasm in the form of meronts with a single or double diplokaryon (Fig. 1.31a and Fig. 1.32b and g). Their characteristic feature is the presence of a dense coat of tubulovesicular strands on the surface of the developmental stages of the parasite (Fig. 1.31b, c, and f and Fig. 1.32f, g and h), sometimes extending a certain distance from the parasite surface (Fig. 1.32g and h). This character is claimed to be more conspicuous in *A. vesicularum* (Fig. 1.31d). The sporogony is disporoblastic, producing spores measuring 4.5 × 3 µm (*A. algerae*, fresh) or 2.9 × 2.0 µm in size (*A. vesicularum* fixed), with 7–10 coils of the polar filament arranged in one (*A. algerae*) to three, usually two, rows (*A. vesicularum*) (Fig. 1.31e). Spores have a thick endospore and a thick, uniform exospore (Fig. 1.31e and Fig. 1.32c). The polar filament is anisofilar, with the last two or three coils being thinner. *A. algerae* and *A. vesicularum* are structurally very similar, if not identical, microsporidia, and their relationship is discussed in Franzen et al. (2006b).

1.10.5.2 Tubulinosema Species

The genus *Tubulinosema* comprises three species formerly ranked into the genus *Nosema*. The late meronts have a tubular coat on the plasma membrane, similar to the genus *Anncaliia*. They are parasites of insects (fruit flies, *Drosophila*, and grasshoppers, *Schistocerca*). The spores have a thick endospore and a thick, uniform exospore and a slightly anisofilar polar filament with 9–14 coils and measure about 4.1–4.3 × 2.5–2.6 µm in size (Fig. 1.32a). For further comparative species data, see Franzen et al. (2006a). A *Tubulinosema* species, with respective 100% and nearly 100% identity of the ssu rRNA gene to *T. acridophagus* from a grasshopper, was identified as the agent of two cases of myositis and disseminated microsporidiosis in immunosuppressed human patients (Choudhary et al. 2011; Meissner et al. 2012).

1.11 STRUCTURE-RELATED TECHNIQUES IN MICROSPORIDIA RESEARCH

Techniques useful for studying microsporidian structure have been summarized by Vávra and Maddox (1976), Hazard et al. (1981), Undeen and Vávra (1997), Becnel (2012), and Solter et al. (2012). Some important and specific methods are reported here. Some of the methods are intended for rapid diagnosis, while others are more or less necessary for type slides or other permanent preparations.

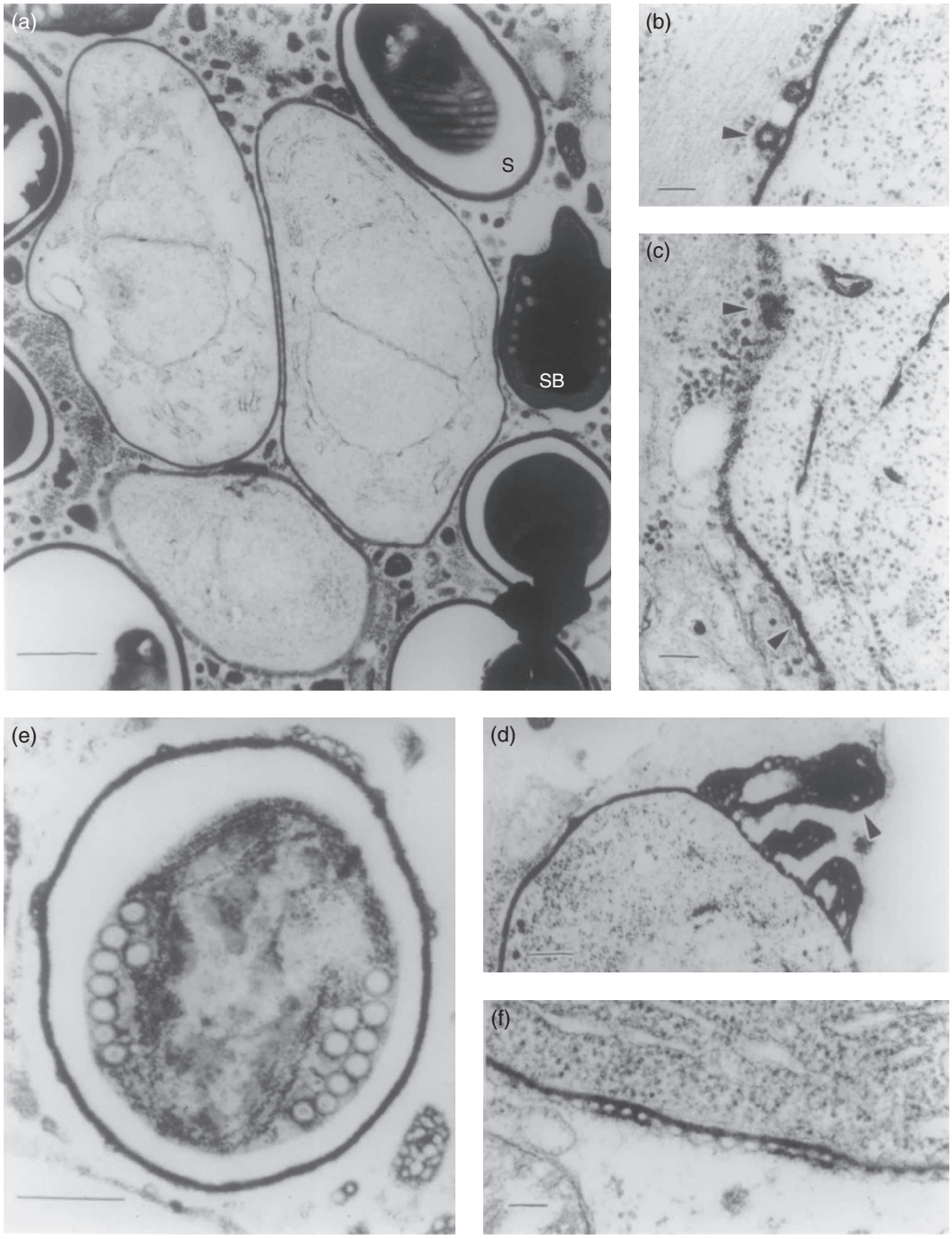

Figure 1.31 *Anncaliia* (formerly *Brachiola*) *vesicularum* from human skeletal muscle (a–e) and *Anncaliia* (formerly *Brachiola*, *Nosema*) *algerae* (f). (a) Developmental stages (meronts), showing the diplokaryotic nuclei. (b, c) Details of electron-dense material deposits in the form of membrane-bound tubules (b) or dense tubular strands (c) at the plasma membrane (arrowhead). (d) Parasite cell showing large expansion of the vesiculotubular electron-dense material at the cell surface (arrowhead). (e) Spore with polar filament arranged as a double coil. (f) The construction of the meront surface of *A. algerae*, a parasite of *Anopheles* mosquito larvae, is to a certain degree similar to the meront surface of *Brachiola*. All images TEM. Scale bars = 1 µm (a), 100 nm (b, c, f), 250 nm (d), 0.5 µm (E). SB, sporoblast; S, spore. Reprinted from Wittner, M., Weiss, L. M. (eds.) 1999. *The Microsporidia and Microsporidiosis*. ASM Press, Washington, DC.

1.11.1 Recognizing Infected Hosts and Making Diagnostic Smears

Spore-filled tissues of a more or less transparent host may exhibit a milky appearance caused by light being scattered off the spores. The milkiness, together with the background coloring of the host, can make the infected host or organs appear milky-greenish yellow or rosy.

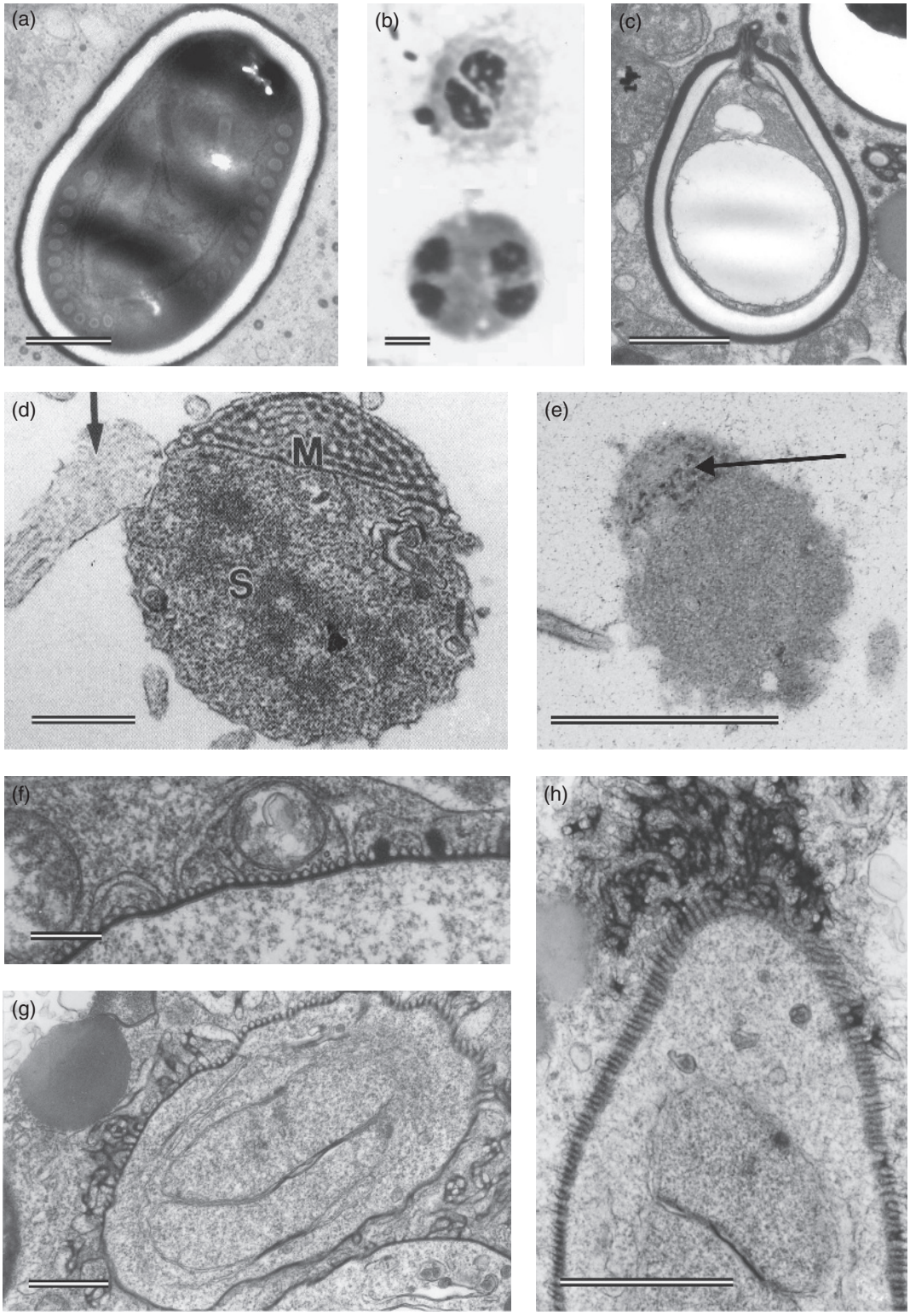

Figure 1.32 *Tubulinosema kingi* (a) and *Anncaliia* (formerly *Brachiola*, *Nosema*) *algerae* (b–h). (a) Spore with thick endospore; thick, single-layer exospore; and a slightly anisofilar polar filament. (b) Binucleate and tetranucleate diplokaryotic cells (Giemsa staining). (c) Germinating spore showing the construction of a spore wall similar to (a). (d) Freshly extruded sporoplasm (S), still attached to the end of the polar tube (arrow). The membranous whorl ("MIN") forming a part of the sporoplasm is at M. (e) "MIN" is derived from Golgi vesicles as demonstrated by histochemical detection of thiamine pyrophosphatase, a Golgi marker (arrow). (f) Tubular layer on plasma membrane of meronts. (g) Binucleate meront with glycocalyx expansions. (h) Detail of tubular expansions protruding from the glycocalyx into the cytoplasm of the host cell. Scale bars = 0.2 µm (f), 1.0 µm (a, c, d, g, h), 2.0 µm (Personal permission of Franzen, C. and Kraaijeveld, A. R. (a), Takvorian, P. M. (e), and Takvorian et al., *Folia Parasitologica* 2005 (d). Original photomicrographs by J. Vávra (b, c, f–h)).

The parasites are normally studied in smears from infected tissues. Thus, in preparing a smear, it is important to use a technique that preserves the dividing stages in a way that allows modes of division to remain visible and avoids destruction of SPOVs. If the smear is prepared like a bacteriological smear, the spore groups, which are the visible sign of sporogony in SPOVs, are lost unless the vesicle envelope is unusually persistent. A squash preparation preserves these features better. Thus, a small piece of microsporidia-filled tissue is squashed in a small drop of water or saline between two microscope slides. When the slides are separated, it is important to avoid gliding one slide over the other (Larsson 1988c).

In most cases, the spores are the useful stage for the diagnosis of a microsporidian infection. Other developmental stages are inconspicuous, and they are not resistant to the environmental conditions after the death of the host. The spores are resistant and persist for years in dead hosts and tissues (Weiser 1961), making them excellent for diagnostic purposes. The diagnosis of human microsporidian infections is treated in detail in Chapter 17.

1.11.2 Recognizing Microsporidian Spores

Microsporidian spores are in most cases similar in size and shape to spores of other organisms, such as other protists, bacteria, and fungi. They may even resemble metazoan sperms, such as those of mites. There are several basic techniques that allow the investigator to determine that the bodies seen in the light microscope are microsporidian spores. Several useful staining methods are based on the ability of spores to retain stain or a stain complex after decolorization of the smear. This is why microsporidian spores are Gram-positive, stain well with carbol-fuchsin stains (Goodpasture–Perrin method, Ziehl–Neelsen standard technique, acid-fast trichrome methods) (Vávra & Maddox 1976; Ignatius et al. 1997). For the specific detection of microsporidia, the PAS staining may be used. Chitin in the spore wall can be detected using fluorescence brighteners. The final light microscopic proof of a spore belonging to a microsporidium is the polar filament extrusion. Electron microscopy is the ultimate technique for the identification of microsporidia spores. An overview of methods used for microsporidia identification in various clinical materials can be found in Garcia (2002).

1.11.2.1 Acid-Fast Trichrome for Microsporidia Identification (Ignatius et al. 1997)

Methanol-fixed smears or tissue sections are flooded with a carbol-fuchsin solution (25.0 g of phenol, 500 ml of distilled water, and 25.0 ml of a saturated alcoholic fuchsin solution consisting of 2.0 g of basic fuchsin in 25 ml of 96% ethanol) for 10 min without heating, washed briefly with tap water, decolorized with 0.5% HCl alcohol, and again washed with tap water. Subsequently, slides are stained for 30 min at 37°C with Didier's trichrome solution (dissolve 6.0 g of chromotrope 2R, 0.5 g of aniline blue, and 0.7 g of phosphotungstic acid in 3 ml of acetic acid at room temperature for 30 min, add 100 ml of distilled water, and adjust to pH 2.5 by 2 N HCl). Rinse slides for 10 s with acid alcohol (4.5 ml of acetic acid in 995.5 ml of 90% ethanol), wash for 30 s with 95% ethanol, and examine either dry or mounted.

1.11.2.2 Periodic Acid–Schiff's (PAS) Staining of the Polar Cap

When spores are subjected to oxidation by periodic acid and then stained by Schiff´s reagent, a minute red granule (a polar cap or a polar sac–anchoring disk complex) stains at one pole of the spore. This method is specific for distinguishing microsporidian spores from similar spores of other organisms (Vávra 1959). The staining reveals polysaccharides with 1,2-glycol groups located in the anchoring apparatus of the filament.

This method can be applied both to smears and to deparaffinized tissue sections. Any fixative can be used, but aldehyde fixatives may give nonspecific staining. (i) Place the material in distilled water. (ii) Allow oxidation in a 0.5–1.0% solution of periodic acid in distilled water for 8–10 min. (iii) Allow reduction for 20 s in a mixture of 100 ml of distilled water, 2.0 g of potassium iodide, 2.0 g of crystalline sodium thiosulfate, and 20 ml of 1N HCl. (iv) Wash in distilled water for 2 min. (v) Stain with Schiff's reagent (leukofuchsin) for 15 min (for preparation, see any histology manual). (vi) Wash twice in water containing SO_2 (5 ml of 1N HCl, 6 ml of 10% sodium bisulfite, and 100 ml of H_2O distilled). The first quick rinse serves to wash out most of the Schiff's reagent, and the second rinse, for 4 min, washes out the remaining traces of the reagent. (vii) Wash well in tap water. (viii) Stain in Harris's hematoxylin (or another hematoxylin stain) and counterstain with 1% light green SF in distilled water. (ix) Dehydrate quickly in ascending ethanol and mount. Spores show a minute red granulum at one spore pole (use oil immersion for observation). A short staining time should be used in the hematoxylin step in order not to mask the PAS-positive structure.

1.11.2.3 Chitin Detection

Microsporidian spores have chitin in the endospore layer of the spore wall (see Section 1.6.3.2). Although this substance is not limited to microsporidian spores, detection of its presence by optical brighteners (e.g., Calcofluor or Uvitex) offers a useful diagnostic technique. Optical brighteners are organic compounds with aromatic rings as part of their structure which emit light in the visible spectrum upon ultraviolet or shortwave light excitation. The theoretical basis of chitin labeling with brighteners is presented in Vávra et al. (1993a). The method can be used both for fresh spores and for histology materials.

Labeling of Microsporidian Spores with Calcofluor White M2R (Vávra et al. 1993)

(i) *Fresh material*. Mix the spore-containing material with a 0.01% solution of Calcofluor White M2R (American Cyanamid Co.) or Fluorescence Brightener 28 (Sigma) in 0.1 M phosphate buffer, pH 8.0. Alternatively, flood a dry smear with the same solution. Apply a coverslip and observe by fluorescence microscopy with a violet or blue excitation filter. The spore wall fluoresces strongly. Fixed (but not in fixatives containing picric acid) or nonfixed material can be equally effective. The same result will be obtained if the Calcofluor solution is washed off after a brief application and replaced by buffered glycerol or another mounting medium suitable for fluorescence. Buffered glycerol is obtained by mixing 0.25 M sodium carbonate buffer, pH 9.5, with glycerol in a proportion of 1:9. (ii) If fresh material (e.g., spores) has been stored for a long period or the material has been fixed, it is suggested that a 0.001% Calcofluor White M2R solution in 1N NaOH is used. This solution is also recommended for rapid examination of tissue biopsy specimens in which the dye achieves fast penetration of tissues crushed between the slide and the coverslip. Fluorescence detection of microsporidia with this method can be completed in minutes (Vávra et al. 1993b). Remark: A number of optical brighteners that give results similar to those obtained with Calcofluor are the active substances of several commercial chitin detection kits used by mycologists. Van Gool et al. (1993) used Uvitex B (Ciba-Geigy, Basel, Switzerland) with success in the clinical diagnosis of microsporidiosis (Chapter 17).

Fluorescent Screening of Microsporidia in Histological Sections (Weir & Sullivan 1989) (Modified)

(i) *Fix material in Carnoy's fixative*. Do not use Bouin's fixative or any other fixative containing picric acid. (ii) Process the material routinely into paraffin. (iii) Stain deparaffinized sections with a hematoxylin stain and do not counterstain with eosin. (iv) Wash off the stain and flood the slides with 1% Uvitex 2B (Ciba-Geigy) or a 001% solution of Calcofluor White M2R in 0.1 M phosphate-buffered saline, pH 7.0–8.0. The staining time is not critical since binding of the fluorescent agent is nearly instantaneous. Wash well in water and either observe wet under a coverslip or mount in buffered glycerol. Observe under fluorescent microscopy with a violet or blue excitation filter.

1.11.2.4 Polar Filament Extrusion

Definite proof of an organism being a microsporidium is obtained when the spore extrudes its filament. Polar filament extrusion is, however, a capricious event. Some microsporidia extrude filaments easily without any special stimulation, whereas others are quite unresponsive to mechanical and chemical stimuli. No single reliable method can be recommended for filament extrusion, and experiments may be necessary for each species. Useful hints for initiating spore germination can be found in Undeen and Vávra (1997). The following methods may be successful, but in any case, not all spores are extruded:

1. *Pressure*. Apply thumb pressure on the coverslip of a wet preparation with spore material (for safety reasons, cover the slide with a piece of filter paper).
2. *Hydrogen peroxide*. Mix a suspension of material containing spores in a 1:1 proportion with 3–6% H_2O_2 or with the same hydrogen peroxide concentration in 0.1 M KCl.
3. *Alkaline priming*. Mix the material to be examined (spore suspension) in a 1:1 proportion with 0.2 M KOH and allow to stand for about 30 min. Centrifuge and discard the supernatant. On a slide, mix a very small portion of the sediment with a large drop of Dulbecco's phosphate-buffered saline, pH 7.3 (without Mg/Ca), containing 0.93 g of KCl in 100 ml, apply a coverslip, and observe (modified method of Yasunaga et al. 1995).
4. *Rewetting of spores*. Try to flood with tap water a freshly dried smear of material with spores.
5. To a drop of material with spores in water on a slide, add a few small crystals of KCl. Cover and observe. Convection currents during salt dissolution will move the spores through different concentrations of KCI; some spores will be primed and probably extruded.

1.11.2.5 Transmission Electron Microscopy

Another unambiguous method for proving that an organism is a microsporidium is TEM. It is important not to fix in ethanol or another alcohol prior to fixation for electron microscopy as the cytology is destroyed by the alcohol.

The recommended handling of microsporidia for TEM has been summarized by Becnel (2012). Routine techniques are used for fixation (two fixation times are recommended: normal for presporal stages and extended periods up to 24 h or more for spores). Spores also require longer infiltration times in the resin. Useful hints for the fixation of spores can be found in Larsson (2005). This author showed that spores can be stored in glutaraldehyde for long periods of time; that paraformaldehyde and formaldehyde, without addition of methanol as a stabilizer, sometimes fix the spores better than the conventional glutaraldehyde; and that freezing does not completely destroy spore ultrastructure. It is worth mentioning that useful ultrastructural information can be obtained even from spores which simply have been dried within their hosts (even for many

years) and then fixed in 4% unstabilized formaldehyde at 60°C for 5 h (Larsson, unpublished). If spore fixation using cold glutaraldehyde fails, it is always worth testing hot formaldehyde. Useful information on the structure of spores can be obtained by reprocessing histological materials embedded in paraffin. Even materials on stained slides provide information on the polar filament structure and the spore wall when processed for electron microscopy. For such purposes, after the mounting medium is removed by soaking in xylene, sections are rehydrated to 50% ethanol and transferred via 0.1 M cacodylate buffer into 1% OsO_4 in a buffer. After they are washed and dehydrated in ethanol, they are transferred to propylene oxide, to mixtures of 70:30 and 30:70 propylene oxide: epoxy embedding resin, and finally to resin alone. A prepolymerized block of resin is placed on top of each section, and the slide is incubated overnight at 65°C to allow polymerization of the new resin. The slide is then placed on a hot plate, and the section, now embedded in resin, is snapped off. Sections are cut from the exposed face of the block (Curry, personal communication). A simpler method using melted agar for the removal and further processing of deparaffinized tissue was described by Larsson (1983c).

1.11.3 Observation and Measuring of Microsporidian Spores

Although microsporidian spores seem to be quite uniform in appearance (spores of most species being oval or pyriform), they are indispensable for diagnosis provided that their shape and size are observed in vivo and properly described. Especially in the case of microsporidia from water-dwelling invertebrate hosts, the spores are equipped with ornamentations or mucous layers on their surfaces that can be used as taxonomic characters (see Sections 1.2.1 and 1.6.3.1).

1.11.3.1 Staining of Microsporidia and Archival Storage

Giemsa staining of methanol-fixed smears is the standard technique for microsporidia. When preparing the smear, it is important to apply the technique described in "The appearance of infected hosts and tissues and the making of smears." Giemsa staining may be used also for sections of paraffin-embedded material (Short & Cooper 1948, see the recipe in Vávra & Maddox 1976). Giemsa stains, although fast and easy, may fade rather quickly, especially when improper mounting medium is used. It is safer to leave Giemsa-stained smears uncovered, and it opens the possibility to isolate DNA from such smears at a later time (Hyliš et al. 2005).

Hematoxylin stains are generally the best for slides intended for storing for a long time as type material. Modified Heidenhain's iron hematoxylin stain is relatively fast and gives excellent results.

Iron Hematoxylin Staining (Sprague 1981)

(i) Place sections in distilled water. (ii) Mordancy in Lang's solution follows (300 ml of 4% ferric ammonium sulfate, 5.0 ml of acetic acid, and 0.6 ml of sulfuric acid) for 10–30 min or longer (time is not critical). (iii) Wash in running tap water for 5 min. (iv) Rinse in distilled water. (v) Stain in 0.5% aqueous hematoxylin (for preparation, see any histology manual) about one or two times as long as the time in mordant (time is not critical). (vi) Destain in a saturated picric acid solution in distilled water for 10–60 min (control the amount of destaining under the microscope). (vii) Wash for 1 h in running tap water. (vii) Counterstain with eosin, light green, etc. (ix) Dehydrate, clear, and mount.

1.11.3.2 Immobilization of Spores

The microscopist is confronted with the fact that spores in fresh mounts are moving as a result of Brownian movement, making it difficult to determine their shape and size. Mounting the spores on an agar monolayer (Vávra 1964) prevents Brownian movement and allows an exact measurement of size and a recording of shape. The method is as follows: (i) Prepare a 1.5% solution of agar melted in hot, distilled water. (ii) Pour a thin layer of agar on a slide and let it cool and congel (the surface of the agar layer should be a little convex and smooth). (iii) Put a small drop of a thick spore suspension on a coverslip. (iv) Invert the coverslip and place it on the agar layer in a single motion. Do not move it any further. There will be areas where the spores are immobilized in a single layer between the agar and the coverslip. Although the preparation can be observed immediately, sometimes it improves after several hours when the agar layer has begun to dry with the effect that the spores are pressed more firmly into the agar layer. The preparation can be stored (in a wet Petri dish or sealed with paraffin or nail polish) for some days. An alternative to this method is the technique described by Hostounský and Žižka (1979) in which agar-coated slides are prepared in advance and afterward dried and stored cold. A coverslip with wet spores is then put on the dried agar, which absorbs the water, swells to some degree, and immobilizes the spores.

1.11.3.3 Recording of Shape

A micrograph of fresh spores provides more information than the best verbal description, and it should be an obligatory component of a description of a new microsporidium. It is surprising that very few descriptions of new microsporidian taxa include good micrographs showing the important features of the spores. Good photographs do not only

show the shape and size of the spores, but they also provide information on the size and position of the posterior vacuole. The light microscopic aspect of the living spore, as shown in a quality micrograph, is sometimes the only means by which the microsporidium studied can be compared with the species described in the first 100 years of microsporidiology.

For photographic recording, it is necessary to use high-contrast camera setting or to use high-contrast negative material (e.g., material for reproduction of line drawings). Do not close the condenser aperture of the microscope excessively and do not use phase contrast because the outline of spore contours is distorted by diffraction lines. The entire photographic process should be aimed at obtaining maximum print contrast.

1.11.3.4 Measuring of Spore Size

The size of spores is an important structural character, but its exact recording is difficult, especially in microsporidia with very small spores. Current ocular micrometers do not provide enough accuracy since it is difficult to superimpose the scale exactly with the refractive spore edge. The use of a special measuring eyepiece (image-splitting eyepiece; Vickers Instruments, Ltd., York, UK) is strongly recommended (Kramer 1964). A more modern method is the use of a computerized image analysis program. Measuring spores on photographs, made with a carefully calibrated microscope and photographic enlarger, is a suitable alternative if a special eyepiece or image analyzer is not available. Fixation causes spores to shrink up to 25%, which means that measurements of spore samples can be compared only if the samples have been treated in an identical way. It is necessary always to specify how the measured spores have been treated.

1.11.3.5 Demonstration of Exospore Ornamentations and the Mucocalyx

Spores of microsporidia infecting aquatic organisms often bear appendages in the form of tails, fibers, mucous layers, etc. (see Section 1.6.3.1). Relatively thick elements of this kind can be shown by negative staining methods, that is, techniques in which the stain does not penetrate the spore structures, and they therefore appear unstained on a stained background. Fine ornamentations, however, can be seen only with electron microscopy. The technique differs if the mucocalyx or spore appendages are demonstrated:

1. *Mucocalyx.* Mix a large drop of a fresh spore suspension in water with a small drop of India ink. Apply a coverslip and observe. If the spores have a mucocalyx, it will appear as a transparent area, that is, a halo, around the spore (Lom & Vávra 1963b) (Fig. 1.1m).
2. *Spore appendages*. Mix a spore suspension in water with a small drop of bacteriological ink (either original Burri ink for bacteriology or a 5–10% solution of water-soluble nigrosine in water employing the modification of Deflandre (1923)). Make a smear and let the preparation dry. Spore appendages are revealed as white fibers on a dark background. The thickness of the smear and the amount of dye are critical. This method is one of the simplest ways to demonstrate spores in a smear (Vávra 1963).

1.11.3.6 Spore Nuclei Techniques

Nuclear configuration is an important structural marker. Current staining methods (e.g., Giemsa stain and hematoxylin) fail to reveal nuclei in spores properly since the spore contents stain too deeply. Also, the Feulgen reaction, which is DNA-specific, stains spore nuclei indistinctly (Jírovec 1932). The best method is Giemsa staining following hydrolysis, which decreases the stainability of the cytoplasm surrounding the nucleus (Piekarski 1937, modified): (i) Fix the smear of spores in any conventional fixative. (ii) Wash in distilled water. (iii) Hydrolyze in 1N HCl at 60°C for 2–10 min. Time is critical and should be adjusted for each species. (iv) Wash well in several changes of tap water followed by distilled water to remove all traces of the acid. (v) Stain in a conventional way with Giemsa stain. The nuclei appear bright red in an almost colorless spore. This technique is practically the only staining method that shows microsporidian nuclei satisfactorily. Do not mistake nuclei for posterosomes (Section 1.5.5.3), which also stain in the posterior portion of young spores. A simple variation of this technique, which provides less control of the process, involves heating of a dried spore smear covered with a large drop of 1N HCl over a small flame of a Bunsen burner (or burning match) until the first fumes appear. Further washing and staining should then proceed as stated earlier (Weiser 1976b).

1.11.3.7 Visualization of Sporophorous Vesicles

Many microsporidia form SPOVs which have relatively thick walls and are persistent. Other microsporidia form thin-walled vesicles, which may be persistent or subpersistent or even disappear upon spore maturation. Some SPOVs are well visible under the light microscope, others are seen only if high magnification is used, and some are nearly invisible. A simple technique using in vivo staining can be applied for revealing the presence of SPOVs. If a drop of spore suspension is mixed in 1:1

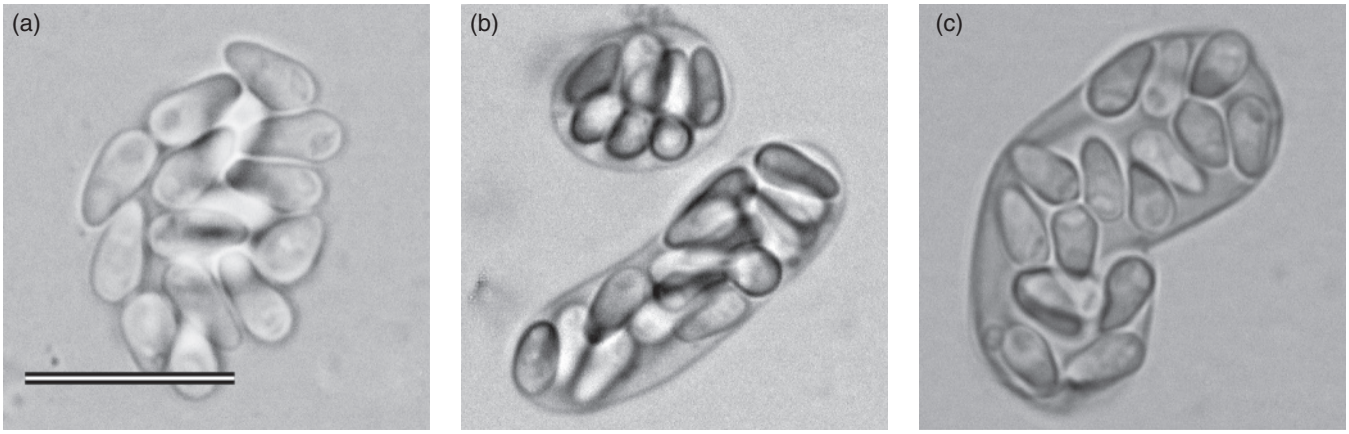

Figure 1.33 Visualization of SPOVs by in vivo staining (*Binucleata daphniae*). (a) In the unstained group of spores, the thin-walled SPOV around the spores is virtually invisible. (b) Addition of Congo Red makes the volume of the SPOV swell and stains the wall. (c) Similar but more distinct staining is achieved by Azidine Scarlett Red ("Vital Red"). Scale bar = 10 μm (Original photos by J. Vávra).

proportion with 1% aqueous solution of Congo Red, the SPOVs swell, and their walls are stained (Solter et al. 2012). Similar, even more distinct staining can be achieved if instead of Congo Red the Azidine Scarlett Red ("Vital Red") is used at the same concentration (Vávra et al. 2011) (Fig. 1.33).

ACKNOWLEDGMENTS

We express our sincere thanks to the following colleagues who kindly contributed to the chapter by providing photomicrographs, material, information, or criticism: J. J. Becnel (USDA, ARS, Gainesville, FL), A. Cali (Rutgers University, Newark, NJ), E. U. Canning (Imperial College, London, UK), A. Curry (Whittington Hospital, Manchester, UK), I. Desportes-Livage (INSERM and Musée d'Histoire Naturelle, Paris, France), I. Fries (Swedish University of Agricultural Sciences, Uppsala, Sweden), M. Hyliš (Faculty of Science, Charles University, Prague, Czech Republic), B. Koudela (Veterinary Research Institute, Brno, Czech Republic), J. M. Orenstein (George Washington University, Washington, DC), E. Porchet-Henneré (Université de Lille, Lille, France), J. Schrével (Musée d'Histoire Naturelle, Paris, France), J. A. Shadduck (Heska Corp., Fort Collins, CO), K. Snowden (Texas A & M University, College Station, TX), M. A. Spycher (University Hospital, Zürich, Switzerland), G. Stentiford (Cefas, UK), P. M. Takvorian (Rutgers University, Newark, NJ), B. S. Toguebaye (Université Cheik Antal Diop, Dakar, Senegal), D. Vinckier (Université de Lille, Lille, France), R. Weber (University Hospital, Zürich, Switzerland), E. Weidner (Louisiana State University, Baton Rouge, LA), J. Weiser (Institute of Entomology, České Budejovice, Czech Republic), and L. M. Weiss (Albert Einstein College of Medicine, Bronx, NY).

REFERENCES

Adl, S. M., Simpson, A. G., Lane, C. E., et al. 2012. The revised classification of eukaryotes. *J. Eukaryot. Microbiol.* 59:429–493.

Agaud, A., Achbarou, A., Desportes-Livage, I. 1997. Cell invasion by the microsporidium *Encephalitozoon intestinalis*. *J. Eukaryot. Microbiol.* 44S:81S.

Alfa, C. E., Hyams, J. S. 1990. Many routes lead to the pole. *Nature* 348:484.

Andreadis, T. G. 1983. Life cycle and epizootiology of *Amblyospora* sp. (Microspora: Amblyosporidae) in the mosquito, *Aedes cantator*. *J. Protozool.* 30:509–518.

Balbiani, G. 1882. Sur les Microsporidies ou Psorospermies des Articules. *C. R. Acad. Sci. Paris* 95:1168–1171.

Barker, R. J. 1975. Ultrastructural observation on *Encephalitozoon cuniculi* Levaditi, Nicolau et Schoen, 1922, from mouse peritoneal macrophages. *Folia Parasitol.* 22:1–9.

Batson, B. S. 1982. A light and electron microscopical study of *Trichoduboscqia epeori* Léger, 1926 (Microspora, Duboscqiidae). *J. Protozool.* 29:202–212.

Batson, B. S. 1983. A light and electron microscope study of *Hirsutosporos austrosimulii* gen. n., sp. n. (Microspora: Nosematidae), a parasite of *Austrosimulium* sp. (Diptera: Simuliidae) in New Zealand. *Protistologica* 19:263–280.

Beard, C. B., Butler, J. F., Becnel, J. J. 1990. *Nolleria pulicis* n. gen., n. sp. (Microsporida: Chytridiopsidae), a microsporidian parasite of the cat flea, *Ctenocephalides felis* (Siphonaptera: Pulicidae). *J. Protozool.* 37:90–99.

Becnel, J. J. 1992. Horizontal transmission and subsequent development of *Amblyospora californica* (Microsporida, Amblyosporidae) in the intermediate and definitive hosts. *Dis. Aquat. Org.* 13:17–28.

Becnel, J. J. 1994. Life cycles and host-parasite relationships of Microsporidia in culicine mosquitoes. *Folia Parasitol.* 41:91–96.

Becnel, J. J. 2012. Complementary techniques: preparations of entomopathogens and diseased specimens for more detailed study using microscopy. *In:* L. A. Lacey (ed.), Manual of Techniques in Insect Pathology, 2nd Ed. Academic Press, Amsterdam, pp. 451–470.

Becnel, J. J., Fukuda, T. 1991. Ultrastructure of *Culicosporella lunata* (Microsporida: Culicosporiidae fam. n.) in the mosquito *Culex pilosus* (Diptera: Culicidae) with new information on the developmental cycle. *Eur. J. Protistol.* 26:319–329.

Becnel, J. J., Hazard, E. I., Fukuda, T., Sprague, V. 1987. Life cycle of *Culicospora magna* (Kudo, 1920) (Microsporida: Culicosporidae) in *Culex restuans* Theobald with special reference to sexuality. *J. Protozool.* 34:313–322.

Becnel, J. J., Sprague, V., Fukuda, T., Hazard, E. I. 1989. Development of *Edhazardia aedis* (Kudo, 1930) n. g., n. comb. (Microsporida: Amblyosporidae) in the mosquito *Aedes aegypti* (L.) (Diptera: Culicidae). *J. Protozool.* 36:119–130.

Becnel, J. J., Sweeney, A. W. 1990. *Amblyospora trinus* n. sp. (Microsporida: Amblyosporidae) in the Australian mosquito *Culex halifaxi* (Diptera: Culicidae). *J. Protozool.* 37:584–592.

Berrebi, P. (1978). Contribution a l'étude biologique des zones saumâtres du littoral mediterranéen français. Biologie d'une Microsporidie: *Glugea atherini* n. sp. parasite de l'Atherine: *Atherina boyeri* Risso, 1810 (Poisson-Teleostéen) des étangs côtiers. Ph.D. Thesis, Université des Sciences et Techniques du Languedoc, Montpellier, France.

Beznoussenko, G. V., Dolgikh, V. V., Seliverstova, E. V., et al. 2007. Analogs of the Golgi complex in microsporidia: structure and avesicular mechanisms of function. *J. Cell Sci.* 120:1288–1298.

Bigliardi, E., Selmi, M. G., Lupetti, P., et al. 1996. Microsporidian spore wall: ultrastructural findings on *Encephalitozoon hellem* exospore. *J. Eukaryot. Microbiol.* 43:181–186.

Bohne, W., Böttcher, K., Großs, U. 2011. The parasitophorous vacuole of *Encephalitozoon cuniculi*: biogenesis and characteristics of the host cell-pathogen interface. *Int. J. Med. Microbiol.* 301:395–399.

Bronnvall, A., Larsson, J. I. R. 1995a. Description of *Binucleospora elongata* gen. et sp. nov. (Microspora, Caudosporidae), a microsporidian parasite of ostracods of the genus *Candona* (Crustacea, Cyprididae) in Sweden. *Eur. J. Protistol.* 31:63–72.

Bronnvall, A., Larsson, J. I. R. 1995b. Description of *Lanatospora tubulifera* sp. n. (Microspora, Tuzetiidae) with emended diagnosis and new systematic position for the genus *Lanatospora*. *Arch. Protistenkd*. 146:69–78.

Brooks, W. M., Becnel, J. J., Kennedy, G. G. 1988. Establishment of *Endoreticulatus* n. g. for *Pleistophora fidelis* (Hostounský and Weiser 1985) (Microsporida: Pleistophoridae) based on the ultrastructure of a microsporidium in the Colorado potato beetle *Leptinotarsa decemlineata* (Say) (Coleoptera: Chrysomelidae). *J. Protozool.* 35:481–488.

Brooks, W. M., Hazard, E. I., Becnel, J. 1985. Two new species of *Nosema* (Microsporida: Nosematidae) from the Mexican bean beetle *Epilachna varivestis* (Coleoptera: Coccinellidae). *J. Protozool.* 32:525–535.

Burges, H. D., Canning, E. U., Hulls, I. K. 1974. Ultrastructure of *Nosema oryzaephili* and the taxonomic value of the polar filament. *J. Invertebr. Pathol.* 23:135–139.

Bylén, E. K. C., Larsson, J. I. R. 1994. *Napamichum cellatum* n. sp. (Microspora, Thelohaniidae), a new parasite of midge larvae of the genus *Endochironomus* (Diptera, Chironomidae) in Sweden. *J. Eukaryot. Microbiol.* 41:450–457.

Bylén, E. K. C., Larsson, J. I. R. 1996. Ultrastructural study and description of *Mrazekia tetraspora* Léger & Hesse, 1922 and transfer to a new genus *Scipionospora* n. g. (Microspora, Caudosporidae). *Eur. J. Protistol.* 32:104–115.

Cali, A., El Garhy, M. 1991. Ultrastructural study of the development of *Pleistophora schubergi* Zwölfer, 1927 (Protozoa: Microsporida) in larva of the spruce budworm, *Choristoneura fumiferana* and its subsequent taxonomic change to the genus *Endoreticulatus*. *J. Protozool.* 38:271–278.

Cali, A., Kotler, D. P., Orenstein, J. M. 1993. *Septata intestinalis* n. g., n. sp., an intestinal microsporidian associated with chronic diarrhea and dissemination in AIDS patients. *J. Eukaryot. Microbiol.* 40:101–112.

Cali, A., Owen, R. L. 1990. Intracellular development of *Enterocytozoon*, a unique microsporidian found in the intestine of AIDS patients. *J. Protozool.* 37:145–155.

Cali, A., Takvorian, P. M., Lewin, S., et al. 1996. Identification of a new *Nosema*-like microsporidian associated with myositis in an AIDS patient. *J. Eukaryot. Microbiol.* 43:108S.

Cali, A., Takvorian, P. M., Lewin, S., et al. 1998. *Brachiola vesicularum*, n. g., n. sp., a new microsporidium associated with AIDS and myositis. *J. Eukaryot. Microbiol.* 45:240–251.

Cali, A., Takvorian, P. M., Weiss, L. M. 2002. *Brachiola algerae* spore membrane systems, their activity during extrusion, and a new structural entity, the multilayered interlaced network, associated with the polar tube and the sporoplasm. *J. Eukaryot. Microbiol.* 49:164–174.

Cali, A., Weiss, L. M., Takvorian, P. M. 1996. Microsporidian taxonomy and the status of *Septata intestinalis*. *J. Eukaryot. Microbiol.* 43:106S–107S.

Canning, E. U. 1988. Nuclear division and chromosome cycle in microsporidia. *BioSystems* 21:333–340.

Canning, E. U., Barker, R. J. Hammond, J. C., Nicholas, J. P. 1983. *Unikaryon slaptonleyi* sp. nov. (Microspora: Unikaryonidae) isolated from echinostome and strigeid larvae from *Lymnaea peregra*: observations on its morphology, transmission and pathogenicity. *Parasitology* 87:175–184.

Canning, E. U., Field, A. S., Hing, M. C., Mariott, D. J. 1994. Further observations on the ultrastructure of *Septata intestinalis* Cali, Kotler et Orenstein, 1993. *Eur. J. Protistol.* 30:414–422.

Canning, E. U., Hazard, E. I. 1982. Genus *Pleistophora* Gurley, 1893: an assemblage of at least three genera. *J. Protozool.* 29:38–49.

Canning, E. U., Lom, J., Nicholas, J. P. 1982. Genus *Glugea* Thélohan, 1891 (Phylum Microspora): redescription of the type species *Glugea anomala* (Moniez, 1887) and recognition of its sporogonic development within sporophorous vesicles (pansporoblastic membranes). *Protistologica* 18:193–210.

Canning, E. U., Nicholas, P. 1980. Genus *Pleistophora* (Phylum Microspora): redescription of the type species, *Pleistophora typicalis* Gurley, 1893 and ultrastructural characterization of the genus. *J. Fish Dis.* 3:317–338.

Canning, E. U., Vávra J. 2000. Phylum Microsporidia Balbiani, 1882. *In:* Lee, J. J., Leedale, G. F., Bradbury, P. (eds.), The Illustrated Guide to the Protozoa, 2nd Ed. Society of Protozoologists Lawrence, Kansas, pp. 39–126.

Cavalier-Smith, T. 2001. What are fungi? *In:* McLaughlin, D. J., McLaughlin, E. G., Lemke, P. A. (eds.), The Mycota, vol. VII, Part A. Systematics and Evolution. Springer Verlag, Berlin, pp. 3–37.

Chen, W. J., Barr, A. R. 1995. Chromosomal evidence on the sporogony of *Amblyospora californica* (Microspora: Amblyosporidae) in *Culex tarsalis* (Diptera: Culicidae). *J. Eukaryot. Microbiol.* 42:103–108.

Choudhary, M. M., Metcalfe, M. G., Arrambide, K., et al. 2011. *Tubulinosema* sp. microsporidian myositis in immunosuppressed patient. *Emerg. Infect. Dis.* 17:1727–1730.

Codreanu, R., Vávra, J. 1970. The structure and ultrastructure of the microsporidian *Telomyxa glugeiformis* Léger and Hesse, 1910, parasite of *Ephemera danica* (Müll) nymphs. *J. Protozool.* 17:374–384.

Corradi, N., Keeling, P. J. 2009. Microsporidia: a journey through radical taxonomical revisions. *Fungal Biol. Rev.* 23:1–8.
Coyle, C. M., Weiss, L. M., Rhodes III, L. V., et al. 2004. Fatal myositis due to the microsporidian *Brachiola algerae*, a mosquito pathogen. *N. Engl. J. Med.* 351:42–47.
Curgy, J. J., Vávra, J., Vivarès, C. 1980. Presence of ribosomal RNAs with prokaryotic properties in Microsporidia, eukaryotic organisms. *Biol. Cell.* 38:49–52.
Deflandre, G. 1923. Emploi de la nigrosine dans l'étude des algues inférieures. *Bull. Soc. Bot. Fr.* 70:738–741.
Desportes, I. 1976. Ultrastructure de *Stempellia mutabilis* Léger & Hesse, Microsporidie parasite de l'Éphémère *Ephemera vulgata* L. *Protistologica* 12:121–150.
Desportes, I., Le Charpentier, Y., Galian, A., et al. 1985. Occurrence of a new microsporidian: *Enterocytozoon bieneusi* n.g., n. sp., in the enterocytes of a patient with AIDS. *J. Protozool.* 32:250–254.
Desportes, I., Théodoridès, J. 1979. Étude ultrastructurale d'*Amphiamblys laubieri* n. sp. (Microsporidie, Metchnikovellidae) parasite d'une Grégarine (*Lecudina* sp.) d'un Echiurien abyssal. *Protistologica* 15:435–457.
Desportes-Livage, I., Chilmonczyk, S., Hedrick, R., et al. 1996. Comparative development of two microsporidian species: *Enterocytozoon bieneusi* and *Enterocytozoon salmonis*, reported in AIDS patients and salmonid fish respectively. *J. Eukaryot. Microbiol.* 43:49–60.
Desportes-Livage, I., Harper, F., Hilmarsdottir, I., Benhamou, Y., Ombrouck, C., Gentilini, M. 1993. The phospholipids in *Enterocytozoon bieneusi*: an electron spectroscopic imaging study. *Folia Parasitol.* 40:275–278.
Desportes-Livage, I., Hilmarsdottir, I., Romana, C., Tanguy, S., Datry, A., Gentilini, M.1991. Characteristics of the microsporidian *Enterocytozoon bieneusi*: a consequence of its development within short-living enterocytes. *J. Protozool.* 38:111S–113S.
Desser, S. S., Hong, H., Yang, Y. J. 1992. Ultrastructure of the development of a species of *Encephalitozoon* cultured from the eye of an AIDS patient. *Parasitol. Res.* 78:677–683.
Dickson, D. L., Barr, A. R. 1990. Development of *Amblyospora campbelli* (Microsporida: Amblyosporidae) in the mosquito *Culiseta incidens* (Thomson). *J. Protozool.* 37:71–78.
Didier, E. S., Didier, P. J., Friedberg, D., et al. 1991. Isolation and characterization of a new human microsporidian *Encephalitozoon hellem* (n. sp.), from three AIDS patients with keratoconjunctivitis. *J. Infect. Dis.* 163:617–621.
Ditrich, O., Lom, J., Dyková, I., Vávra, J. 1994. First case of *Enterocytozoon bieneusi* infection in the Czech Republic: comments on the ultrastructure and teratoid sporogenesis of the parasites. *J. Eukaryot. Microbiol.* 41:35S–36S.
Fasshauer, V., Gross, U., Bohne, W. 2005. The parasitophorous vacuole membrane of *Encephalitozoon cuniculi* lacks host cell membrane proteins immediately after invasion. *Eukaryot. Cell* 4:221–224.
Faye, N., Toguebaye, B. S., Bouix, G. 1991. *Microfilum lutjani* n. g., sp. n. (Protozoa, Microsporidia), a gill parasite of the golden African snapper *Lutjanus fulgens* (Valenciennes, 1830) (Teleost Lutjanidae): developmental cycle and ultrastructure. *J. Protozool.* 38:30–40.
Field, A. S., Paik, J. Y., Stark, D., et al. 2012. Myositis due to the microsporidian *Anncaliia* (Brachiola) *algerae* in a lung transplant recipient. *Transp. Infect. Dis.* 14:169–176.
Flegel, T. W., Pasharawipas, T. 1995. A proposal for typical eukaryotic meiosis in microsporidians. *Can. J. Microbiol.* 41:1–11.
Franzen, C., Fischer, S., Schroeder, J., Schölmerich, J., Schneuwly, S. 2005. Morphological and molecular investigations of *Tubulinosema ratisbonensis* gen. nov., sp. nov. (Microsporidia: Tubulinosematidae fam. nov.), a parasite infecting a laboratory colony of *Drosophila melanogaster* (*Diptera*: Drosophilidae). *J. Eukaryot. Microbiol.* 52:141–152.
Franzen, C., Futerman, P. H., Schroeder, J., Salzberger, B., Kraaijeveld, A. R. 2006a. An ultrastructural and molecular study of *Tubulinosema kingi* Kramer (Microsporidia: Tubulinosematidae) from *Drosophila melanogaster* (*Diptera*: Drosophilidae) and its parasitoid *Asobara tabida* (Hymenoptera: Braconidae). *J. Invertebr. Pathol.* 91:158–167.
Franzen, C., Nassonova, E. S., Schölmerich, J., Issi, I. V. 2006b. Transfer of the members of the genus *Brachiola* (Microsporidia) to the genus *Anncaliia* based on ultrastructural and molecular data. *J. Eukaryot. Microbiol.* 53:26–35.
Freeman, M. A., Sommerville, C. 2011. Original observations of *Desmozoon lepeophtherii*, a microsporidian hyperparasite infecting the salmon louse *Lepeophtheirus salmonis*, and its subsequent detection by other researchers. *Parasit. Vec.*, 4:231.
Garcia, L. S. 2002. Laboratory identification of microsporidia. *J. Clin. Microbiol.* 40:1892–1901.
Ghosh, K., Nieves, E., Keeling, P., et al. 2011. Branching network of proteinaceous filaments within the parasitophorous vacuole of *Encephalitozoon cuniculi* and *Encephalitozoon hellem*. *Infect. Immun.* 79:1374–1385.
Haag, K. L., Traunecker, E., Ebert, D. 2013. Single-nucleotide polymorphisms of two closely related microsporidian parasites suggest a clonal population expansion after the last glaciation. *Mol. Ecol.* 22:314–326.
Hazard, E. I., Brookbank, J. W. 1984. Karyogamy and meiosis in an *Amblyospora* sp. (Microspora) in the mosquito *Culex salinarius*. *J. Invertebr. Pathol.* 44:3–11.
Hazard, E. I., Ellis, E. A., Joslyn, D. J. 1981. Identification of microsporidia. *In:* Burges, H. D. (ed.), Microbial Control of Plant Diseases 1970-1980. Academic Press, London, pp. 163–182.
Hazard, E. I., Fukuda, T., Becnel, J. J. 1985. Gametogenesis and plasmogamy in certain species of Microspora. *J. Invertebr. Pathol.* 46:63–69.
Hazard, E. I., Oldacre, S. W. 1975. Revision of Microsporida (Protozoa) Close to *Thelohania*, with Descriptions of One New Family, Eight New Genera, and Thirteen New Species. U.S. Dept. Agric. Tech. Bull. 1530. U.S. Department of Agriculture, Washington, DC.
Hedrick, R. P., Groff, J. M., Baxa, D. V. 1991. Experimental infections with *Nucleospora salmonis* n. g., n. sp.: an intranuclear microsporidium from chinook salmon (*Oncorhynchus tshawitscha*). *Fish Health Sect./Am. Fish. Soc. Newsl.* 19:5.
Henneguy, F., Thélohan, P. 1892. Sur un Sporozoaire parasite des muscles des Crustacés decapods. *C. R. Acad. Sci. Paris* 114:1552–1555.
Hildebrand, H., Vivier, E. 1971. Observations ultrastructurales sur le sporoblaste de *Metchnikovella wohlfarthi* n. sp. (Microsporidies), parasite de la Grégarine *Lecudina tuzetae*. *Protistologica* 7:131–139.
Hilmarsdottir, I., Desportes-Livage, I., Datry, A., Gentilini, M. 1993. Morphogenesis of the polaroplast in *Enterocytozoon bieneusi* Desportes et al., 1985, a microsporidian parasite of HIV infected patients. *Eur. J. Protistol.* 29:88–97.
Hollande, A. 1972. Le déroulement de la cryptomitose et les modalités de la ségrégation des chromatides dans quelques groupes de Protozoaires. *Ann. Biol.* 11:427–466.
Hollister, W. S., Canning, E. U., Weidner, E., Field, A. S., Kench, J., Marriott, D. J. 1996. Development and ultrastructure of *Trachipleistophora hominis* n. g., n. sp., after in vitro isolation from an AIDS patient and inoculation into athymic mice. *Parasitology* 112:143–154.
Hostounský, Z., Žižka, Z. 1979. A modification of the "agar cushion method" for observation and photographic recording microsporidian spores. *J. Protozool.* 26:41A–42A.

Hurst, L. D. 1993. Drunken walk of the diploid. *Nature* 365:206–207.
Hyliš, M., Weiser, J., Oborník, M., Vávra, J. 2005. DNA isolation from museum and type collection slides of microsporidia. *J. Invertebr. Pathol.* 88:257–260.
Ignatius, R., Lehmann, M., Miksits, K., et al. 1997. A new acid-fast trichrome stain for simultaneous detection of *Cryptosporidium parvum* and microsporidial species in stool specimens. *J. Clin. Microbiol.* 35:446–449.
International Commission on Zoological Nomenclature 1999. *International Code of Zoological Nomenclature.* 4th Ed. International Trust for Zoological Nomenclature, London.
Ironside, J. E. 2013. Diversity and recombination of dispersed ribosomal DNA and protein coding genes in microsporidia. *PLoS One* 8:e55878.
Ishihara, R., Hayashi, Y. 1968. Some properties of ribosomes from the sporoplasm of *Nosema bombycis*. *J. Invertebr. Pathol.* 11:377–385.
Issi, I. V. 1986. Microsporidia as a phylum of parasitic protozoa. *In* Beyer, T. V., Issi, I. V. (eds.), Protozoology, vol 10. USSR, Nauka, Leningrad, pp. 6–136 (In Russian with English summary.)
James, T. Y., Kauff, F., Schoch, C. L., et al. 2006. Reconstructing the early evolution of Fungi using a six-gene phylogeny. *Nature* 443:818–822.
Jírovec, O. 1932. Ergebnisse der Nuclealfarbung an den Sporen den Microsporidien nebst einigen Bemerkungen über *Lymphocystis*. *Arch. Protistenk.* 77:379–390.
Koudela, B., Visvesvara, G. S., Moura, H., Vávra, J. 2001. The human isolate of *Brachiola algerae* (Phylum Microspora): development in SCID mice and description of its fine structure features. *Parasitology* 123:153–162.
Kramer, J. P. 1964. *Nosema kingi* sp. n., a microsporidian from *Drosophila willistoni* Sturtevant, and its infectivity for other muscoids. *J. Insect. Pathol.* 6:491–499.
Larsson, J. I. R. 1980. Insect pathological investigations on Swedish Thysanura. II. A new microsporidian parasite of *Petrobius brevistylis* (Microcoryphia, Machilidae); description of the species and creation of two new genera and a new family. *Protistologica* 16:85–101.
Larsson, J. I. R. 1981a. The ultrastructure of the spore and sporogonic stages of *Telomyxa glugeiformis* Léger and Hesse 1910 (Microsporida: Telomyxidae). *Zool. Anz.* 206:137–153.
Larsson, J. I. R. 1981b. A new microsporidium *Berwaldia singularis* gen. et sp. nov. from *Daphnia pulex* and a survey of microsporidia described from Cladocera. *Parasitology* 83:325–342.
Larsson, J. I. R. 1981c. Description of *Nosema tractabile* n. sp. (Microspora, Nosematidae), a parasite of the leech *Helobdella stagnalis* (L.) (Hirudinea, Glossiphoniidae). *Protistologica* 17:407–422.
Larsson, J. I. R. 1982. Cytology and taxonomy of *Helmichia aggregata* gen. et sp. nov. (Microspora, Thelohaniidae), a parasite of *Endochironomus* larvae (Diptera, Chironomidae). *Protistologica* 18:355–370.
Larsson, J. I. R. 1983a. *Thelohania capillata* n. sp. (Microspora, Thelohaniidae)—an ultrastructural study with remarks on the taxonomy of the genus *Thelohania* Henneguy, 1892. *Arch. Protistenkd.* 127:21–46.
Larsson, J. I. R. 1983b. On two microsporidia of the amphipod *Rivulogammarus pulex*: light microscopical and ultrastructural observations on *Thelohania muelleri* (Pfeiffer, 1895) and *Nosema rivulogammari* n. sp. (Microspora, Thelohaniidae and Nosematidae). *Zool. Anz.* 211:299–323.
Larsson, J. I. R. 1983c. Description of *Hyalinocysta expilatoria* n. sp. a microsporidian parasite of the blackfly *Odagmia ornata*. *J. Invertebr. Pathol.* 42:348–356.
Larsson, J. I. R. 1983d. A revisionary study of the taxon *Tuzetia* Maurand, Fize, Fenwick and Michel, 1971 and related forms (Microspora). *Protistologica* 19:323–355.
Larsson, J. I. R. 1984. Ultrastructural study and description of *Chapmanium dispersus* sp. n. (Microspora. Thelohaniidae), a microsporidian parasite of *Endochironomus* larvae (Diptera, Chironomidae). *Protistologica* 20:547–563.
Larsson, J. I. R. 1985. On the cytology, development and systematic position of *Thelohania asterias* Weiser, 1963, with creation of the new genus *Bohuslavia* (Microspora, Thelohaniidae). *Protistologica* 21:235–248.
Larsson, J. I. R. 1986a. Development, ultracytology and taxonomical position of *Thelohania corethrae* Schuberg and Rodriguez, 1915 (Microspora, Thelohaniidae). *Arch. Protistenkd.* 132:245–264.
Larsson, J. I. R. 1986b. Ultrastructure, function and classification of microsporidia. *In:* Corliss, J. O., Patterson, D. J. (eds.), Progress in Protistology, vol. I. Biopress, Ltd., Bristol, pp. 325–390.
Larsson, J. I. R. 1986c. Ultrastructural investigation of two microsporidia with rod-shaped spores. with descriptions of *Cylindrospora fasciculata* sp. nov. and *Resiomeria odonatae* gen. et sp. nov. (Microspora, Thelohaniidae). *Protistologica* 22:379–398.
Larsson, J. I. R. 1986d. Ultrastructural study and description of *Vavraia holocentropi* n. sp. (Microspora, Pleistophoridae), a parasite of larvae of the caddisfly *Holocentropus dubius* (Trichoptera, Polycentropodidae). *Protistologica*, 22:441–452.
Larsson, J. I. R. 1986e. Ultracytology of a tetrasporoblastic microsporidium of the caddisfly *Holocentropus picicornis* (Trichoptera, Polycentropodidae), with description of *Episeptum inversum* gen. et sp. nov. (Microspora, Gurleyidae). *Arch. Protistenkd.* 131:257–279.
Larsson, J. I. R. 1987. Ultrastructure and development of a microsporidium of the genus *Pegmatheca* with description of *P. lamellata* sp. nov. (Microspora, Thelohaniidae). *Zool. Anz.* 218:304–320.
Larsson, J. I. R. 1988a. On the taxonomy of the genus *Systenostrema* Hazard & Oldacre. 1975 (Microspora, Thelohaniidae), with description of two new species. *Syst. Parasitol.* 11:3–17.
Larsson, J. I. R. 1988b. Isometric viruslike particles in spores of two microsporidia belonging to the Thelohaniidae. *J. Invertebr. Pathol.* 51:163–165.
Larsson, J. I. R. 1988c. Identification of microsporidian genera (Protozoa, Microspora)—a guide with comments on the taxonomy. *Arch. Protistenkd.* 136:1–37.
Larsson, J. I. R. 1989a. On the ultrastructure of *Hyalinocysta expilatoria* (Microspora, Thelohaniidae) and the taxonomy of the species. *J. Invertebr. Pathol.* 54:213–223.
Larsson, J. I. R. 1989b. Light and electron microscope studies on *Jirovecia involuta* sp. nov. (Microspora, Bacillidiidae): a new microsporidian parasite of oligochaetes in Sweden. *Eur. J. Protistol.* 25:172–181.
Larsson, J. I. R. 1989c. The light and electron microscopic cytology of *Bacillidium filiferum* sp. nov. (Microspora, Bacillidiidae). *Arch. Protistenkd.* 137:345–355.
Larsson, J. I. R. 1990a. Description of a new microsporidium of the water mite *Limnochares aquatica* and establishment of the new genus *Napamichum* (Microspora, Thelohaniidae). *J. Invertebr. Pathol.* 55:152–161.
Larsson, J. I. R. 1990b. On the cytology of *Jirovecia caudata* (Léger and Hesse, 1916) (Microspora, Bacillidiidae). *Eur. J. Protistol.* 25:321–330.
Larsson, J. I. R. 1990c. On the cytology and taxonomic position of *Nudispora biformis* n. g., n. sp. (Microspora. Thelohaniidae), a microsporidian parasite of the dragon fly *Coenagrion hastulatum* in Sweden. *J. Protozool.* 37:310–318.

Larsson, J. I. R. 1990d. *Rectispora reticulata* gen. et sp. nov. (Microspora, Bacillidiidae), a new microsporidian parasite of *Pomatothrix hammoniensis* (Michaelsen 1901) (Oligochaeta, Tubificidae). *Eur. J. Protistol.* 26:55–64.

Larsson, J. I. R. 1992. The ultrastructural cytology of *Bacillidium strictum* (Léger and Hesse, 1916) Jírovec, 1936 (Microspora, Bacillidiidae). *Eur. J. Protistol.* 28:175–183.

Larsson, J. I. R. 1993. Description of *Chytridiopsis trichopterae*, n. sp. (Microspora, Chytridiopsidae), a microsporidian parasite of the caddis fly *Polycentropus flavomaculatus* (Trichoptera, Polycentropodidae), with comments on relationships between the families Chytridiopsidae and Metchnikovellidae. *J. Eukaryot. Microbiol.* 40:37–48.

Larsson, J. I. R. 1994a. Characteristics of the genus *Bacillidium* Janda, 1928 (Microspora, Mrazekiidae): reinvestigation of the type species *B. criodrili* and improved diagnosis of the genus. *Eur. J. Protistol.* 30:85–96.

Larsson, J. I. R. 1994b. *Trichoctosporea pygopellita* gen. et sp. nov. (Microspora: Thelohaniidae), a microsporidian parasite of the mosquito *Aedes vexans* (Diptera, Culicidae). *Arch. Protistenk.* 144:147–161.

Larsson, J. I. R. 1995. A light microscopic and ultrastructural study of *Gurleya legeri* sensu Mackinnon (1911)—with establishment of the new species *Gurleya dorisae* sp. n. (Microspora, Gurleyidae). *Acta Protozool.* 34:45–56.

Larsson, J. I. R. 1996. Two tetrasporoblastic microsporidian parasites of caddis flies (Trichoptera) with description of the new species *Episeptum invadens* sp. n. *and Episeptum circumscriptum* sp. n. (Microspora, Gurleyidae*). Arch. Protistenk.* 146:349–362.

Larsson, J. I. R. 1999. Identification of microsporidia. *Acta Protozool.* 38:161–197.

Larsson, J. I. R. 2000. The hyperparasitic microsporidium *Amphiacantha longa* Caullery et Mesnil, 1914 (Microspora: Metchnikovellidae)—description of the cytology, redescription of the species, emended diagnosis of the genus *Amphiacantha* and establishment of the new family Amphiacanthidae. *Folia Parasitol.* 47:241–256.

Larsson, J. I. R. 2005. Fixation of microsporidian spores for electron microscopy. *J. Invertebr. Pathol.* 90:47–50.

Larsson, J. I. R., Ebert, D., Mangin, K. L., Vávra, J. 1998. Ultrastructural study and description *of Flabelliforma magnivora* sp. n. (Microspora, Duboscqiidae), a microsporidian parasite of *Daphnia magna* (Crustacea: Cladocera: Daphniidae). *Acta Protozool.* 37:41–52.

Larsson, J. I. R., Ebert, D., Vávra, J. 1997a. Ultrastructural Study and description of *Ordospora colligata* gen. et sp. nov. (Microspora, Ordosporidae fam. nov.), a new microsporidian parasite of *Daphnia magna* (Crustacea, Cladocera). *Eur. J. Protistol.* 33:432–443.

Larsson, J. I. R., Ebert, D., Vávra, J., Voronin, V. N. 1996. Redescription of *Pleistophora intestinalis* Chatton, 1907, a microsporidian parasite of *Daphnia magna* and *Daphnia pulex*, with establishment of the new genus *Glugoides* (Microspora, Glugeidae). *Eur. J. Protistol.* 32:251–261.

Larsson, J. I. R., Eilenberg, J., Bresciani, J. 1995. Ultrastructural study and description of *Cystosporogenes deliaradicae* n. sp. (Microspora, Glugeidae), a microsporidian parasite of the cabbage root fly *Delia radicum* (Linnaeus, 1758) (Diptera, Anthomyidae). *Eur. J. Protistol.* 31:275–285.

Larsson, J. I. R., Götz, P. 1996. Ultrastructural evidence for the systematic position of *Jirovecia brevicauda* (Léger and Hesse, 1916) Weiser, 1985 (Microspora, Mrazekiidae). *Eur. J. Protistol.* 32:366–371.

Larsson, J. I. R., Køie, M. 2006. The ultrastructure and reproduction of *Amphiamblys capitellides* (Microspora, Metchnikovellidae), a parasite of the gregarine *Ancora sagittata* (Apicomplexa, Lecudinidae), with redescription of the species and comments on the taxonomy. *Eur. J. Protistol.* 42:233–248.

Larsson, J. I. R., Steiner, M., Bjørnson, S. 1997b. *lntexta acarivora* gen. et sp. n. (Microspora: Chytridiopsidae)—ultrastructural study and description of a new microsporidian parasite of the forage mite *Tyrophagus putrescentiae* (Acari: Acaridae). *Acta Protozool.* 36:295–304.

Larsson, J. I. R., Vávra, J., Schrével, J. 1993. *Bacillidium cyclopis* Vávra, 1962. Description of the ultrastructural cytology and transfer to the genus *Mrazekia* Léger and Hesse, 1916 (Microspora, Mrazekiidae). *Eur. J. Protistol.* 29:49–60.

Léger, L. 1926. Une Microsporidie nouvelle à spores épineux. *C. R. Acad. Sci.* 182:727–729.

Léger, L., Hesse, E. 1910. Cnidosporidies des larves d'Éphémères. *C. R. Acad. Sci.* 150:411–414.

Léger, L., Hesse, E. 1916. *Mrazekia*, genre nouveau de Microsporidies à spores tubuleuses. *C. R. Soc. Biol.* 79:345–348.

Levaditi, C., Nicolau, S., Schoen, R. 1923. L'agent étiologique de l'encéphalite épizootique du lapin (*Encephalitozoon cuniculi*). *C. R. Acad. Sci. Biol.* 89:984–986.

Liu, T. P. 1972. Ultrastructural changes in the nuclear envelope of larval fat body cells of *Simulium vittatum* (Diptera) induced by microsporidian infection of *Thelohania bracteata*. *Tissue Cell* 4:493–502.

Liu, T. P. 1984. Virus-like cytoplasmic particles associated with lysed spores of *Nosema apis*. *J. Invertebr. Pathol.* 44:103–105.

Liu, T. P., Myrick, G. R. 1989. Deformities in the spore of *Nosema apis* as induced by intraconazole. *Parasitol. Res.* 75:498–502.

Liu, Y. J., Hodson, M. C., Hall, B. D. 2006. Loss of the flagellum happened only once in the fungal lineage: phylogenetic structure of Kingdom Fungi inferred from RNA polymerase II subunit genes. *BMC Evol. Biol.* 6:74.

Lom, J. 1953. Contribution to the development of *Mrazekia caudata* Léger et Hesse 1916. *Česk. Parasitol.* 5:147–151 (in Czech with English summary).

Lom, J. 1972. On the structure of the extruded microsporidian polar filament. *Z. Parasitenkd.* 38:200–213.

Lom, J., Corliss, J. O. 1967. Ultrastructure observations on the development of the microsporidian protozoon *Plistophora hyphessobryconis* Schaeperclaus. *J. Protozool.* 14:141–152.

Lom, J., Dyková, I. 1990. *Hrabyeia xerkophora* n. gen. n. sp., a new microsporidian with tailed spores from the oligochaete *Nais christinae* Kasprzak, 1973. *Eur. J. Protistol.* 25:243–248.

Lom, J., Dyková, I. 2005. Microsporidian xenomas in fish seen in wider perspective. *Folia Parasitol.* 52:69–81.

Lom, J., Vávra, J. 1963a. The mode of sporoplasm extrusion in microsporidian spores. *Acta Protozool.* 1:81–89.

Lom, J., Vávra, J. 1963b. Mucous envelopes of spores of the subphylum Cnidospora (Doflein, 1901). *Věst. Česk. Spol. Zool.* 27:4–6.

Loubès, C. 1979. Recherches sur la meiose chez les Microsporidies: consequences sur les cycles biologiques. *J. Protozool.* 26:200–208.

Loubès, C., Akbarieh, M. 1977. Étude ultrastructurale de *Nosemoides simocephali* n. sp. (Microsporidie), parasite intestinal de la Daphnie *Simocephalus vetulus* (Muller, 1776). *Z. Parasitenk.* 54:125–137.

Loubès, C., Akbarieh, M. 1978. Étude ultrastructurale de la Microsporidie *Baculea daphniae* n. g, n. sp., parasite de l'épithélium intestinal de *Daphnia pulex* Leydig, 1860 (Crustacé, Cladocère). *Protistologica* 14:23–38.

Loubès, C., Maurand, J. 1976. Étude ultrastructurale de *Pleistophora debaisieuxi* Jírovec, 1943 (Microsporida): son transfert dans le genre *Tuzetia* Maurand, Fize, Michel et Fenwick, 1971 et rémarques sur la structure et la genèse du filament polaire. *Protistologica* 12:577–591.

Loubès, C., Maurand, J., Ormières, R. 1979. Étude ultrastructurale de *Spraguea lophii* (Doflein, 1898), Microsporidie parasite de la Baudroi: éssai d'interpretation du dimorphisme sporal. *Protistologica* 15:43–54.

Loubès, C., Maurand, J., Rousset-Galangau, V. 1976. Présence de complexes synaptonématiques dans le cycle biologique de *Gurleya chironomi* Loubès et Maurand, 1975: un argument en faveur d'une sexualité chez les Microsporidies? *C. R. Acad. Sci.* 282:1025–1027.

Lowman, P. M., Takvorian, P. M., Cali, A. 2000. The effects of elevated temperatures and various time-temperature combinations on the development of *Brachiola* (*Nosema*) *algerae* N. Comb. in mammalian cell culture. *J. Eukaryot. Microbiol.* 47:221–234.

Martins, R. R., Perondini, A. L. P. 1974. Hipertrofia nuclear e síntese de RNA em células de *Rhynchosciara* infectadas por microsporídeos. *Cién. Cult.* 27:961–968.

Maurand, J. 1973. Recherches biologiques sur les Microsporidies des larves des Simulies. Thesis. Université des Sciences et Techniques du Languedoc, Académie de Montpellier, Montpellier, France.

Maurand, J., Fize, A., Fenwick, B., Michel, R.1971. Étude au microscope électronique de *Nosema infirmum* Kudo 1921, Microsporidie parasite d'un Copépode cyclopoïde; création du genre nouveau *Tuzetia*: à propos de cette éspèce. *Protistologica* 7:221–225.

Meissner, E. G., Bennett, J. E., Qvarnstrom, Y., et al. 2012. Disseminated microsporidiosis in an immunosuppressed patient. *Emerg. Infect. Dis.* 18:1155–1158.

Metenier, G., Vivarés, C. P., 2001. Molecular characteristics and physiology of microsporidia. *Microb. Infect.* 3, 407–415.

Milner, R. J., Mayer, J. A. 1982. *Tuzetia boeckella* sp. nov. (Protozoa: Microsporida), a parasite of *Boeckella triarticulata* (Copepoda: Calanoidea) in Australia. *J. Invertebr. Pathol.* 39:174–184.

Mitchell, M. J., Cali, A. 1993. Ultrastructural study of the development of *Vairimorpha necatrix* (Kramer, 1965) (Protozoa, Microsporida) in larvae of the corn earworm, *Heliothis zea* (Boddie) (Lepidoptera, Noctuidae) with emphasis on sporogony. *J. Eukaryot. Microbiol.* 40:701–710.

Moore, C. B., Brooks, W. M. 1992. An ultrastructural study of *Vairimorpha necatrix* (Microspora, Microsporida) with particular reference to episporontal inclusions during octosporogony. *J. Protozool.* 39:392–398.

Moore, C. B., Brooks, W. M.. 1994. An ultrastructural study of the episporontal inclusions produced during octosporogony by five species/isolates of *Vairimorpha* (Microspora: Microsporida). *J. Invertebr. Pathol.* 63:197–206.

Morrison, C. M., Sprague, V. 1981. Electron microscopical study of a new genus and new species of microsporida in the gills of Atlantic cod *Gadus morhua*. *J. Fish Dis.* 4:15–32.

Nägeli C. 1857. Über die neue Krankheit der Seidenraupe und verwandte Organismen. *Bot. Zeitung* 15:760–761.

Nassonova, E. S., Smirnov, A. V. 2005. Synaptonemal complexes as evidence for meiosis in the life cycle of the monomorphic diplokaryotic microsporidium *Paranosema grylli*. *Eur. J. Protistol.* 41:175–181.

Olson, R. B., Tiekotter, K. L., Reno, P. W. 1994. *Nadelspora canceri* n. g., n. sp., an unusual microsporidian parasite of the Dungeness crab, *Cancer magister*. *J. Eukaryot. Microbiol.* 41:349–359.

Orenstein, J. M. 1991. Microsporidiosis in the acquired immunodeficiency syndrome. *J. Parasitol.* 77:843–864.

Ormières, R., Loubès, C., Maurand, J. 1981. *Amphiamblys bhatiellae* n. sp., Microsporidie parasite de *Bhatiella marphysae* Setna, 1931, Eugrégarine d'Annélide polychète. *Protistologica* 17:273–280.

Overstreet, R. M., Weidner, E. 1974. Differentiation of microsporidian spore-tails in *Inodosporus spraguei* gen. et sp. n. *Z. Parasitenkd.* 44:169–186.

Pavan, C., Perondini, A. L. P., Picard, T. 1969. Changes in chromosomes and in development of cells of *Sciara ocellaris* induced by microsporidian infections. *Chromosoma* 28:328–345.

Piekarski, G. 1937. Cytologische Untersuchungen an Paratyphus und Colibakterien. *Arch. Mikrobiol.* 8:428–438.

Pilley, B. M. 1976. A new genus *Vairimorpha* (Protozoa: Microsporida) for *Nosema necatrix* Kramer I965: pathogenicity and life cycle in *Spodoptera exempta* (Lepidoptera: Noctuidae). *J. Invertebr. Pathol.* 28:177–183.

Purrini, K., Weiser, J. 1984. Light and electron microscopic studies of *Chytridiopsis typographi* (Weiser, 1954) Weiser, 1970 (Microspora) parasitizing the barkbeetle *Hylastes cunicularius* Er. *Zool. Anz.* 212:369–376.

de Puytorac, P., Tourret, M. 1963. Études de kystes d'origine parasitaire (Microsporidie ou Grégarines) sur la paroi interne du corps des vers Megascolecidae. *Ann. Parasitol. Hum. Comp.* 38:861–874.

Raikov, I. 1982. The Protozoan Nucleus, Morphology and Evolution. Cell Biology Monographs, vol. 9. Springer-Verlag, Vienna, pp. 1–474.

Rausch, M., Grunewald, J. 1980. Light and stereoscan electron microscopic observations on some microsporidian parasites (Cnidosporidia: Microsporidia) of blackfly larvae (Diptera: Simuliidae). *Z. Parasitenkd.* 63:1–11.

Redhead, S. A., Kirk, P. M., Keeling, P. J., Weiss, L. M. 2009. Proposals to exclude the phylum Microsporidia from the Code. *Taxon* 58:669.

Richards, C. S., Sheffield, H. G. 1970. Unique host relations and ultrastructure of a new microsporidian of the genus *Coccospora* infecting *Biomphalaria glabrata*. *In:* Proceedings of the IVth International Colloquium on Insect Pathology, College Park, MD, August 25–28. Society for Invertebrate Pathology, Gainesville, FL, pp. 439–452.

Schubert, G. 1969. Ultracytologische Untersuchungen an der Spore der Mikrosporidienart, *Heterosporis finki*, gen. et sp. n. *Z. Parasitenkd.* 32:59–79.

Shadduck, J. A., Meccoli, R. A., Davis, R., Font, R. L. 1990. Isolation of a microsporidian from a human patient. *J. Infect. Dis.* 162:773–776.

Short, H. E., Cooper, W. 1948. Staining of microscopical sections containing protozoal parasites by modification of McNamara's method. *Trans. R. Soc. Trop. Med. Hyg.* 41:427–428.

Silveira, H., Canning, E. U. 1995. *Vittaforma corneae* n. comb. for the human microsporidium *Nosema corneum* Shadduck, Meccoli, Davis and Font, 1990, based on its ultrastructure in the liver of experimentally infected athymic mice. *J. Eukaryot. Microbiol.* 42:158–165.

Slamovits, C. H., Williams, B. A. P., Keeling, P. J. 2004. Transfer of *Nosema locustae* (Microsporidia) to *Antonospora locustae* n. comb. based on molecular and ultrastructural data. *J. Eukaryot. Microbiol.* 51:207–213.

Sokolova, Y. Y., Fuxa, J. R. 2008. Biology and life-cycle of the microsporidium *Kneallhazia solenopsae* Knell Allan Hazard 1977 gen. n., comb. n., from the fire ant *Solenopsis invicta*. *Parasitology* 135:903–929.

Solter, L. F, Becnel, J. J., Vávra, J. 2012. Research methods for entomopathogenic microsporidia and other protists. *In:* Lacey, L.A (ed.), Manual of Techniques in Invertebrate Pathology. 2nd Ed. Academic Press, Amsterdam, pp. 329–370.

Sprague, V. 1977. Systematics of the Microsporidia. *In:* Bulla Jr., L. A., Cheng, T. C. (eds.), Comparative Pathobiology, vol. 2. Plenum Press, New York, pp. 1–510.

Sprague, V. 1981. Iron haematoxylin staining. *In:* Clark, C. (ed.), Staining Procedures. William and Wilkins, Baltimore, pp. 271–272.

Sprague, V., Becnel, J. J., Hazard, E. I. 1992. Taxonomy of phylum microspora. *Crit. Rev. Microbiol.* 18:285–395.

Sprague, V., Ormières, R., Manier, J.-F. 1972. Creation of a new genus and a new family in the Microsporida. *J. Invertebr. Pathol.* 20:228–231.

Sprague, V., Vernick, S. H., Lloyd Jr., B. J. 1968. The fine structure of *Nosema* sp. Sprague, 1965 (Microsporida, Nosematidae) with particular reference to stages in sporogony. *J. Invertebr. Pathol.* 12:105–117.

Stentiford, G. D., Bateman, K. S. 2007. *Enterospora* sp., an intranuclear microsporidian infection of hermit crab *Eupagurus bernhardus*. *Dis. Aquat. Org.* 75:73–78.

Stentiford, G. D., Bateman, K. S., Feist, S. W., Chambers, E., Stone, D. M. 2013. Plastic parasites: extreme dimorphism creates a taxonomic conundrum in the phylum Microsporidia. *Int. J. Parasitol.* 43:339–352.

Stentiford, G. D., Bateman, K. S., Longshaw, M., Feist, S. W. 2007. *Enterospora canceri* n. gen., n. sp., intranuclear within the hepatopancreatocytes of the European edible crab *Cancer pagurus*. *Dis. Aquat. Org.* 75:61–72.

Sweeney, A. W., Hazard, E. I., Graham, M. F. 1985. Intermediate host for an *Amblyospora* sp. (Microspora) infecting the mosquito, *Culex annulirostris*. *J. Invertebr. Pathol.* 46:98–102.

Takizawa, H., Vivier, E., Petitprez, A. 1973. Développement intranucléaire de la Microsporidie *Nosema bombycis* dans les cellules de vers à soie après infestation expérimentale. *C. R. Acad. Sci.* 277:1769–1772.

Takvorian, P. M., Buttle, K. F., Mankus, D., Mannella, C. A., Weiss, L. M., Cali, A. 2013. The multilayered interlaced network (MIN) in the sporoplasm of the microsporidium *Anncaliia algerae* is derived from Golgi. *J. Eukaryot. Microbiol.* 60:166–178.

Takvorian, P. M., Cali, A. 1983. Appendages associated with *Glugea stephani*, a microsporidian found in flounder. *J. Protozool.* 30:251–256.

Takvorian, P. M., Cali, A. 1994. Enzyme histochemical identification of the Golgi apparatus in the microsporidian, *Glugea stephani*. *J. Eukaryot. Microbiol.* 41:633–643.

Takvorian, P. M., Cali, A. 1996. Polar tube formation and nucleoside diphosphatase activity in the microsporidian, *Glugea stephani*. *J. Eukaryot. Microbiol.* 43:102S–103S.

Takvorian, P. M., Weiss, L. M., Cali, A. 2005. The early events of *Brachiola algerae* (Microsporidia) infection: spore germination, sporoplasm structure, and development within host cells. *Folia Parasitol*. 52:118–129.

Taupin, V., Garenaux, E., Mazet, M., et al. 2007. Major O-glycans in the spores of two microsporidian parasites are represented by unbranched manno-oligosaccharides containing α-1,2 linkages. *Glycobiology* 17:56–67.

Taupin, V., Metenier, G., Delbac, F., Vivarès, C. P., Prensier, G. 2006. Expression of two cell wall proteins during the intracellular development of *Encephalitozoon cuniculi*: an immunocytochemical and in situ hybridization study with ultrathin frozen sections. *Parasitology* 132:815–825.

Thiéry, J. P. 1972. Mise en évidence des polysaccharides sur coupes fines en microscopie électronique. *J. Microsc.* 6:987–1018.

Thomarat, F., Vivarès, C. P., Gouy, M. 2004. Phylogenetic analysis of the complete genome sequence of *Encephalitozoon cuniculi* supports the fungal origin of Microsporidia and reveals a high frequency of fast-evolving genes. *J. Mol. Evol.* 59**:**780–791.

Toguebaye, B. S., Marchand, B. 1985. Pathogénie, cycle de développement et ultrastructure d'*Amblyospora culicis* n. sp. (Protozoa: Microspora), parasite du moustique *Culex quinquefasciatus* Say, 1823 (Diptera, Culicidae). *Can. J. Zool.* 63:1197–1809.

Toguebaye, B. S., Marchand, B.1986. Genèse des différents organites de la spore uninuclée d' *Amblyospora culicis* (Protozoa, Microspora). *Arch. Protistenkd.* 132:231–244.

Tonka, T., Weiser Jr., J., Weiser, J. 2010. Budding: a new stage in the development of *Chytridiopsis typographi* (Zygomycetes: Microsporidia). *J. Invertebr. Pathol.* 104:17–22.

Undeen, A. H. 1990. A proposed mechanism for the germination of microsporidian (Protozoa: Microspora) spores. *J. Theor. Biol.* 142:223–235.

Undeen, A. H., Frixione, E. 1991. Structural alteration of plasma membrane in spores of the microsporidium *Nosema algerae* on germination. *J. Protozool.* 38:511–518.

Undeen, A. H., Solter, L. F., 1996. Sugar content of and density of living and dead microsporidian (Protozoa: Microspora) spores. *J. Invertebr. Pathol.* 67: 80–91.

Undeen, A. H., Vander Meer, R. K.. 1994. Conversion of intrasporal trehalose into reducing sugars during germination of *Nosema algerae* (Protista: Microspora) spores: a quantitative study. *J. Eukaryot. Microbiol.* 41:129–132.

Undeen, A. H., Vávra, J. 1997. Research methods for entomopathogenic protozoa. *In:* L. Lacey (ed.), Manual of Techniques in Insect Pathology. Academic Press, San Diego, pp. 117–151.

Van Gool, T., Snijders, F., Reiss, P., et al. 1993. Diagnosis of intestinal and disseminated microsporidial infections in patients with HIV by a new rapid fluorescence technique. *J. Clin. Pathol.* 46:694–699.

Vávra, J. 1959. Beitrag zur Cytologie einiger Mikrosporidien. *Věst. Česk. Spol. Zool.* 23:347–350.

Vávra, J. 1962. *Bacillidium cyclopis* n. sp. (Cnidospora, Microsporidia), a new parasite of copepods. *Věst. Česk. Spol. Zool.* 26:295–299.

Vávra, J. 1963. Spore projection in microsporidia. *Acta Protozool.* 1:153–155.

Vávra, J. 1964. Recording microsporidian spores. *J. Insect. Pathol.* 6:258–260.

Vávra, J. 1965. Étude au microscope électronique de la morphologie et du développement de quelques Microsporidies. *C. R. Acad. Sci.* 261:3467–3470.

Vávra, J. 1972. Detection of polysaccharides in microsporidian spores by means of periodic acid-thiosemicarbazide-silver proteinate test. *J. Microsc.* 14:357–360.

Vávra, J. 1975. Scindosome-a new microsporidian organelle. *J. Protozool.* 22:69A.

Vávra, J. 1976a. Structure of the microsporidia. *In:* Bulla Jr., L. A., Cheng, T. C. (eds.), Comparative Pathobiology, vol. 1. Plenum Press, New York , pp. 1–85.

Vávra, J. 1976b. The development of microsporidia. *In:* Bulla Jr., L. A., Cheng, T. C. (eds.), Comparative Pathobiology, vol. 1. Plenum Press, New York, pp. 87–110.

Vávra, J. 1976c. The occurrence of paramural bodies in microsporidia. *J. Protozool.* 23:21A.

Vávra, J. 1984. *Norlevinea* n. g., a new genus for *Glugea daphniae* (Protozoa: Microspora), a parasite of *Daphnia longispina* (Crustacea: Phyllopoda). *J. Protozool.* 31:508–513.

Vávra, J. 2005. "Polar vesicles" of microsporidia are mitochondrial remnants ("mitosomes")? *Folia Parasitol.* 52:193–195.

Vávra, J., Barker, R. J., Vivarès, C. P. 1981. A scanning electron microscope study of a microsporidian with pansporoblast: *Thelohania maenadis*. *J. Invertebr. Pathol.* 37:47–53.

Vávra, J., Bedrník, P., Činátl, J. 1972. Isolation and in vitro cultivation of the mammalian microsporidian *Encephalitozoon cuniculi*. *Folia Parasitol.* 19:349–354.

Vávra, J., Chalupský, J. 1982. Fluorescence staining of microsporidian spores with the brightener "Calcofluor White M2R". *J. Protozool.* 29:503.

Vávra, J., Dahbiová, R., Hollister, W. S., Canning, E. U. 1993a. Staining of microsporidia spores by optical brighteners with remarks on the use of brighteners for the diagnosis of AIDS associated human microsporidioses. *Folia Parasitol.* 40:267–272.

Vávra, J., Hyliš, M., Vossbrinck, C., et al. 2006. *Vairimorpha disparis* n. comb. (Microsporidia: Burenellidae): a redescription and taxonomic revision of *Thelohania disparis* Timofejeva 1956, a microsporidian parasite of the gypsy moth *Lymantria dispar* (L.) (Lepidoptera: Lymantriidae). *J. Eukaryot. Microbiol.* 53:292–304.

Vávra, J., Kamler, M., Modrý, D., Koudela, B. 2011. Opportunistic nature of the mammalian microsporidia: experimental transmission of *Trachipleistophora extenrec* (Fungi: Microsporidia). between mammalian and insect hosts. *Parasitol. Res.* 108:1565–1573.

Vávra, J., Larsson, J. I. R. 1994. *Berwaldia schaefernai* (Jírovec, 1937) comb. n. (Protozoa, Microsporida), fine structure, life cycle and relationship to *Berwaldia singularis* Larsson, 1981. *Eur. J. Protistol.* 30:45–54.

Vávra, J., Larsson, J. I. R., Baker, M. D. 1997. Light and electron microscopic study of *Trichotuzetia guttata* gen. et sp. n. (Microspora, Tuzetiidae), a microsporidian parasite of *Cyclops vicinus* Uljanin, 1875 (Crustacea, Copepoda). *Arch. Protistenkd.* l47:293–306.

Vávra, J., Lukeš, J. 2013. Microsporidia and "the art of living together". *In:* Rollinson, D. (ed.), Advances in Parasitology, vol. 82**.** Academic Press, New York, pp. 253–320.

Vávra, J., Maddox, J. V. 1976. Methods in microsporidiology. *In:* Bulla Jr., L. A., Cheng, T. C. (eds.), Comparative Pathobiology, vol. 1. Plenum Press, New York, pp. 281–319.

Vávra, J., Nohynková, E., Machala, L., Špála, J. 1993b. An extremely rapid method for detection of microsporidia in biopsy materials from AIDS patients. *Folia Parasitol.* 40:273–274.

Vávra, J., Sprague, V. 1976. Glossary for the microsporidia. *In:* Bulla Jr., L. A., Cheng, T. C. (eds.), Comparative Pathobiology, vol. 1. Plenum Press, New York, pp. 341–363.

Vávra, J., Undeen, A. H. 1970. *Nosema algerae* sp. (Cnidospora: Microsporida) a pathogen in a laboratory colony of *Anopheles stephensi* Liston (Diptera, Culicidae). *J. Protozool.* 17:240–249.

Vávra, J., Vinckier, D., Torpier, G., Porchet, E., Vivier, E. 1986. A freeze-fracture study of microsporidia (Protozoa: Microspora). I. The sporophorous vesicle, the spore wall, the spore plasma membrane. *Protistologica* 22:143–154.

Vávra, J., Yachnis, A. T., Shadduck, J. A., Orenstein, J. M. 1998. Microsporidia of the genus *Trachipleistophora* - causative agents of human microsporidiosis: description of *Trachipleistophora anthropophthera* n. sp. (Protozoa: Microsporidia). *J. Eukaryot. Microbiol.* 45:273–283.

Vinckier, D. 1973. Étude des cycles et de l'ultrastructure de *Lecudina linei* n. sp. (Grégarine parasite de Nemerte) et de son parasite, la Microsporidie *Nosema vivieri* (V. D. et P.). Thesis. Université des Sciences et Techniques de Lille, Lille, France.

Vinckier, D. 1975. *Nosemoides* gen. n., *N. vivieri* (Vinckier, Devauchelle & Prensier, 1970) comb. nov. (Microsporidie): étude de la différenciacion sporoblastique et genèse des differentes structures de la spore. *J. Protozool.* 22:170–184.

Vinckier, D. 1990. Différenciation cellulaire chez les Microsporidies: étude ultrastructurale du développement de *Nosemoides vivieri* V. D. et P. et *Nosema apis* Zander et mise en évidence de l'évolution des systemes membranaires par la technique de cryofracture. Thesis. Université des Sciences et Techniques de Lille Flandres Artois, Lille, France.

Vinckier, D., Porchet, E., Vivier, E., Vávra, J., Torpier, G. A. 1993. A freeze-fracture study of microsporidia (Protozoa: Microspora). II. The extrusion apparatus: polar filament, polaroplast, posterior vacuole. *Eur. J. Protistol.* 29:370–380.

Vivarès, C. P. 1980. Étude ultrastructurale de *Thelohania maenadis* Pérez (Microspora: Microsporida) et données nouvelles sur le genre *Thelohania* Henneguy. *Arch. Protistenkd.* 123:44–60.

Vivarès, C. P., Bouix, G., Manier, J. F. 1977. *Ormieresia carcini*, gen. n., sp.n., Microsporidie du crabe méditerranéen, *Carcinus mediterraneus* Czerniavsky, 1884: cycle évolutif et étude ultrastructurale. *J. Protozool.* 24:83–94.

Vivier, E. 1975. The microsporidia of the Protozoa. *Protistologica* 11:345–361.

Vivier, E., Schrével, J. 1973. Étude en microscopic photonique et électronique de differents stades du cycle de *Metchnikovella hovassei* et observations sur la position systématique des Metchnikovellidae. *Protistologica* 9:95–118.

Voronin, V. N. 1989a. Classification of the polar filaments of microsporidia on the base of their ultrastructure. *Citologia* 31:1010–1015 (in Russian with English summary).

Voronin, V. N. 1989b. The ultrastructure of *Lanatospora macrocyclopis* (Protozoa: Microsporida) from the cyclope *Macrocyclops albidus* (Jur.) (Crustacea, Copepoda). *Arch. Protistenkd.* 137:357–366.

Voronin, V. N. 1994. *Microsporidium fluviatilis* sp. n. (Protozoa: Microsporidia) from the cyclope *Eucyclops serratulus* (Fisch.) with description of a new type of polaroplast. *Parazitologiya* 28:48–51 (in Russian with English summary).

Vossbrinck, C. R., Andreadis, T. G., Vávra, J., Becnel, J. J. 2004. Molecular phylogeny and evolution of mosquito parasitic microsporidia (Microsporidia: Amblyosporidae). *J. Eukaryot. Microbiol.* 51:88–95.

Vossbrinck, C. R., Debrunner-Vossbrinck, B. A. 2005. Molecular phylogeny of the Microsporidia: ecological, ultrastructural and taxonomic considerations. *Folia Parasitol.* 52:131–142.

Vossbrinck, C. R., Woese, C. R. 1986. Eukaryotic ribosomes that lack a 5.8 S RNA. *Nature* 320:287–288.

Walker, M. H., Hinsch, G. W. 1972. Ultrastructural observations of a microsporidian protozoan parasite in *Libnia dubia* (Decapoda). I. Early spore development. *Z. Parasitenkd.* 39:17–26.

Weidner, E. 1972. Ultrastructural study of microsporidian invasion into cells. *Z. Parasitenkd.* 40:227–242.

Weidner, E. 1975. Interactions between *Encephalitozoon cuniculi* and macrophages. *Z. Parasitenkd.* 47:1–9.

Weidner, E. 1976a. The microsporidian spore invasion tube. The ultrastructure, isolation, and characterization of the protein comprising the tube. *J. Cell Biol.* 71:23–34.

Weidner, E. 1976b. Some aspects of microsporidian physiology. *In:* Bulla Jr., L. A., Cheng, T. C. (eds.), Comparative Pathobiology, vol. 1. Plenum Press, New York, pp. 111–126.

Weidner, E. 1982. The microsporidian spore invasion tube. lII. Tube extrusion and assembly. *J. Cell Biol.* 93:976–979.

Weidner, E., Byrd, W., Scarborough, A., Pleshinger, J., Sibley, D. 1984. Microsporidian spore discharge and the transfer of polaroplast organelle membrane into plasma membrane. *J. Protozool.* 31:195–198.

Weidner, E., Canning, E. U., Hollister, W. S. 1997. The plaque matrix (PQM) and tubules at the surface of intramuscular parasite *Trachipleistophora hominis*. *J. Eukaryot. Microbiol.* 44:359–365.

Weidner, E., Canning, E. U., Rutledge, C. R., Meek, C. L. 1999. Mosquito (*Diptera*: *Culicidae*) host compatibility and vector competency for the human myositic parasite *Trachipleistophora hominis* (Phylum Microspora). *J. Med. Entomol.* 36:522–525.

Weidner, E., Manale, S. B., Halonen, S. K., Lynn J. W. 1995. Protein-membrane interaction is essential to normal assembly of the microsporidian spore invasion tube. *Biol. Bull.* 188:128–135.

Weidner, E., Overstreet, R. M., Tedeschi, B., Fuseler, J. 1990. Cytokeratin and desmoplakin analogues within an intracellular parasite. *Biol. Bull.* 179:237–242.

Weir, G. O., Sullivan, J. T. 1989. A fluorescence screening technique for microsporidia in histological sections. *Trans. Am. Microsc. Soc.* 108:208–210.

Weiser, J. 1961. Die Mikrosporidien als Parasiten der Insekten. Monographien zur Angewandte Entomologie, vol. 17. Paul Parey Verlag, Hamburg, 149 pp.
Weiser, J. 1976a. The *Pleistophora debaisieuxi* xenoma. *Z. Parasitenkd.* 48:263–270.
Weiser, J. 1976b. Staining of the nuclei of microsporidian spores. *J. Invertebr. Pathol.* 28:147–149.
Weiser, J. 1977. Contribution to the classification of microsporidia. *Věst. Česk. Spol. Zool.* 41:308–320.
Weiser, J., Purrini, K. 1985. Light- and electron-microscopic studies on the microsporidian *Vairimorpha ephestiae* (Mattes) (Protozoa, Microsporidia) in the meal moth *Ephestia kuehniella*. *Arch. Protistenkd.* 130:179–189.
Weiser, J., Žižka, Z. 1974. Stages in sporogony of *Pleistophora debaisieuxi* (Microsporidia). *J. Protozool.* 21:477 (abstr.).
Weiser, J., Žižka, Z. 1975. Stages in sporogony of *Plistophora debaisieuxi* Jírovec (Microsporidia). *Acta Protozool.* 14:185–194.
Weissenberg, R. 1976. Microsporidian interactions with host cells. *In:* Bulla Jr., L. A., Cheng, T. C. (eds.), Comparative Pathobiology, vol. 1. Plenum Press, New York, pp. 203–237.
Williams, B. A. P., Cali, A., Takvorian, P. M., Keeling, P. J. 2008. Distinct localization patterns of two putative mitochondrial proteins in the microsporidian *Encephalitozoon cuniculi*. *J. Eukaryot. Microbiol.* 55:131–133.
Williams, B. A. P., Hirt, R. P., Lucocq, J. M., Embley, T. M. 2002. A mitochondrial remnant in the microsporidian *Trachipleistophora hominis*. *Nature* 418:865–869.
Wittner, M., Weiss, L. M. (eds.) 1999. *The Microsporidia and Microsporidiosis*. ASM Press, Washington, DC.
Yasunaga, C., Shino, I., Funakoshi, M., Kawarabata, T., Hayasaka, S. 1995. A new method for inoculation of poor germinator *Nosema* sp. NIS M11 (Microsporida: Nosematidae) into an insect cell culture. *J. Eukaryot. Microbiol.* 42:191–195.
Zickler, D., Olson, L. W. 1975. The synaptonemal complex and the spindle plaque during meiosis in yeast. *Chromosoma* 50:1–23.